

**DOKUZ EYLÜL UNIVERSITY
GRADUATE SCHOOL OF NATURAL AND APPLIED
SCIENCES**

**SHUNT VOLTAGE REGULATION OF SELF-
EXCITED INDUCTION GENERATOR**

By

Changiz SALIMIKORDKANDI

October 2012

İZMİR

SHUNT VOLTAGE REGULATION OF SELF- EXCITED INDUCTION GENERATOR

**A Thesis Submitted to the
Graduate School of Natural and Applied Sciences of Dokuz Eylül
University In Partial Fulfillment of the Requirements for the Degree
of Master of Science in Electric and Electronic Engineering**

**by
Changiz SALIMIKORDKANDI**

October 2012

İZMİR

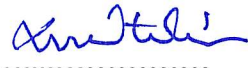
M.Sc THESIS EXAMINATION RESULT FORM


We have read the thesis entitled “**SHUNT VOLTAGE REGULATION OF SELF-EXCITED INDUCTION GENERATOR**” completed by **CHANGIZ SALIMIKORDKANDI** under supervision of **ASSIST.PROF.DR. TOLGA SÜRGEVİL** and we certify that in our opinion it is fully adequate, in scope and in quality, as a thesis for the degree of Master of Science.




Assist.Prof.Dr. Tolga SÜRGEVİL

(Supervisor)


.....
Yrd. Doç. Dr. Levent ÇETKİN


.....
Prof. Dr. Eyüp ALPİNAR


.....
.....

Prof.Dr. Mustafa SABUNCU
Director
Graduate School of Natural and Applied Sciences

Acknowledgements

I would like to express my sincere gratitude and appreciation to my supervisor Assist.Prof.Dr. Tolga SÜRGEVİL for his guidance and fruitful discussions.

I would like to thank to Prof.Dr. Eyüp AKPINAR for his encouragement and recommendations.

I also sincerely thank to my parents, Ebadollah and Nahid, for providing continuous guidance and support throughout the project.

Changiz Salimikordkandi

SHUNT VOLTAGE REGULATION OF SELF-EXCITED INDUCTION GENERATOR

ABSTRACT

In this thesis, the excitation methods for stand-alone self-excited induction generator (SEIG) using fixed capacitor bank, voltage source inverter (VSI) and static synchronous compensator (STATCOM) are presented. The steady-state analyses of the SEIG with fixed capacitor excitation for constant frequency and constant speed operation are performed in MATLAB environment. Stand-alone SEIG's dynamic characteristics are examined using the simulation models in stationary reference frame based on q-d reference frame theory. In order to verify the machine models, an experimental setup of SEIG with fixed capacitor bank was built in the laboratory. The results obtained from steady-state and dynamic model of the induction machine are compared by the laboratory tests results. The shunt voltage regulator schemes for stand-alone SEIG based on VSI and STATCOM under constant speed and variable load conditions are studied. The performances of these regulation schemes are examined through simulations in MATLAB/Simulink using the developed models for this purpose.

Keywords: Induction generator, self-excitation, voltage regulation, STATCOM, VSI, dynamic modeling.

KENDİNDEN UYARTIMLI ENDÜKSİYON JENETATÖRÜNÜN ŞÖNT GERİLİM REGÜLASYONU

ÖZ

Bu tez çalışmasında, sabit kondansatörlü, gerilim kaynaklı evirici (VSI) ve statik senkron kompensatör (STATCOM) kullanarak bağımsız kendinden uyartımlı endüksiyon jeneratörü (SEIG) için uyartım metotları sunulmuştur. Sabit kondansatör uyartımlı jeneratörün sürekli-hal analizleri, sabit frekans ve sabit hız için MATLAB ortamında gerçekleştirilmiştir. SEIG' in dinamik karakteristikleri q-d referans çerçevesi teorisine dayalı durağan referans çerçevesinde oluşturulan benzetim modelleri kullanılarak incelenmiştir. Makina modellerini doğrulamak için sabit kondansatörlü SEIG deney düzeneği laboratuarda kurulmuştur. Endüksiyon makinasının sürekli-hal ve dinamik modelinden elde edilen sonuçlar laboratuvar test sonuçları ile karşılaştırılmıştır. SEIG için VSI ve STATCOM kullanan şönt gerilim düzenleyici dizgelerinin çalışması sabit hızda ve değişken yük koşulları altında incelenmiştir. Bu gerilim düzenleyici dizgelerin performansı bu amaç için MATLAB/Simulink' te oluşturulan modeller kullanılarak incelenmiştir.

Anahtar sözcükler: Endüksiyon jeneratörü, kendinden uyartım, gerilim regülasyonu, STATCOM, VSI, dinamik modelleme.

CONTENTS

	Page
THESIS EXAMINATION RESULT FORM	ii
ACKNOWLEDGEMENTS	iii
ABSTRACT	iv
ÖZ	v
CHAPTER ONE - INTRODUCTION.....	1
CHAPTER TWO - LITERATURE SURVEY ON INDUCTION GENERATORS.....	3
2.1 Self Excitation Process.....	5
2.2 Excitation Methods	7
2.2.1 Excitation by Capacitor Bank	7
2.2.2 Excitation by Controlled Rectifier.....	8
2.2.3Excitation by Capacitor Bank and Controlled Rectifier.....	9
2.2.4 Excitation by SVC and STATCOM	10
CHAPTER THREE-STEADY STATE ANALYSIS OF FIXED CAPACITOR STAND-ALONE SELF-EXCITED INDUCTION ENERATOR.....	12
3.1 Per-Phase Equivalent Circuit of Self Excited Induction Generator (SEIG) Excited by Fixed Shunt Capacitor.....	12
3.2 Operation Condition of Stand-Alone SEIG.....	15
3.2.1 Constant Frequency Operation.....	15
3.2.2 Constant Speed Operation	18
3.3 Comparison of Analysis and Experimental Results	20
3.3.1 No-Load Characteristics of Induction Machine.....	21
3.3.2 Constant Frequency Operation Results.....	22
3.3.3 Constant Speed Operation Results.....	24

CHAPTER FOUR - DYNAMICAL MODEL OF INDUCTION MACHINE....29

4.1 Dynamical Model of Three Phase Induction Machine	29
4.1.1 Voltage Equations in qd0 Reference Frame	31
4.1.2 Modeling of Induction Machine in the Stationary Reference Frame.....	34
4.1.3 Saturation Model.....	37
4.2 Simulation Model of Induction Motor in MATLAB/SIMULINK.....	40
4.2.1 Comparison of Simulation and Experimental Results of Induction Motor.....	43
4.3 Dynamical Model of Fixed Capacitor Self-Excited Induction Generator.....	45
4.3.1 Comparison of Simulation Results with Experimental and Steady-State Analysis Results of SEIG.....	47
4.3.1.1 Voltage Buildup Under No-Load.....	48
4.3.1.2 Load Variation after Full Excitation.....	50

CHAPTER FIVE - VOLTAGE REGULATION OF STAND ALONE SELF EXCITED INDUCTION GENERATOR.....51

5.1 Voltage Regulation by using Variable Capacitor Bank.....	51
5.1.1 Simulation Model of Voltage Regulation by Variable Capacitor Bank.....	52
5.1.2 Simulation Results of using Variable Capacitor Bank.....	53
5.2 Regulation of the Generated Voltage by using Voltage Source Inverter.....	56
5.2.1 Modeling of the VSI and dc Load	57
5.2.2 Simulation Model of SEIG and VSI.....	59
5.2.3 Results of Voltage Regulation by using VSI.....	61
5.3 Regulation of the Generated Voltage by using STATCOM.....	65
5.3.1 Modeling of the Connected ac Load and STATCOM	66
5.3.2 Simulation Model of Shunt Voltage Regulation by using STATCOM.....	68
5.3.3 Results of Shunt Voltage Regulation by using STATCOM.....	71
5.4 Shunt Voltage Regulation using Feedback from Stator Voltage.....	79

CHAPTER SIX - CONCLUSION.....80

REFERENCES.....85

CHAPTER ONE

INTRODUCTION

In the past, nearly half century ago, electricity was important but not essential. But today, the social living has more problems such as traffic problems, no heating, no light and communication without electricity. On the other hand, the traditional methods to produce electricity need to consume other energy sources such as gas, fuel, nuclear energy. By increasing cost of the gas and fuel in the past decade, the electricity cost is increased dependently. Also, the environmental pollution problems due to usage of these sources have led to interest in alternative energy sources such as solar and wind energy.

The synchronous machine and induction machine can be used as a generator in renewable energy plants. When the losses of transferring energy is an important point to decrease cost of electricity, production of electricity in local is the other important point of scientists' view. When the local production is our aim, we need a machine that doesn't need maintenance and also it is independent from other sources like as battery (DC source). Therefore, induction machine can be a good candidate in local energy conversion such as in wind farms. These machines are inexpensive and reliable, but they need an extra reactive power source to control the voltage, typically by means of a capacitor bank at the terminals of self-excited induction generator (SEIG). The advantages of the induction machine against synchronous machine are well known. These are simplicity, reliability, self-protection against short circuit faults, low cost, minimum service requirement and good efficiency. Despite these advantages, SEIG have two major disadvantages. The magnitude and frequency of voltage generated by SEIG will vary under variable speed, variable excitation and variable load operation.

The objective of this thesis is to examine the methods of stator voltage control in SEIG by using shunt regulation techniques. In this scope, capacitor excitation, voltage source inverter (VSI) excitation and static synchronous compensator (STATCOM) excitation methods were examined by means of computer simulations.

The results show that by using these methods, it is possible to achieve acceptable voltage regulation on the stator terminals of the induction generator.

The studies accomplished in this thesis are summarized in the following chapters: Chapter 2 contains a literature survey on excitation methods of the stand-alone self-excited induction generators. In Chapter 3, the steady-state analyses of fixed capacitor SEIG are performed for both constant speed and constant frequency operating conditions. In order to observe the dynamic behavior of the induction machine, its q-d reference frame model is presented in Chapter 4. In Chapter 5, the methods of voltage control are discussed and specific control strategies are examined through dynamic simulations. In Chapter 6, conclusions and future work are given.

CHAPTER TWO

LITERATURE SURVEY ON INDUCTION GENERATORS

Induction machines have some advantages when compared to other electrical machines. These are simplicity, reliability, low cost, minimum service requirement and good efficiency. Induction machines can be operated without needing a separate source for supplying the rotor field current; instead, these currents are applied to the rotor by electromagnetic induction from stator. These advantages make this machine popular in applications as a generator in renewable energy, especially in remote applications of wind and hydro energy (Haque, 2008). These machines absorb the fluctuation of mechanical power delivered by the wind source. Therefore, induction machine become a suitable generator to produce energy from the wind (Meier, 2006).

Induction generators can be classified according to the structure of rotor and connection of the machine's stator windings to the external electrical circuit. If the rotor of induction generator consists of windings similar to its stator windings, it is called wound rotor induction generator. These types of machines are more expensive and less robust. The generator is called squirrel cage induction generator, if the rotor has short-circuited conducting bars parallel to the generator shaft instead of windings. Because of its being inexpensive and robust, the squirrel cage induction generators are more common (Meier, 2006). Classification of induction generator with respect to connection of the machine to external electrical circuit divided into two categories. Induction generator can be connected to the electrical power grid, which is called grid connected induction generator, which is shown in Figure 2.1. In this mode, the machine supplies active power to the grid and absorbs reactive power from grid. Also, both amplitude and frequency of the generated voltage will be determined by the electrical grid (Haque, 2008; Joshi, Sandhu & Soni, 2006). It is also possible to supply the reactive power requirement of the induction generator locally. In this case, the machine is called stand-alone self-excited induction generator (SEIG). This machine is able to generate voltage if the required reactive power of machine is supplied by an appropriate capacitor bank connected to the

stator. At startup, there must be a residual voltage at the stator terminals to provide self-excitation. The capacitor bank provides the reactive power requirement of the machine and load, which is illustrated in Figure 2.2.

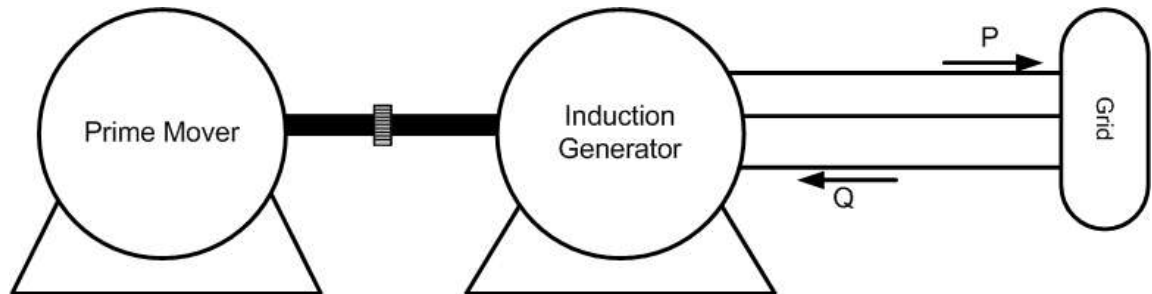


Figure 2.1 Grid Connected Induction Generator scheme

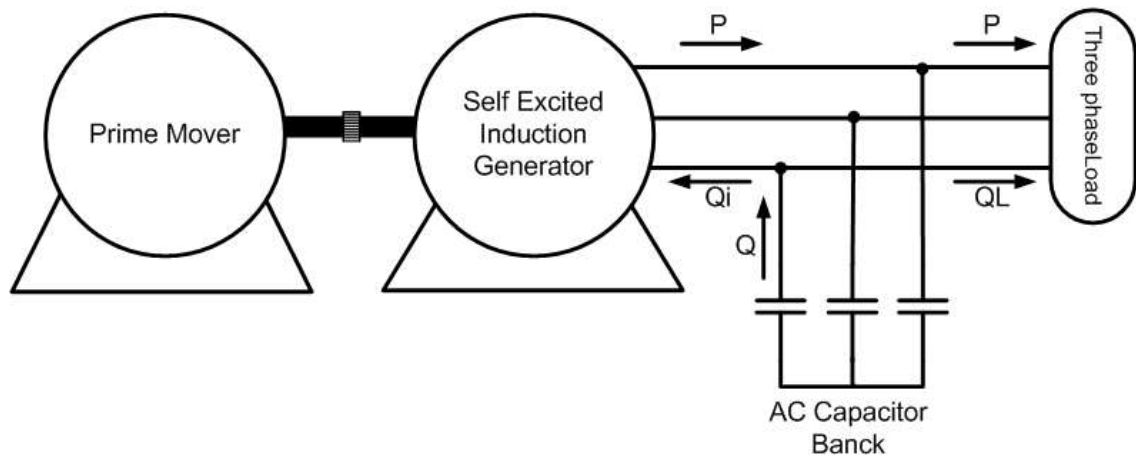


Figure 2.2 Stand-alone self-excited induction generator scheme

The advantages of SEIG are well known; ruggedness, simple structure, low cost, self-protection against short circuit faults (Singh, 2003). Unfortunately, these machines have some major disadvantages that restrict the application of this machine in sensitive loads. These are large variation and deregulation of terminal voltage and frequency under varying load conditions. (Mosaad, 2011; Singh, 2003; Sharma & Sandhu, 2008).

In literature, there are survey studies that classify the structures and analysis methods of self-excited induction generators (Bansal, 2005; Singh, 2003). To analyze the induction machine in steady-state and transient, the per-phase equivalent circuit

and q-d models are used, respectively. In steady-state analysis, by using some methods such as loop impedance (Ahmad & Noro, 2003; Chan & Lai, 2001; Haque, 2008; Murthy, Bhuvaneswari, Ahuja & Gao, 2010) and nodal admittance (Anagreh & Al-Refae'e, 2003; Ahmed, Noro, Matso, Shindo & Nakaoka, 2003; Hashemnia, Kashiha & Ansari, 2010; Ouazene & Mcpherson 1983), the performance of machine can be analyzed. On the other hand, in transient analysis of machine, q-d model has been extensive because it simplifies the complex equations of the machine (Krause, 2002; Ong, 1998; Wang, & Su, 1997). These analysis methods are explained in Chapter 3 and Chapter 4 in details.

2.1 Self Excitation Process

It is well known that, by a suitable capacitor bank across the induction generator terminals and driving the rotor at a suitable speed, voltage can be induced at the stator windings because of the residual magnetism that initially exists in the machine. This method is called self-excitation and in order that self-excitation occurs, the following conditions should be satisfied:

- There should be enough residual magnetism in the machine, if not, by using a battery connected at two terminals of stator or starting the machine in motoring case, it can be produced.
- The capacitor bank across the stator terminal of machine must have a suitable value.

The EMF induce in the induction machine due to residual magnetism initially circulates a leading current on the capacitor and then the flux produced by this current increase the induced EMF. As the voltage of the machine increases then the capacitor current will also increase. As a result, the stator voltage will increase until the generated reactive power by the capacitor bank and the reactive power consumed by the generator are equal. The no-load terminal voltage of induction generator is dependent on the value of capacitor curve and machine's magnetizing curve. Intersection of these two curves is the magnitude of generated voltage by the

machine at no-load (Anagreh & Al-Refae'e, 2003; Phumiphak & Uthai, 2009). This process is illustrated in Figure 2.3. This point will be changed by any change in the rotor speed, capacitor value and load conditions.

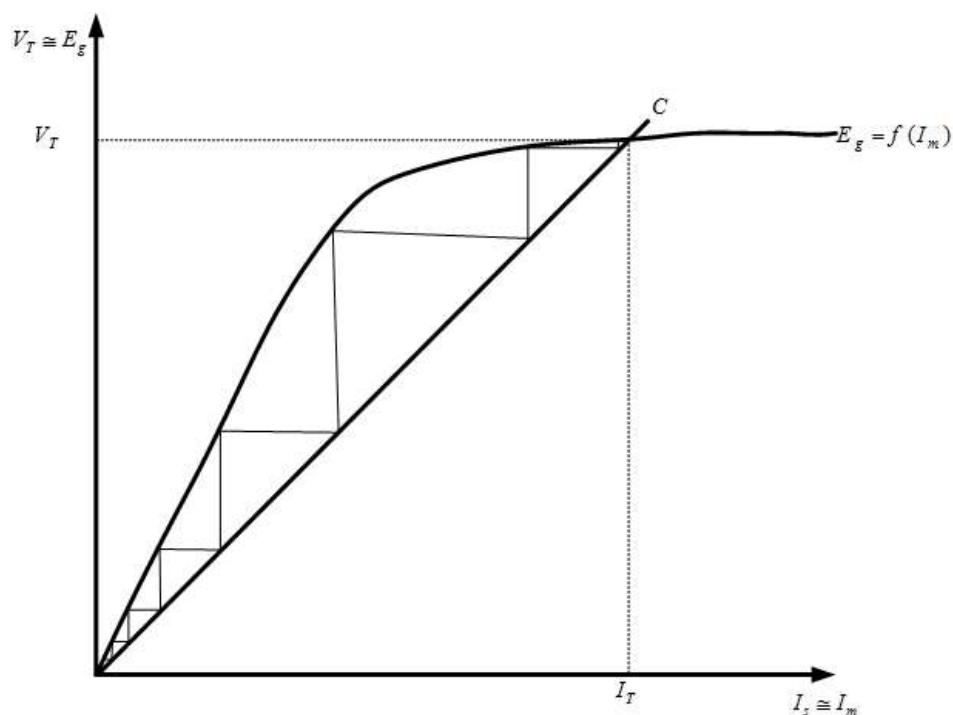


Figure 2.3 Voltage build-up process of SEIG

The excitation time is dependent on the values of residual magnetism and the capacitor. Obtaining the critical and maximum value of connected capacitor is important, because SEIG terminal voltage will collapse or no excitation will occur if the capacitor value (C_1) is less than the critical capacitor value (C_2) as shown in Figure 2.4. However, if the value of capacitance is selected much higher, the operating frequency of machine will decrease. Because, by increasing the capacitor value, magnetizing current in the machine will be increased. As the magnetizing current increases, the copper losses on the stator will be increased. This causes an increase in the generator slip and the frequency of the voltages will be decreased (Anagreh & Al-Refae'e, 2003). As a result, more ohmic losses and thus less efficiency will occur. Usually, the capacitor value is chosen to be some more than the critical value (C_3) as shown in Figure 2.4 (Hashemnia, Kashiha & Ansari, 2010; Wang & Cheng, 2000).

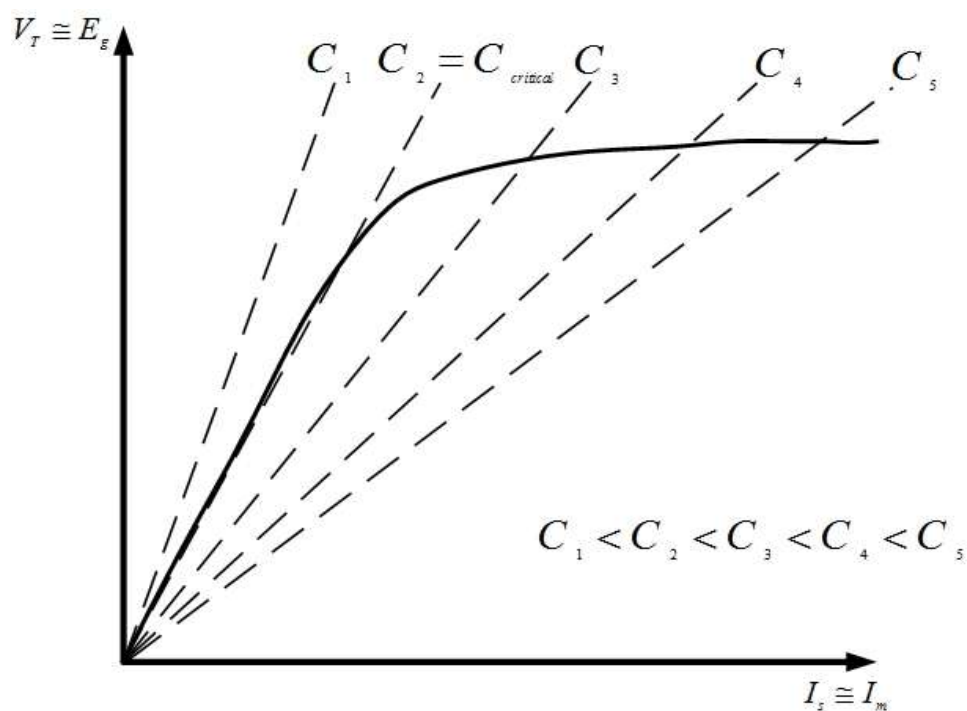


Figure 2.4 Induction generator and capacitor voltage curves

2.2 Excitation Methods

In stand-alone self-excited condition, the required reactive power is supplied from an external circuit. Therefore, a fixed capacitor bank or other electronic controller methods can be employed for the excitation of the generator.

2.2.1 Excitation by Capacitor Bank

The SEIG scheme with fixed capacitor excitation was shown in Figure 2.2. This type of excitation is suitable when the load is constant and also the prime mover provides constant speed to the rotor of the generator. Any change in the load and speed will affect the frequency and the magnitude of the stator terminal voltage. In the literature, a Genetic Algorithm based approach to obtain constant voltage and constant frequency operation of SEIG was proposed where the terminal voltage magnitude was regulated by adjusting the capacitor value and the frequency was regulated by adjusting the rotor speed (Joshi, Sandhu & Soni, 2006).

To feed dc loads or regulate ac output for stand-alone or grid connected systems, ac-dc power conversion interface is required (Wu, 2008). In order to obtain constant frequency on the connected load, an ac-dc-ac converter can be also connected to the stator of machine. In this case, voltage across the load is variable and constant in frequency if this scheme shown in Figure 2.5 is used. In order to obtain constant voltage on the stator/load terminals, the value of the capacitor bank can be changed by using additional capacitor banks and switching these capacitors depending on any change in the load and speed. The disadvantage of this method is that the rectifier will generate harmonics and it may cause power resonance and noise in the machine (Wu, 2008).

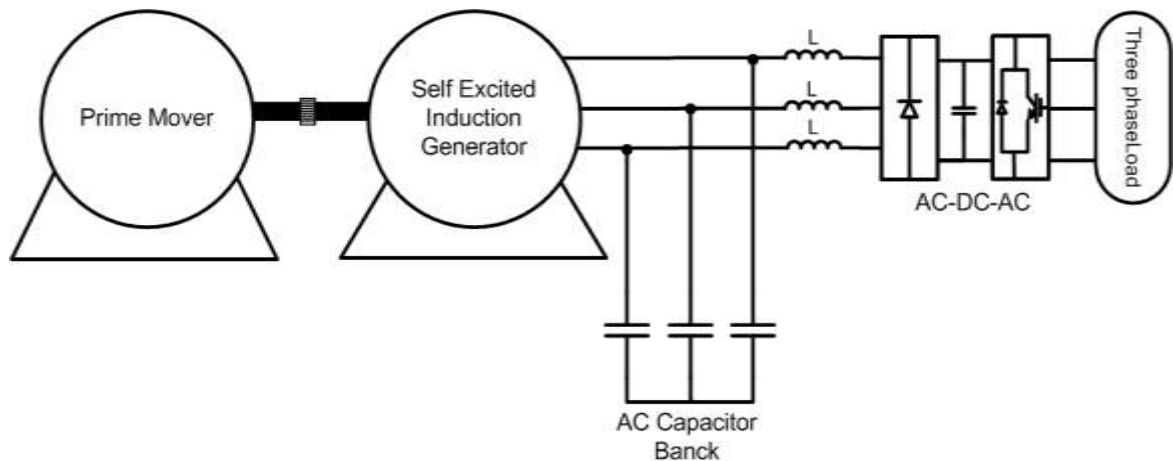


Figure 2.5 Excitation and ac/dc power conversion interface by using a fixed capacitor bank

2.2.2 Excitation by Controlled Rectifier

In this method, the VSI supplies active power to the dc load and the reactive power required by SEIG. Hence, the power capability of VSI is large, and it increases the cost and loss (Hazra & Sensarma, 2010; Jayaramaiah & Fernandes, 2006). This method is illustrated in Figure 2.6. The simulation model is built and analysis of the dynamic behavior of this method is examined in Chapter 5.

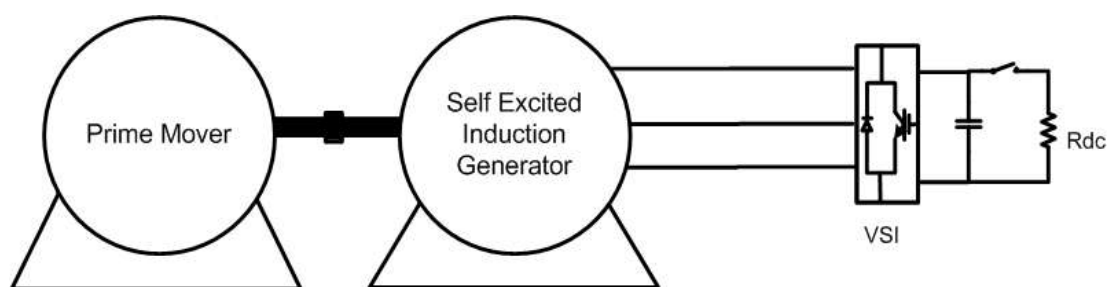


Figure 2.6 Excitation and control of terminal voltage by using VSI

Also, for supplying the reactive power needed by SEIG and obtaining a regulated ac output, back to back converters that consist of a controlled rectifier and an inverter can be used (Dastagir & Lopes, 2007). This process is illustrated in Figure 2.7. The reactive power demand of the machine is provided by the voltage source converter (VSC). Also, it transfers the active power generated to the load side and regulates the dc bus voltage. Usage of voltage source inverter (VSI) allows us to supply a three phase ac load at fixed frequency. The advantage of this method is that the machine can be operated in variable speed and variable load conditions (Wu, 2008). The main disadvantage of this method is that the converters have to be rated to at least rated generator power (Dastagir & Lopes, 2007).

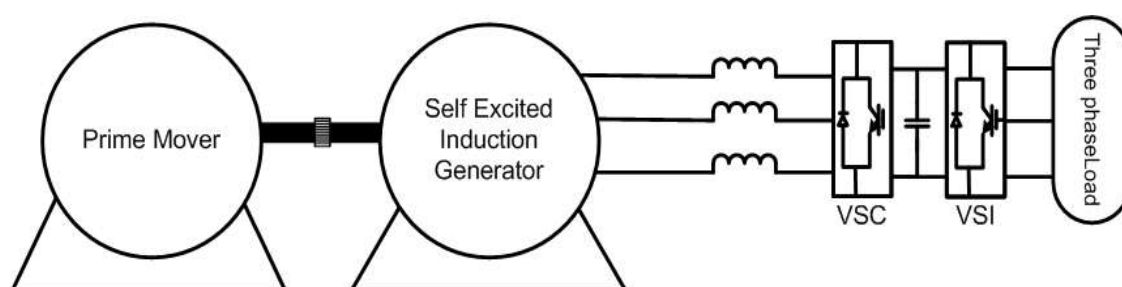


Figure 2.7 Excitation and control of load voltage and frequency by using ac/dc/ac power converter interface

2.2.3 Excitation by Capacitor Bank and Controlled Rectifier

Disadvantage of previous method (cost and losses in excitation by voltage source converter) can be handled by employing the method shown in Figure 2.8. In this method, the amplitude and frequency of generated voltage by induction generator are

regulated by using back to back converters between induction generator and load. The major reactive power that the induction generator demands is supplied by the ac capacitor bank and the VSC supplies the fine tune reactive power depending on any change in load and speed. In this scheme, the losses and cost of the VSC is reduced since it supplies a portion of reactive power required by the induction generator. As a result, cost of the system is decreased. The VSI still supplies full active power to the load (Wu, 2008).

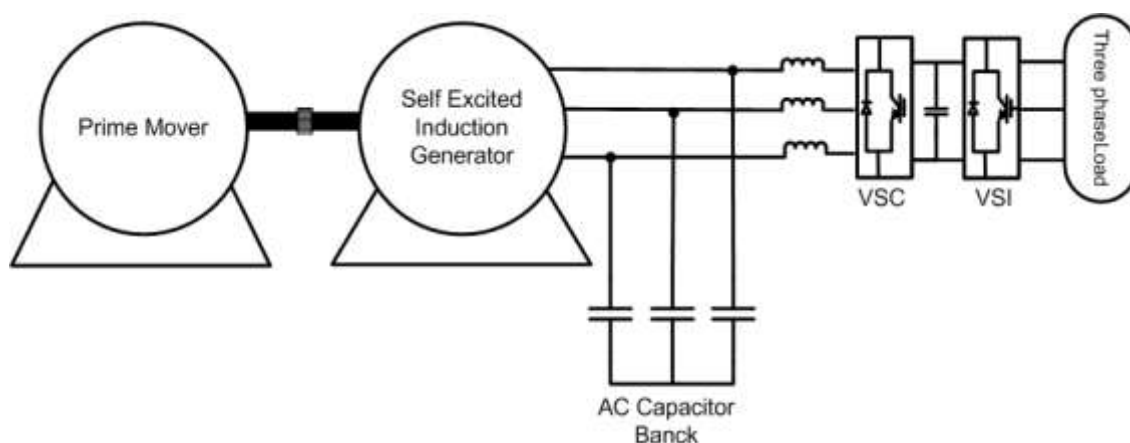


Figure 2.8 Excitation and control of load voltage and frequency by using AC capacitor bank and ac/dc/ac power converter

2.2.4 Excitation by SVC and STATCOM

Excitation of the machine is not restricted by above methods. In order to excite the machine and regulate the generated voltage by the machine, static VAR compensator (SVC) or static synchronous compensator (STATCOM) can be used as shown in Figure 2.9 (Ahmed & Noro, 2003; Singh, Murthy & Gupta, 2004). Using this method, the magnitude of the terminal voltages can be maintained constant under variable load. By controlling the reactive power supplied by STATCOM/SVC in shunt with the SEIG. For supplying the major reactive power requirement by SEIG, a fixed capacitor bank is used. Also, for supplying the additional reactive power needed by the machine and load depending on conditions STATCOM or SVC is used. In this case, the machine is able to deliver constant voltage and variable

frequency to the load (Kuperman & Rabinovici, 2005). This method is also examined in Chapter 5.

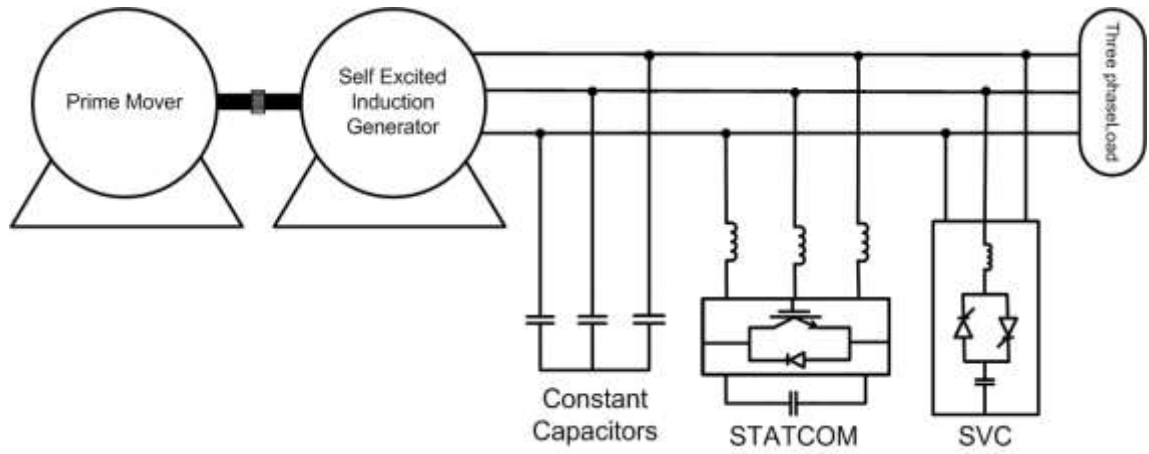


Figure 2.9 Excitation and control of terminal voltage by STATCOM/SVC

CHAPTER THREE
STEADY STATE ANALYSIS OF FIXED CAPACITOR STAND-ALONE
SELF-EXCITED INDUCTION GENERATOR

Steady state analysis is useful to determine the operation of stand-alone SEIG and also design and usage of this machine for appropriate application. To analyze the stand-alone SEIG with fixed capacitor in steady-state condition, its per-phase equivalent circuit is required. From dc test, blocked-rotor test, and no-load test, the parameters of the equivalent circuit are obtained. The performance of machine is calculated when the speed, excitation capacitors, and the value of load across the stator of machine are known. To estimate the performance of the machine, loop impedance (Ahmad & Noro, 2003; Chan & Lai, 2001; Haque, 2008; Murthy, Bhuvaneshwari, Ahuja & Gao, 2010) and nodal admittance (Anagreh & Al-Refae'e, 2003; Ahmed, Noro, Matso, Shindo & Nakaoka, 2003; Hashemnia, Kashiha & Ansari, 2010; Ouazene & Mcpherson 1983) methods have been developed in literature. In all these analysis methods, it is assumed that magnetizing reactance is the only element affected by magnetic saturation and other circuit parameters are considered as constant.

3.1 Equivalent Circuit of Self-Excited Induction Generator with Fixed Shunt Capacitor

The per phase equivalent circuit of a three-phase SEIG with shunt excitation capacitor and resistance load is shown in Figure 3.1. The rotor parameters are referred to the stator of the machine.

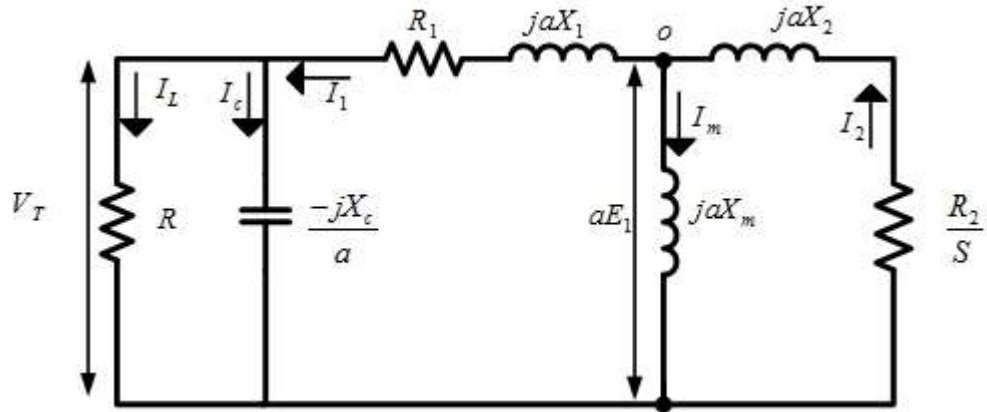


Figure 3.1 Per-phase equivalent circuit of SEIG with fixed shunt capacitor and resistive load

The difference between synchronous speed and rotor speed is determining the value of slip, which can be written as

$$S = \frac{W_s - W_r}{W_s} = \frac{a - b}{a} \quad (3.1)$$

where W_s is the synchronous speed, W_r is the rotor speed, a is the per unit frequency and b is speed value in per unit.

On the rotor side, substituting slip from equation (3.1) in $\frac{R_2}{S}$

$$\frac{R_2}{S} = \frac{aR_2}{a-b} \quad (3.2)$$

To obtain the normalized form of circuit, all parameters in Figure 3.1 are divided by base frequency (a), which is shown in Figure 3.2.

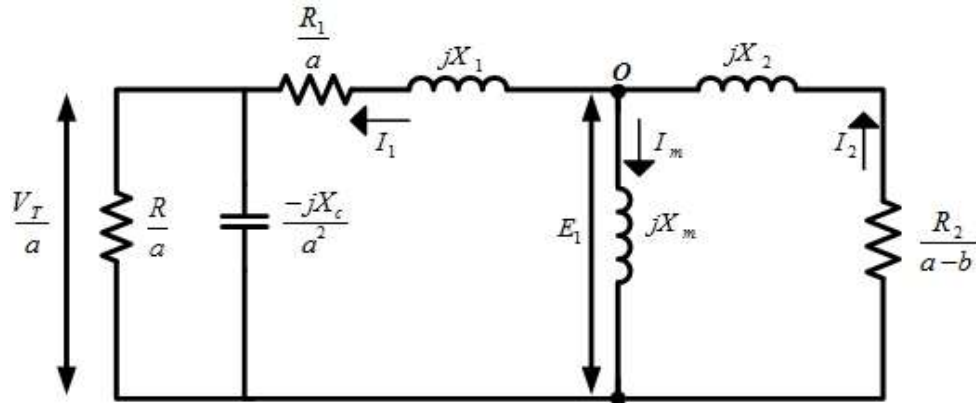


Figure 3.2 Normalized equivalent circuit of SEIG

The symbols in these equivalent circuits indicate the following:

R_1, R_2 Stator and rotor resistance in ohms, respectively

X_1, X_2 Stator and rotor reactance parameters in ohms, respectively

X_m Machine magnetizing reactance in ohms

E_1 Air gap voltage in volts at rated frequency

S Slip factor

a Per unit frequency

b Per unit speed of rotor

V_T Terminal voltage in volts

R Resistance load in ohms

It must be noted that, the core loss resistance is neglected because of its large value. In this case

$$I_2 = I_m + I_1 \quad (3.3)$$

where, I_1 is the stator current, I_m is the magnetizing reactance current, I_2 is the rotor branch current (Boldea, 2006; Ouazene & Mcpherson, 1983).

3.2 Operating Conditions of Stand-Alone SEIG

Depending on the prime mover's control, the induction generator can be operated in three modes. (a) Constant speed, (b) constant frequency and (c) variable speed variable frequency (Anagreh & Al-Refae'e, 2003). In this thesis, the second order slip equation model is used (Boldea, 2006) to analyze the machine in constant frequency and to analyze machine in constant speed the nodal admittance method is used (Ouazene & Mcpherson 1983).

3.2.1 Constant Frequency Operation

Constant frequency operation is shown in Figure 3.3 and can be obtained by controlling the speed such that the frequency of the generated voltage is held constant. In this mode of operation, the value of X_m is variable depending on load and speed, therefore, it is assumed as an unknown. The other unknown is slip (S), when the machine is operated in constant frequency. Once X_m and S are calculated, the terminal voltage, stator current, rotor current and the performance of machine can be calculated (Boldea, 2006; Joshi, Sandhu & Soni, 2006; Sandhu & Jain, 2008).

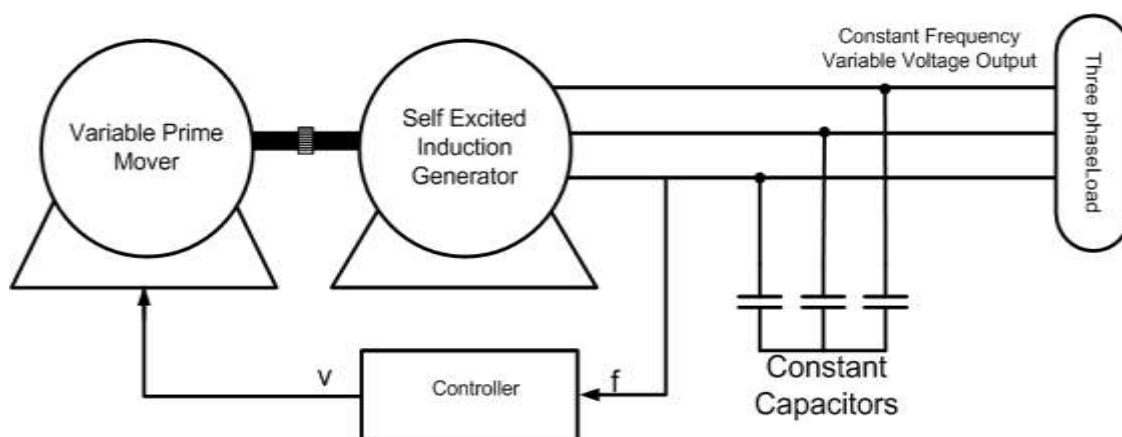


Figure 3.3 Constant frequency SEIG scheme

Considering a resistive load connected to the stator terminals, from equivalent circuit given in Figure 3.1

$$R_L = \frac{RX_c^2}{a^2R^2 + X_c^2} \quad (3.4)$$

$$X_L = \frac{aR^2X_c}{a^2R^2 + X_c^2} \quad (3.5)$$

where $R_L - jX_L$ is the parallel equivalent of the load and capacitive branches (Boldea, 2006).

Analysis of circuit at node 0 gives

$$I_m + I_1 - I_2 = 0 \quad (3.6)$$

Substitution of current values gives

$$aE_1 \left(\frac{1}{jaX_m} + \frac{1}{R_{1L} + jX_{1L}} + \frac{S}{R_2 + jSaX_2} \right) = 0 \quad (3.7)$$

where

$$R_{1L} = R_1 + R_L \quad X_{1L} = X_1 - X_L \quad (3.8)$$

Real part of equation (3.7) can be written as

$$\frac{R_{1L}}{R_{1L}^2 + X_{1L}^2} + \frac{SR_2}{R_2^2 + S^2a^2X_2^2} = 0 \quad (3.9)$$

And the imaginary part equation (3.7) is equal to

$$-\frac{1}{aX_m} - \frac{X_{1L}}{R_{1L}^2 + X_{1L}^2} - \frac{aS^2X_2}{R_2^2 + S^2a^2X_2^2} = 0 \quad (3.10)$$

Solution of (3.9) is used to find the operating slip such that

$$K_1S^2 + K_2S + K_3 = 0 \quad (3.11)$$

where

$$K_1 = a^2X_2^2R_{1L}, \quad K_2 = R_2(R_{1L}^2 + X_{1L}^2), \quad K_3 = R_{1L}R_2^2 \quad (3.12)$$

and

$$S_{1,2} = \frac{-K_2 \pm \sqrt{K_2^2 - 4K_1K_3}}{2K_1} \quad (3.13)$$

Equation (3.14) provide two values of slip (S_1 and S_2) that only the lower real one is acceptable for generator mode. Once the slip is calculated the speed of machine can be calculated from

$$b = a(1-s) \quad (3.14)$$

After obtaining the slip from equation (3.13), the magnetizing reactance can be determined from (3.10) such that

$$X_m = \frac{(R_2^2 + S^2a^2X_2^2)(R_{1L}^2 + X_{1L}^2)}{-(X_{1L}(R_2^2 + S^2a^2X_2^2) + aS^2X_2(R_{1L}^2 + X_{1L}^2))a} \quad (3.15)$$

The no-load saturation curve that is obtained from no-load motoring operation is used to define relation between X_m and E_1 , which is given in section 3.4. The relation between X_m and E_1 can be written as a fifth order polynomial

$$E_1 = p_1 X_m^5 + p_2 X_m^4 + p_3 X_m^3 + p_4 X_m^2 + p_5 X_m + p_6 \quad (3.16)$$

As E_1, S, F and X_m are known, the machine efficiency can be obtained (Boldea, 2006).

3.2.2 Constant Speed Operation

For steady state analysis of machine in constant speed operation mode, the equivalent circuit given in Figure 3.2 can be used. As indicated in previous operation mode, it is assumed that only magnetizing reactance is affected by the saturation and also the core losses are ignored (Ouazene & Mcpherson, 1983).

For a resistive load, the combination of shunt branch, $-j \frac{X_c}{a^2}$ and $\frac{R}{a}$, in per phase equivalent circuit can be written as (Ouazene & Mcpherson, 1983).

$$R_L = \frac{RXc^2}{a(a^2R^2 + X_c^2)} \quad (3.17)$$

$$X_L = \frac{R^2Xc}{(a^2R^2 + X_c^2)} \quad (3.18)$$

From nodal admittance method the three branches admittance in equivalent circuit must be equal to zero

$$Y_s + Y_m + Y_r = 0 \quad (3.19)$$

The real and imaginary part of equation (3.19) yields, respectively

$$\frac{\left(R_L + \frac{R_1}{a}\right)}{(X_1 - X_L)^2 + \left(R_L + \frac{R_1}{a}\right)^2} + \frac{\frac{R_2}{(a-b)}}{X_2^2 + \left(\frac{R_2}{(a-b)}\right)^2} = 0 \quad (3.20)$$

$$-\frac{1}{X_m} - \frac{X_2}{X_2^2 + \left(\frac{R_2}{(a-b)}\right)^2} - \frac{(X_1 - X_L)}{(X_1 - X_L)^2 + \left(R_L + \frac{R_1}{a}\right)^2} = 0 \quad (3.21)$$

If the value of speed, load resistance and excitation capacitor are given, the two unknowns in machine are frequency and magnetizing reactance. When the speed is known, the only unknown is the frequency of machine and it can be calculated from real part of total admittance. From equation (3.20), the following expression can be written as a fifth order polynomial

$$Q_5 a^5 + Q_4 a^4 + Q_3 a^3 + Q_2 a^2 + Q_1 a + Q_0 = 0 \quad (3.22)$$

Where $Q_0 - Q_5$ are functions of equivalent circuit parameters, which are expressed as

$$Q_0 = -bR_2 \left(\frac{R_3}{R}\right)^2 \quad (3.23)$$

$$Q_1 = R_2 \left(\frac{R_3}{R}\right)^2 + R_3 \left(\frac{R_2}{R}\right)^2 + b^2 R_3 \left(\frac{X_2}{R}\right)^2 \quad (3.24)$$

$$Q_2 = -2bR_3 \left(\frac{X_2}{R}\right)^2 - bR_2 \left[\left(\frac{R_1}{X_c}\right)^2 + \left(\frac{X_1}{R}\right)^2 - 2\left(\frac{X_1}{X_c}\right) \right] \quad (3.25)$$

$$Q_3 = R_2 \left[\left(\frac{X_1}{R}\right)^2 + \left(\frac{R_1}{X_c}\right)^2 - 2\left(\frac{X_1}{X_c}\right) \right] + R_3 \left(\frac{X_2}{R}\right)^2 + R_1 \left(\frac{R_2}{X_c}\right)^2 + b^2 R_1 \left(\frac{X_2}{X_c}\right)^2 \quad (3.26)$$

$$Q_5 = R_2 \left(\frac{X_1}{X_c}\right)^2 + R_1 \left(\frac{X_2}{X_c}\right)^2 \quad (3.27)$$

$$Q_4 = -b[Q_5 + R_1 \left(\frac{X_2}{X_c}\right)^2] \quad (3.28)$$

where

$$R_3 = R_1 + R \quad (3.29)$$

Equation (3.22) can be solved in MATLAB program by root command. The roots of this equation are imaginary and real, but only the real roots are acceptable in practice (Ouazene & Mcpherson, 1983).

After calculating the machine operating frequency, magnetizing reactance can be determined from equation (3.21) by following equation: (Ouazene & Mcpherson, 1983)

$$X_m = \frac{\left(R_L + \frac{R_1}{a}\right)\left(X_2^2 + (a-b)^2\right)}{\left(\frac{R_2}{a-b}\right)(X_1 - X_L) - X_2\left(R_L + \frac{R_1}{a}\right)} \quad (3.30)$$

And similar to the constant frequency operation, the value of air gap voltage can be obtained from equation (3.16). The values of p1- p6 are obtained from no-load curve of induction machine tested in the laboratory and results are given in the next section.

3.3 Comparison of Analysis and Experimental Results

Steady-state analysis and experimental results of SEIG with a resistive load between infinite and 160 ohm are compared in this section. The test machine is a 1.1 kW, 4-pole, 400-V, 50/60-Hz, Y-connected squirrel-cage induction machine having a rated current of 2.8 A. From dc test, blocked-rotor test, and no-load test the circuit parameters of the machine are calculated and shown in Table 3.1. The value of each capacitor in the Y-connected excitation capacitor bank is 30 μ F.

Table 3.1 1.1 kW induction machine parameters obtained from tests

$R_s \Omega$	$X_1 \Omega$	$R_2 \Omega$	$X_2 \Omega$	$X_m \Omega$	$X_{m-uns} \Omega$
7.9	8.1	8.2	8.1	96.5	140

3.3.1 No-load Characteristics of Induction Machine

By applying variable voltage to the stator terminals of the machine at rated frequency (50 Hz), the no load characteristics of the machine can be obtained. In above condition, according to slip concept, its value will be very small (in practice it is assumed zero), and with respect to the rotor equation $\frac{R_2}{S} + jX_2$, this branch can be assumed as an open circuit. Therefore, by measuring the applied voltage to the stator of machine and stator current that is approximately equal to the magnetizing current, saturation curve of machine can be obtained (E_1 Versus I_m). The no-load curve obtained in experimental setup and 30 μF capacitor voltage line are shown in Figure 3.4, where the interaction of two curves determine the generator terminal (line - to - line) voltage at steady-state and no-load.

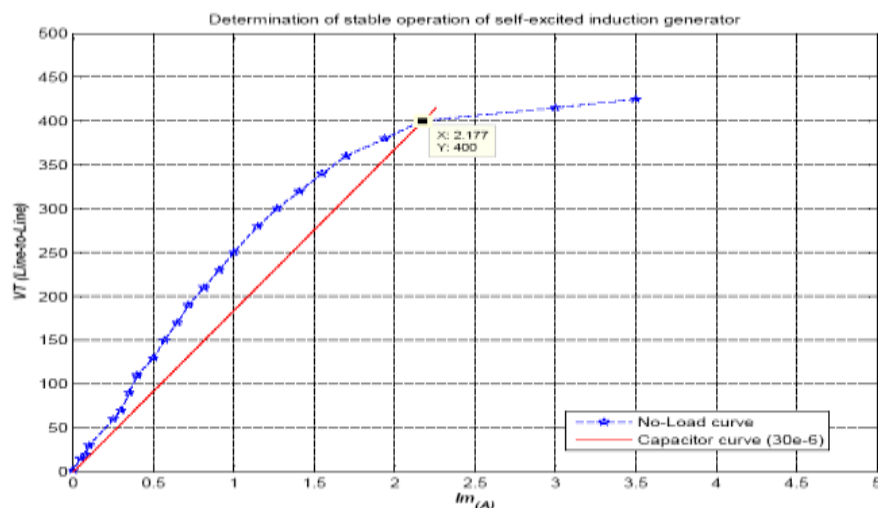


Figure 3.4 Capacitor and no-load curves of SEIG

From curve fitting tool (CFTOOL) in MATLAB, a fifth order polynomial can be determined to obtain the value of X_m versus E_1 , which is illustrated in Figure 3.5.

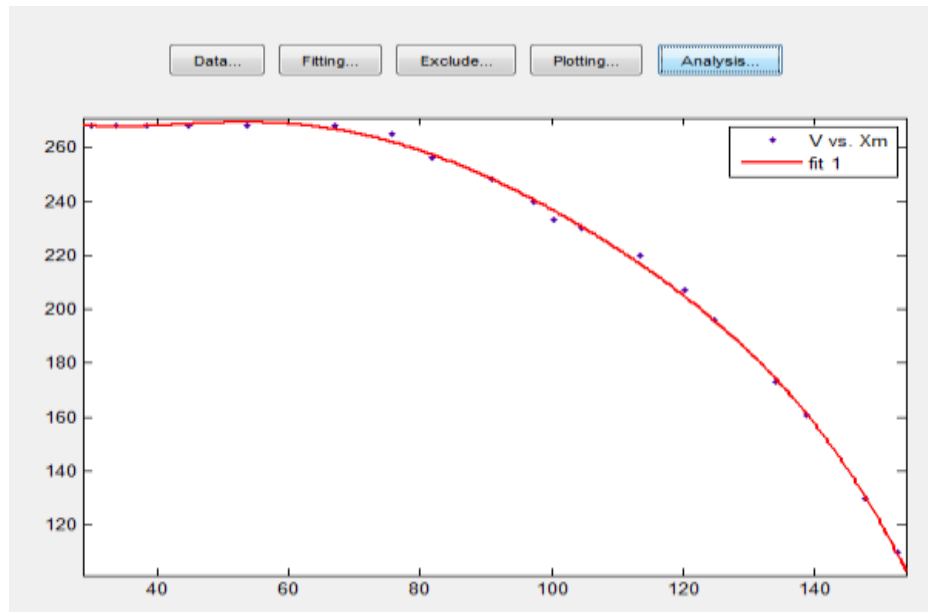


Figure 3.5 Magnetizing reactance (Ω) versus air gap voltage (V)

With the experimental test data that are fitted to a 5th order polynomial, the following polynomial coefficients are obtained:

$$p1 = -2.443e-008;$$

$$p2 = 1.613e-005;$$

$$p3 = -0.0042;$$

$$p4 = 0.5139;$$

$$p5 = -30.29;$$

$$p6 = 927.9;$$

3.3.2 Constant Frequency Operation Results

Constant frequency operation is implemented by changing the machine's rotor speed to obtain constant frequency on the laboratory setup. In this test the stator voltage, stator current, load current, frequency and rotor speed had measured. The experimental results are shown in Table 3.2. Also the machine steady state analysis results and comparison between these two results (experimental and simulation) are shown in Table 3.3 and Figure 3.6, respectively.

Table 3.2 Experimental results of constant frequency operation

Load (Ω)	Stator Voltage (V)	Stator Current (A)	Load Current (A)	Stator Frequency (HZ)	Rotor Speed (RPM)
∞	228	2.25	0	50	1500
384	211	2.15	0.55	50	1524
288	205	2.15	0.71	50	1536
192	190	2.14	0.98	50	1560
160	175	2.06	1.09	50	1575

Table 3.3 Computer analysis results of constant frequency operation

Load (Ω)	Stator Voltage (V)	Stator Current (A)	Load Current (A)	Stator Frequency (HZ)	Rotor Speed (RPM)
∞	228	2.2	0	50	1500
384	210	2.1	0.55	50	1546
288	204	2.1	0.7	50	1558
192	188	2.1	0.97	50	1580
160	174	2	1.08	50	1594

From above test, it is obvious that terminal voltage continue to decreasing by any increasing in the load current. This procedure is illustrated in Figure 3.6. The analysis results are almost verified by the experiments

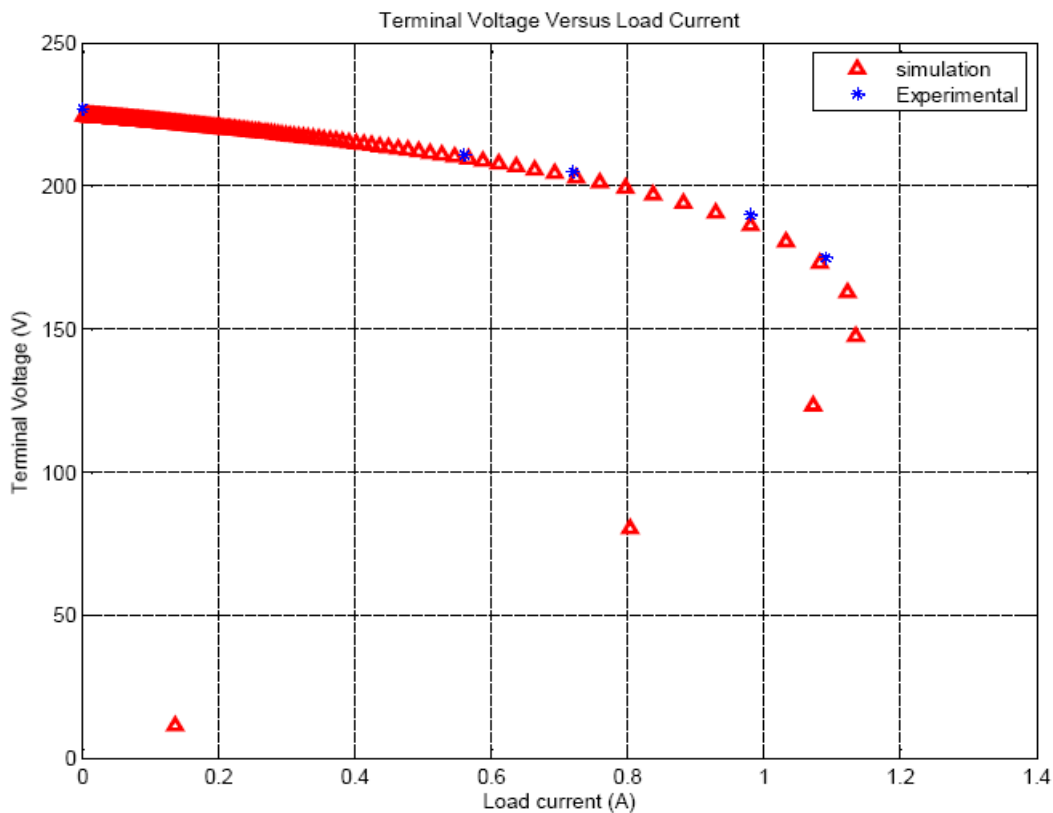


Figure 3.6 Terminal voltage (V) of SEIG in constant frequency (Hz) operation

3.3.3 Constant Speed Operation Results

When the machine is operated in constant speed, stator frequency and voltage is changed by load variation. Experimental and analysis results of machine in constant speed are shown in Table 3.4 and Table 3.5, respectively.

Table 3.4 Experimental results of constant speed operation

Load (Ω)	Stator Voltage (V)	Stator Current (A)	Load Current (A)	Stator Frequency (HZ)	Rotor Speed (RPM)
∞	228	2.25	0	50	1500
384	204	2.07	0.53	49.5	1500
288	193	2	0.67	49	1500
192	164	1.78	0.85	48.1	1500
160	131	1.5	0.81	47.6	1500

Table 3.5 Computer analysis results of constant speed operation

Load (Ω)	Stator Voltage (V)	Stator Current (A)	Load Current (A)	Stator Frequency (HZ)	Rotor Speed (RPM)
∞	227	2.2	0	49.8	1500
384	197	2	0.51	49.5	1500
288	186	1.88	0.65	48.5	1500
192	157	1.67	0.8	48	1500
160	133	1.5	0.83	47.2	1500

Similar to the constant frequency operation mode, the terminal voltage of SEIG is varied by any variation on the load resistance. From Figure 3.7 it could be seen that, when the load current is increased, the generated voltage by SEIG will be decreased. Closeness between the experimental and simulation results verify the computer simulation.

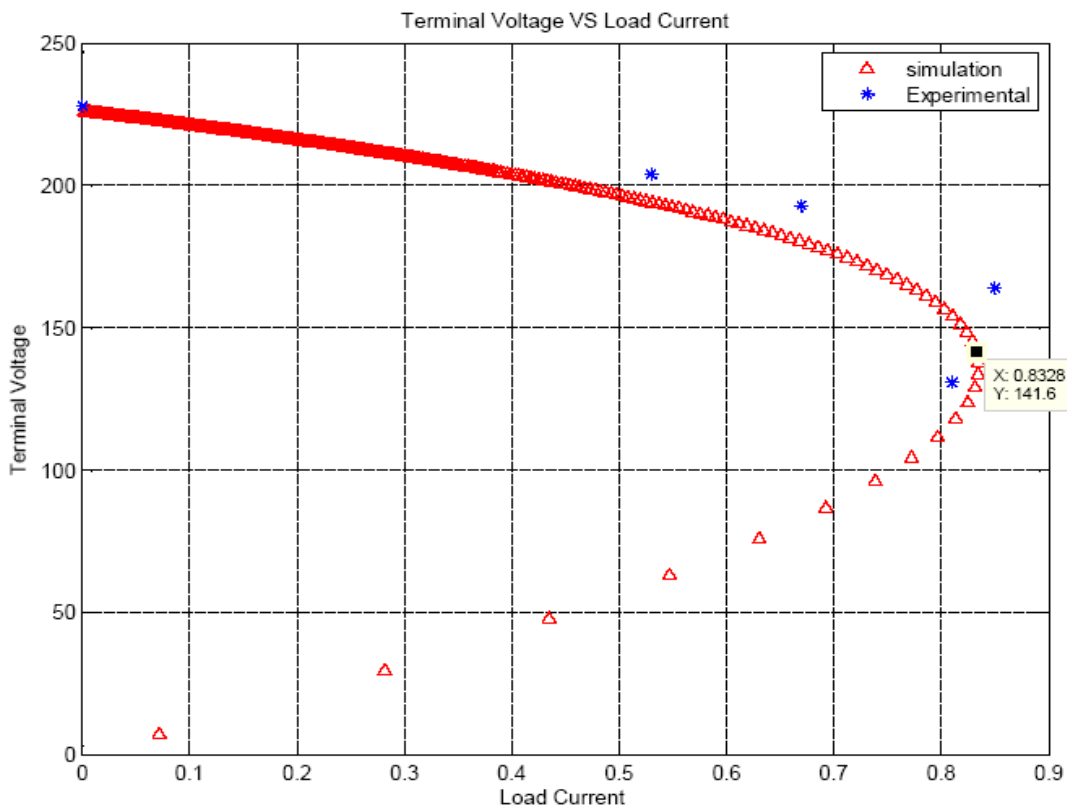


Figure 3.7 Terminal voltage (V) versus load current (A) in constant speed operation

Figure 3.8 shows the stator frequency of SEIG, in both laboratory and computer analysis. The stator frequency of SEIG decreased when the load current is increased. Figure 3.9 shows the generated voltage versus load resistance values. The generated voltage by the SEIG will be decreased by decreasing the connected resistive load. As shown in Figure 3.7 and Figure 3.9, the terminal voltage is collapsed when the value of the load is decreased to its critical value of 180Ω .

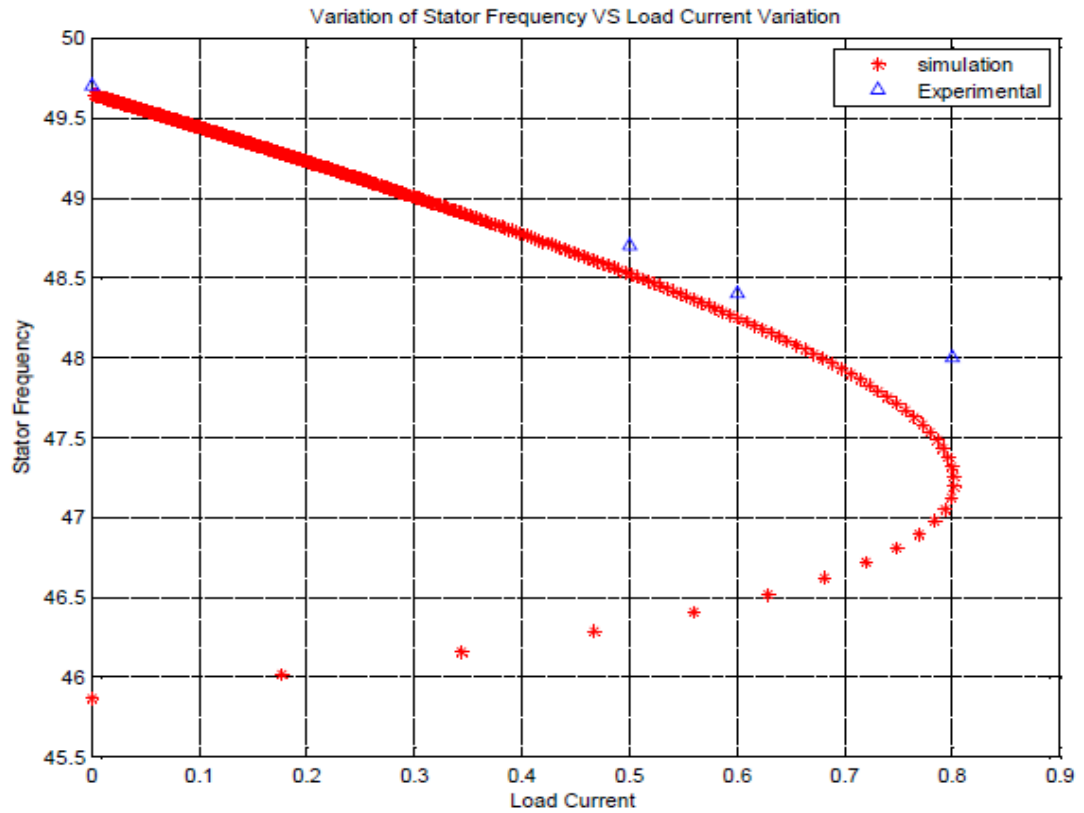


Figure 3.8 Terminal frequency (Hz) versus load current (A) in constant speed operation

Any reduction in the load will cause output power increment and terminal voltage reduction. Figure 3.11 shows the generated voltage versus output power by changing the connected load. From this figure, it is possible to determine the maximum loading capacity of the generator at constant speed mode.

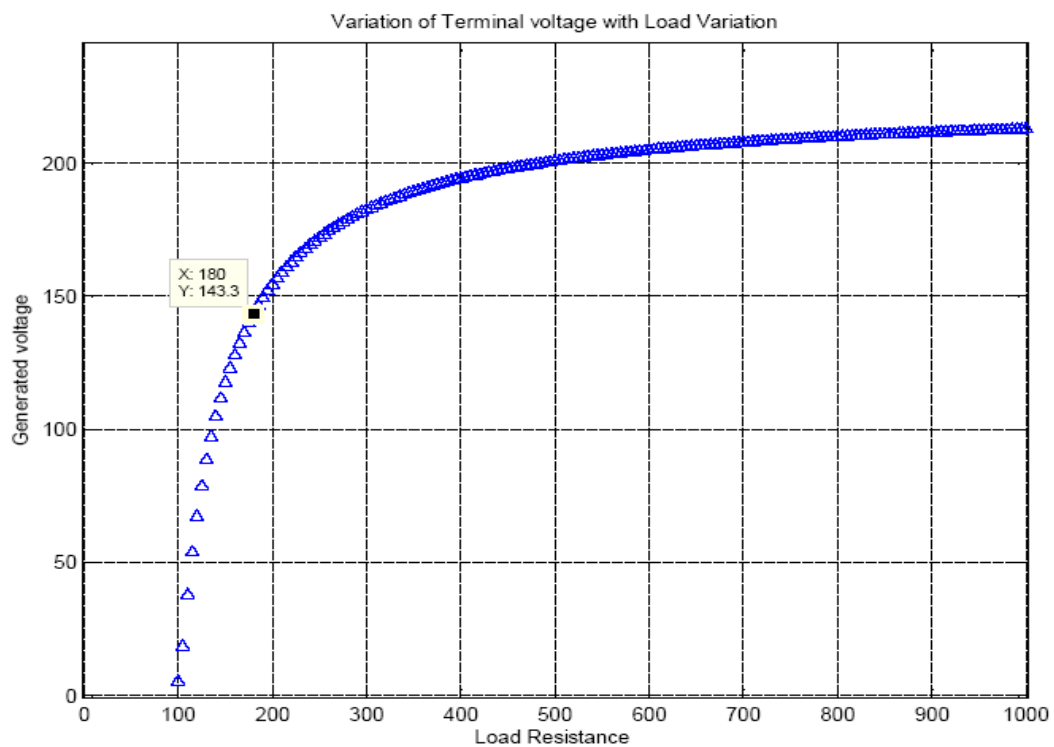


Figure 3.9 Terminal voltage (V) versus resistive load (Ω)

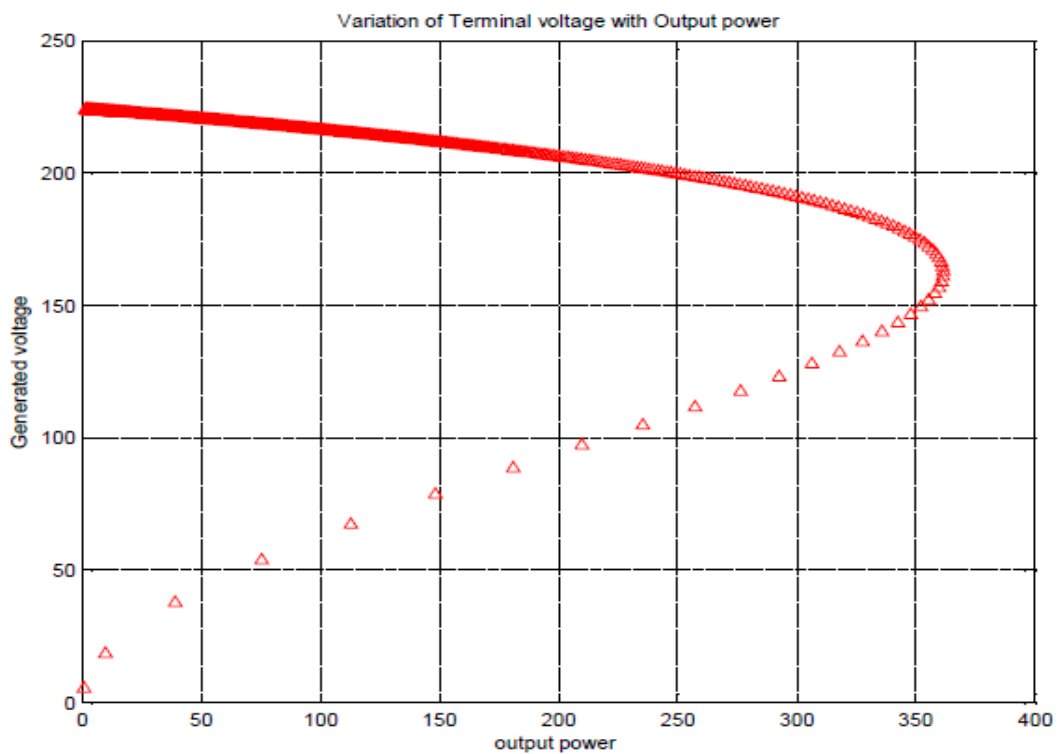


Figure 3.10 Variation of terminal voltage (V) versus output power (W)

CHAPTER FOUR

DYNAMICAL MODEL OF INDUCTION MACHINE

In this chapter, the dynamical model of induction machine in both motor under load and generator mode with fixed excitation capacitors connected to the stator of induction generator will be studied by using the qd0 transformation theory. State-space dynamical model of induction machine taking magnetic saturation into account will be presented in stationary reference frame. The induction machine model has been built in MATLAB/SIMULINK tool and simulation results are verified by the experiments carried out in laboratory setup.

4.1 Dynamical Model of Three Phase Induction Machine

In this modeling, the machine will be considered as a three phase induction motor with balanced three-phase windings and direction of currents is into the terminals. The MMF distribution in the machine is assumed to be sinusoidal. The stator voltages in terms of resistance and inductance voltages can be written as

$$v_{abc} = r_s i_{abc} + \frac{d(\lambda_{abc})}{dt} \quad (4.1)$$

where v_{abc} , i_{abc} and λ_{abc} are the stator voltages, stator currents and flux linkages, respectively, and are 3×1 vectors defined by:

$$v_{abc} = \begin{bmatrix} v_{as} \\ v_{bs} \\ v_{cs} \end{bmatrix} \quad i_{abc} = \begin{bmatrix} i_{as} \\ i_{bs} \\ i_{cs} \end{bmatrix} \quad \lambda_{abc} = \begin{bmatrix} \lambda_{as} \\ \lambda_{bs} \\ \lambda_{cs} \end{bmatrix} \quad (4.2)$$

Similarly, rotor voltage equations in terms of rotor variables can be written as

$$v_{abcr} = r_r i_{abcr} + \frac{d(\lambda_{abcr})}{dt} \quad (4.3)$$

where v_{abcr} , i_{abcr} and λ_{abcr} are the rotor voltages, and are 3×1 vectors defined by

$$v_{abcr} = \begin{bmatrix} v_{ar} \\ v_{br} \\ v_{cr} \end{bmatrix} \quad i_{abcr} = \begin{bmatrix} i_{ar} \\ i_{br} \\ i_{cr} \end{bmatrix} \quad \lambda_{abcr} = \begin{bmatrix} \lambda_{ar} \\ \lambda_{br} \\ \lambda_{cr} \end{bmatrix} \quad (4.4)$$

Referring all quantities to the stator of the machine, flux linkage equations in terms of the winding inductances and currents can be written as (Krause, 2002).

$$\begin{bmatrix} \lambda_{abcs} \\ \lambda'_{abcr} \end{bmatrix} = \begin{bmatrix} L_s & L'_{sr} \\ L'_{sr}{}^T & L_r \end{bmatrix} \begin{bmatrix} i_{abcs} \\ i'_{abcr} \end{bmatrix} \quad (4.5)$$

where

$$L_s = \begin{bmatrix} L_{ls} + L_{ms} & -\frac{1}{2}L_{ms} & -\frac{1}{2}L_{ms} \\ -\frac{1}{2}L_{ms} & L_{ls} + L_{ms} & -\frac{1}{2}L_{ms} \\ -\frac{1}{2}L_{ms} & -\frac{1}{2}L_{ms} & L_{ls} + L_{ms} \end{bmatrix} \quad (4.6)$$

$$L'_r = \begin{bmatrix} L'_{lr} + L_{ms} & -\frac{1}{2}L_{ms} & -\frac{1}{2}L_{ms} \\ -\frac{1}{2}L_{ms} & L'_{lr} + L_{ms} & -\frac{1}{2}L_{ms} \\ -\frac{1}{2}L_{ms} & -\frac{1}{2}L_{ms} & L'_{lr} + L_{ms} \end{bmatrix} \quad (4.7)$$

$$L'_{sr} = L_{ms} \begin{bmatrix} \cos \theta_r & \cos(\theta_r + \frac{2\pi}{3}) & \cos(\theta_r - \frac{2\pi}{3}) \\ \cos(\theta_r - \frac{2\pi}{3}) & \cos \theta_r & \cos(\theta_r + \frac{2\pi}{3}) \\ \cos(\theta_r + \frac{2\pi}{3}) & \cos(\theta_r - \frac{2\pi}{3}) & \cos \theta_r \end{bmatrix} \quad (4.8)$$

where

$$\theta_r = \int_0^t \omega_r dt + \theta_r(0) \quad (4.9)$$

and ω_r is the rotor speed in electrical radians per second.

In above equations, the stator leakage and magnetizing inductance are denoted by L_{ls} and L_{ms} , respectively. L_{lr} is the leakage inductance of rotor windings. The inductance L_{ms} is also the amplitude of the mutual inductance between stator and rotor windings as rotor equations are referred to the stator (Krause, 2002).

4.1.1 Voltage Equations in $qd0$ Reference Frame

The voltage equations of stator and rotor in abc variables, are transferred to the arbitrary $qd0$ reference frame by using the following transformations (Krause, 2002).

$$\begin{bmatrix} f_{qs} \\ f_{ds} \\ f_{0s} \end{bmatrix} = K_s \begin{bmatrix} f_{as} \\ f_{bs} \\ f_{cs} \end{bmatrix} \quad (4.10)$$

$$\begin{bmatrix} f_{qr} \\ f_{dr} \\ f_{0r} \end{bmatrix} = K_r \begin{bmatrix} f_{ar} \\ f_{br} \\ f_{cr} \end{bmatrix} \quad (4.11)$$

where the symbol f is used to represent the three phase stator and rotor variables such as voltages, currents and flux linkages (Krause, 2002).

The transformation matrices K_s and K_r are

$$K_s = \frac{2}{3} \begin{bmatrix} \cos \theta & \cos(\theta - \frac{2\pi}{3}) & \cos(\theta + \frac{2\pi}{3}) \\ \sin \theta & \sin(\theta - \frac{2\pi}{3}) & \sin(\theta + \frac{2\pi}{3}) \\ \frac{1}{2} & \frac{1}{2} & \frac{1}{2} \end{bmatrix} \quad (4.12)$$

$$K_r = \frac{2}{3} \begin{bmatrix} \cos \beta & \cos(\beta - \frac{2\pi}{3}) & \cos(\beta + \frac{2\pi}{3}) \\ \sin \beta & \sin(\beta - \frac{2\pi}{3}) & \sin(\beta + \frac{2\pi}{3}) \\ \frac{1}{2} & \frac{1}{2} & \frac{1}{2} \end{bmatrix} \quad (4.13)$$

where

$$\theta = \int_0^t \omega(\tau) d\tau + \theta(0) \quad (4.14)$$

and

$$\beta = \theta - \theta_r \quad (4.15)$$

Finally, the voltage equations in arbitrary reference frame by using the above transformations are obtained as

$$v_{qs} = r_s i_{qs} + \omega \lambda_{ds} + p \lambda_{qs} \quad (4.16)$$

$$v_{ds} = r_s i_{ds} - \omega \lambda_{qs} + p \lambda_{ds} \quad (4.17)$$

$$v_{qr}' = r_r i_{qr}' + (\omega - \omega_r) \lambda_{dr}' + p \lambda_{qr}' \quad (4.18)$$

$$v_{dr}' = r_r i_{dr}' - (\omega - \omega_r) \lambda_{qr}' + p \lambda_{dr}' \quad (4.19)$$

where the symbol p represents the derivative operator $\left(\frac{d}{dt}\right)$. It must be noted that the rotor parameters are referred to the stator side and the zero sequence equations are omitted since the conditions in the machine are assumed to be balanced.

The flux linkages are expressed as

$$\lambda_{qs} = L_{ls}i_{qs} + L_m(i_{qs} + i'_{qr}) \quad (4.20)$$

$$\lambda_{ds} = L_{ls}i_{ds} + L_m(i_{ds} + i'_{dr}) \quad (4.21)$$

$$\lambda'_{qr} = L_{lr}i'_{qr} + L_m(i_{qs} + i'_{qr}) \quad (4.22)$$

$$\lambda'_{dr} = L_{lr}i'_{dr} + L_m(i_{ds} + i'_{dr}) \quad (4.23)$$

where $L_m = \frac{3}{2}L_{ms}$

Substituting $\lambda_{qd} = \frac{\psi_{qd}}{\omega_b}$ in the equations (4.16) - (4.19), they can be written in

terms of flux linkages per second as

$$v_{qs} = r_s i_{qs} + \frac{\omega}{\omega_b} \psi_{ds} + \frac{p}{\omega_b} \psi_{qs} \quad (4.24)$$

$$v_{ds} = r_s i_{ds} - \frac{\omega}{\omega_b} \psi_{qs} + \frac{p}{\omega_b} \psi_{ds} \quad (4.25)$$

$$v'_{qr} = r_r i'_{qr} + \frac{(\omega - \omega_r)}{\omega_b} \psi'_{dr} + \frac{p}{\omega_b} \psi'_{qr} \quad (4.26)$$

$$v'_{dr} = r_r i'_{dr} - \frac{(\omega - \omega_r)}{\omega_b} \psi'_{qr} + \frac{p}{\omega_b} \psi'_{dr} \quad (4.27)$$

where ω_b is the base electrical angular velocity and ψ is the flux linkages in per second, which are expressed as

$$\Psi_{qs} = x_{ls} i_{qs} + x_m (i_{qs} + i_{qr}') \quad (4.28)$$

$$\Psi_{ds} = x_{ls} i_{ds} + x_m (i_{ds} + i_{dr}') \quad (4.29)$$

$$\Psi_{qr}' = x_{lr}' i_{dr}' + x_m (i_{qs} + i_{qr}') \quad (4.30)$$

$$\Psi_{dr}' = x_{lr}' i_{dr}' + x_m (i_{ds} + i_{dr}') \quad (4.31)$$

By using equations (4.24) - (4.27) the q and d axis equivalent circuits can be obtained as shown in Figure 4.1.

4.1.2 Modeling of Induction Machine in the Stationary Reference Frame

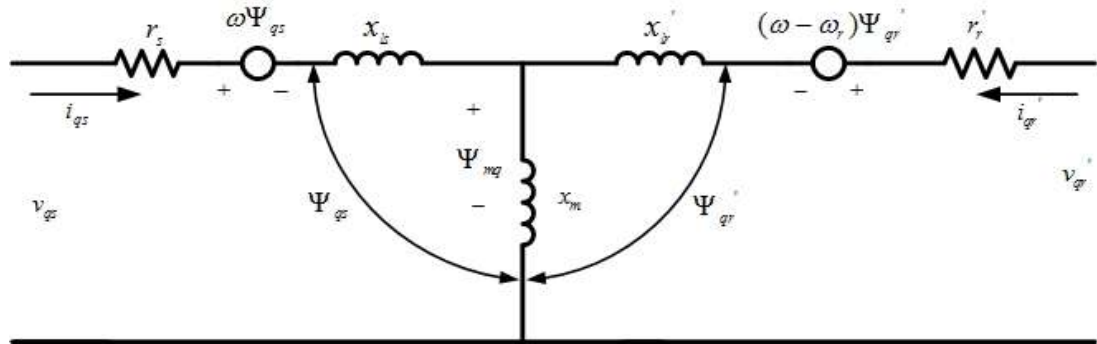
In the stationary reference frame, the speed of the rotating frame is $\omega = 0$. Thus, the voltage equations can be written as

$$v_{qs} = r_s i_{qs} + \frac{p}{\omega_b} \psi_{qs} \quad (4.32)$$

$$v_{ds} = r_s i_{ds} + \frac{p}{\omega_b} \psi_{ds} \quad (4.33)$$

$$v_{qr}' = r_r i_{qr}' - \frac{\omega_r}{\omega_b} \psi_{dr}' + \frac{p}{\omega_b} \psi_{qr}' \quad (4.34)$$

$$v_{dr}' = r_r i_{dr}' + \frac{\omega_r}{\omega_b} \psi_{qr}' + \frac{p}{\omega_b} \psi_{dr}' \quad (4.35)$$



(a)

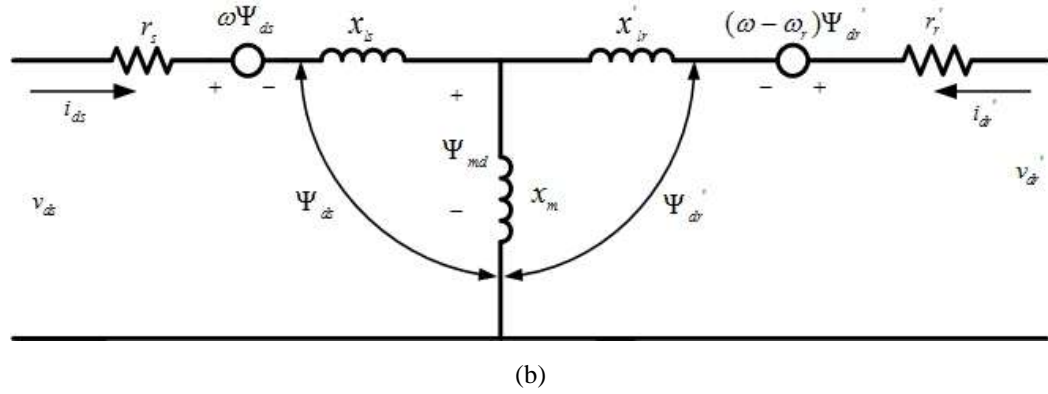


Figure 4.1 Equivalent circuits for a three phase induction machine in arbitrary reference frame (a) q-axis circuit and (b) d-axis circuit

From Figure 4.1, by neglecting the effects of saturation the stator and rotor flux linkages per second can be written as (Ong, 1998).

$$\Psi_{qs} = x_{ls} i_{qs} + \Psi_{mq} \quad (4.36)$$

$$\Psi_{ds} = x_{ls} i_{ds} + \Psi_{md} \quad (4.37)$$

$$\Psi_{qr} = x_{lr}' i_{qr}' + \Psi_{mq} \quad (4.38)$$

$$\Psi_{dr} = x_{lr}' i_{dr}' + \Psi_{md} \quad (4.39)$$

From above equations, the stator and rotor currents can be obtained as

$$i_{qs} = \frac{\Psi_{qs} - \Psi_{mq}}{x_{ls}} \quad (4.40)$$

$$i_{ds} = \frac{\Psi_{ds} - \Psi_{md}}{x_{ls}} \quad (4.41)$$

$$i_{qr}' = \frac{\Psi_{qr}' - \Psi_{mq}}{x_{lr}'} \quad (4.42)$$

$$i_{dr}' = \frac{\Psi_{dr}' - \Psi_{md}}{x_{lr}'} \quad (4.43)$$

By substituting equations (4.40) – (4.43) into (4.32) – (4.35), the flux linkages per second can be expressed as follows (Barrado, Grino & Valderrama, 2007; Ong, 1998).

$$\Psi_{qs} = \omega_b \int \left\{ v_{qs} + \frac{r_s}{x_{ls}} (\Psi_{mq} - \Psi_{qs}) \right\} dt \quad (4.44)$$

$$\Psi_{ds} = \omega_b \int \left\{ v_{ds} + \frac{r_s}{x_{ls}} (\Psi_{md} - \Psi_{ds}) \right\} dt \quad (4.45)$$

$$\Psi'_{qr} = \omega_b \int \left\{ v'_{qr} - \frac{\omega_r}{\omega_b} \Psi'_{dr} + \frac{r'_r}{x'_{lr}} (\Psi_{mq} - \Psi'_{qr}) \right\} dt \quad (4.46)$$

$$\Psi'_{dr} = \omega_b \int \left\{ v'_{dr} - \frac{\omega_r}{\omega_b} \Psi'_{qr} + \frac{r'_r}{x'_{lr}} (\Psi_{md} - \Psi'_{dr}) \right\} dt \quad (4.47)$$

where the mutual flux in linear region is

$$\Psi_{mq} = x_m (i_{qs} + i'_{dr}) \quad (4.48)$$

$$\Psi_{md} = x_m (i_{ds} + i'_{qr}) \quad (4.49)$$

By substituting (4.40) – (4.43) into (4.48) and (4.49), the mutual flux linkage in q and d axes can be written as

$$\Psi_{mq} = X_M \left(\frac{\Psi_{qs}}{x_{ls}} + \frac{\Psi'_{qr}}{x'_{lr}} \right) \quad (4.50)$$

$$\Psi_{md} = X_M \left(\frac{\Psi_{ds}}{x_{ls}} + \frac{\Psi'_{dr}}{x'_{lr}} \right) \quad (4.51)$$

where

$$\frac{1}{X_M} = \frac{1}{x_m} + \frac{1}{x_{ls}} + \frac{1}{x'_{lr}} \quad (4.52)$$

Finally, the motor motion and electromagnetic torque equations of the induction motor can be written as

$$J \frac{d\omega_r}{dt} = T_{em} - T_{mech} - T_{damp} \quad (4.53)$$

$$T_{em} = \frac{3}{2} \frac{P}{2\omega_b} (\Psi_{ds} i_{qs} - \Psi_{qs} i_{ds}) \quad (4.54)$$

where

$$T_{damp} = B \times \omega_r \quad (4.55)$$

and T_{mech} is the mechanical torque applied to the shaft of the machine.

In experimental setup, the combined moment of inertia of the driving dc motor and induction generator setup is $J=0.042 \text{ kg.m}^2$ and the friction coefficient of the drive train is $B= 0.006 \text{ Nm.s/rad}$. These values are used in simulations.

4.1.3 Saturation Model

Saturation of iron in induction machine affects the mutual and leakage flux. In the analysis of the machine, the magnetizing reactance will be assumed the only affected element by the saturation. Therefore, the main factor in induction machine analysis is determining its magnetizing inductance (Ong, 1998).

The magnetizing inductance is obtained by the no-load motor test, by driving induction motor speed close to synchronous speed (i.e. $S \approx 0$) and measure the variable applied voltage and resulting stator current. Magnetizing reactance of machine can be calculated from

$$x_m = \frac{E_g}{I_m} \quad (4.56)$$

where E_g is the air gap voltage and its value will be assumed the applied voltage to the terminal of machine and I_m is the stator current when the value of slip (s) in the rotor side is zero because the rotor rotates nearly at synchronous speed.

The effect of the saturation is same in both q and d axes. Therefore, by using Figure 4.2, the reduction of flux linkages per second in q and d axes can be expressed as (Ong, 1998).

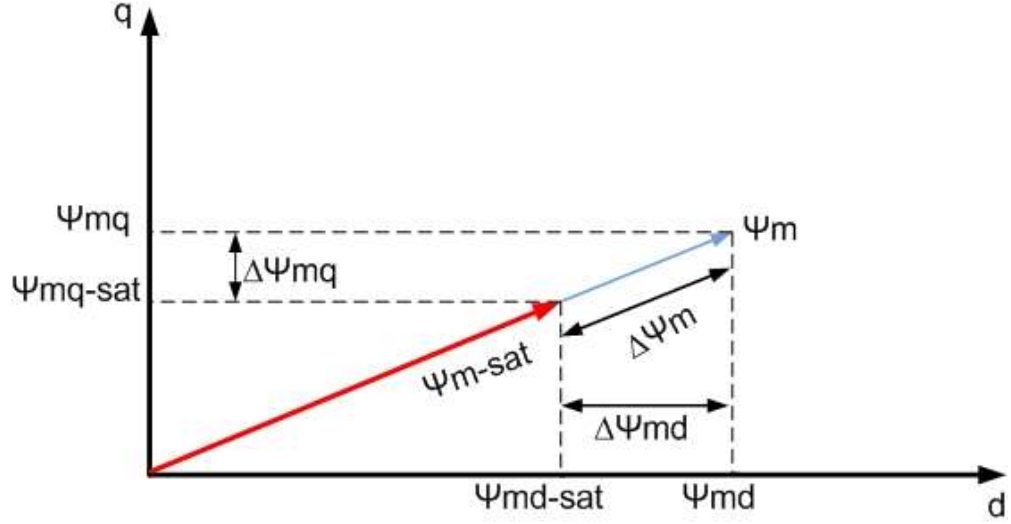


Figure 4.2 Illustration of saturation in d-q components

$$\Psi_{mq}^{sat} = \Psi_{mq} - \Delta\Psi_{mq} \quad (4.57)$$

$$\Psi_{md}^{sat} = \Psi_{md} - \Delta\Psi_{md} \quad (4.58)$$

By using equations (4.50) and (4.51), the saturated value of the q and d axis mutual flux linkage can be written as

$$\Psi_{mq}^{sat} = X_M \left(\frac{\Psi_{qs}}{x_{ls}} + \frac{\Psi'_{qr}}{x'_{lr}} - \frac{\Delta\Psi_{mq}}{x_{m-uns}} \right) \quad (4.59)$$

$$\Psi_{md}^{sat} = X_M \left(\frac{\Psi_{ds}}{x_{ls}} + \frac{\Psi'_{dr}}{x'_{lr}} - \frac{\Delta\Psi_{md}}{x_{m-uns}} \right) \quad (4.60)$$

where x_{m-uns} is the value of the unsaturated magnetizing reactance.

The relationship between $\Delta\Psi_m$ and $\Delta\Psi_{mq}$, $\Delta\Psi_{md}$ can be written from Figure 4.2, such that

$$\Delta\Psi_{md} = \frac{\Psi_{md}^{sat}}{\Psi_m^{sat}} \Delta\Psi_m \quad (4.61)$$

$$\Delta\Psi_{mq} = \frac{\Psi_{mq}^{sat}}{\Psi_m^{sat}} \Delta\Psi_m \quad (4.62)$$

$$\Delta\Psi_m = \sqrt{(\Psi_{mq}^{sat})^2 + (\Psi_{md}^{sat})^2} \quad (4.63)$$

The amount of decrease in the mutual flux linkage per second ($\Delta\Psi_m$) due to saturation can be determined from the saturation curve of the machine. Figure 4.3 shows the 1.1 kW induction machine's saturation curve, which is obtained experimentally in the laboratory. As shown in Figure 4.4, the reduction in flux linkage per second ($\Delta\Psi_m$) can be determined by obtaining the difference between saturation curve and linear air gap line (Ong, 1998). The saturation characteristics of induction machine were obtained using the calculations below and shown in Table 4.1, which is defined as a look up table in computer simulations.

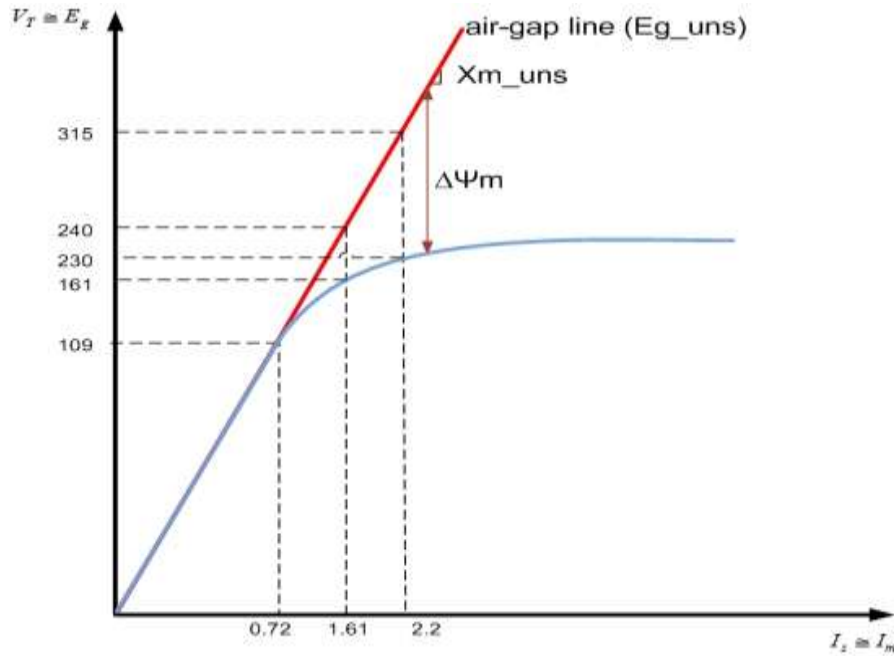


Figure 4.3 Saturation curve of the 1.1kW induction machine

$$x_{m-uns} = \frac{E_{g-uns}}{I_m} = \frac{109}{0.72} = 151\Omega \quad (4.64)$$

the value of I_m is equal to the stator current and is obtained from no-load test.

$$\Delta\Psi_m = E_{g-ims} - E_g \quad (4.65)$$

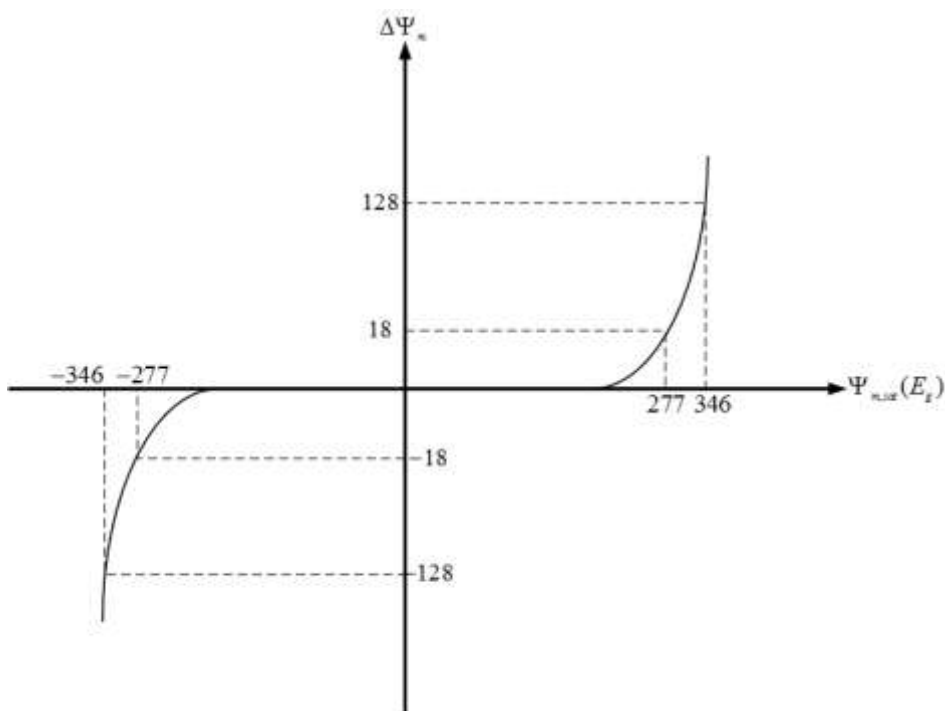


Figure 4.4 Saturation characteristics of the 1.1kW induction machine

Table 4.1 Saturation characteristics of the 1.1kW induction machine defined in the lookup table.

E_g (V)	86	117	148	178	233	277	319	328	346
$\Delta\Psi_m$ (V)	0	0	0	6	10.5	18	61	91	128

4.2 Simulation Model of Induction Motor in MATLAB/SIMULINK

In order to verify the experimental results for motoring operation, the machine model including saturation was constructed in MATLAB/SIMULINK using equations (4.32) – (4.63). Figure 4.5 shows a complete diagram of an induction motor in stationary reference frame. The details of main blocks are shown in Figure

4.6(a), 4.6(b), Figure 4.7 and Figure 4.8. Figure 4.6(a), 4.6(b) show the implementation of equations in both q and d axis circuits of three phase induction machine. The equations (4.40) – (4.43) and (4.44) - (4.47) are implemented in the induction machine sub-block.

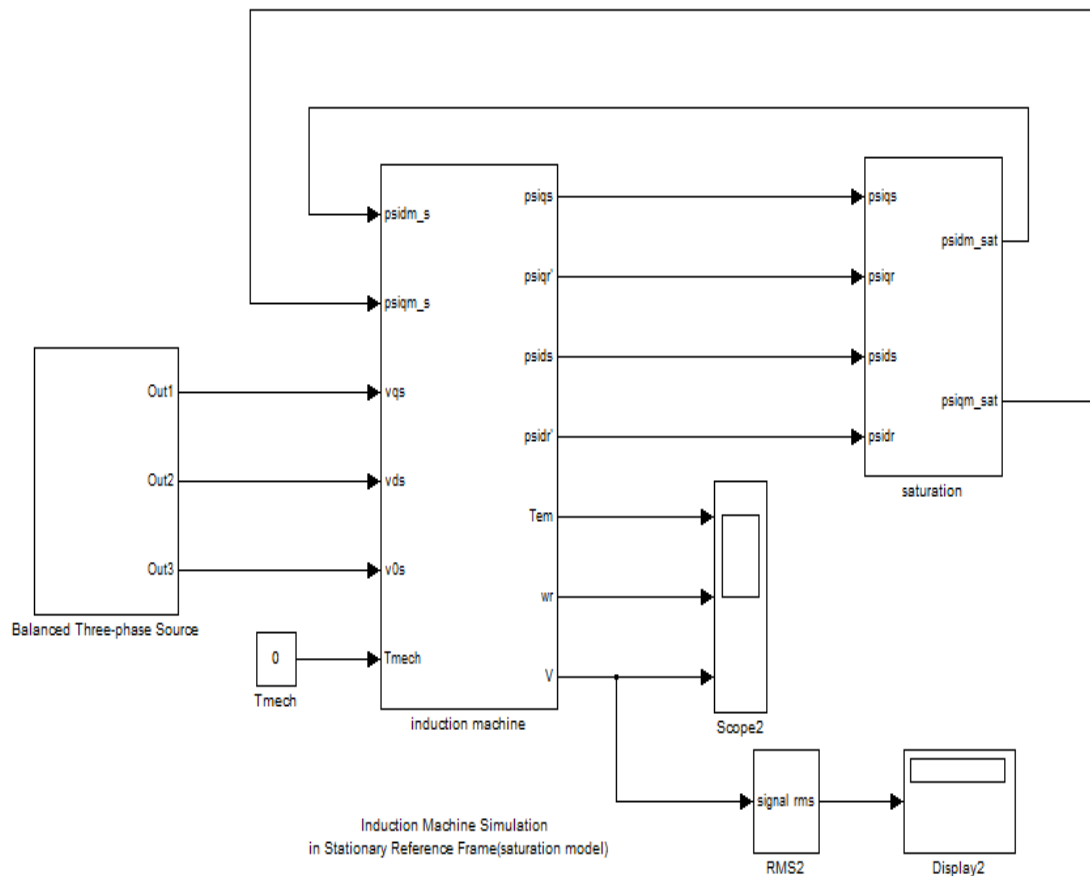
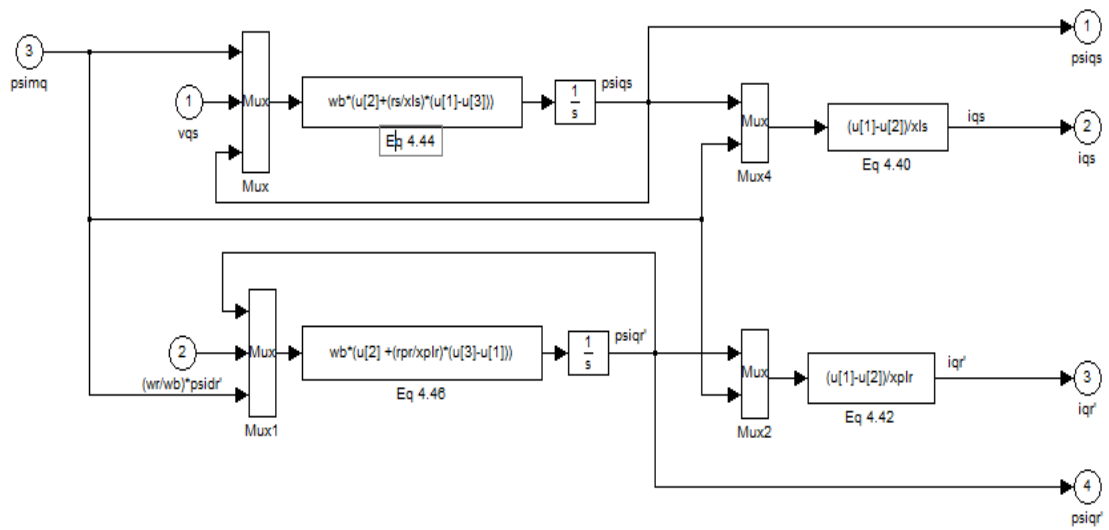
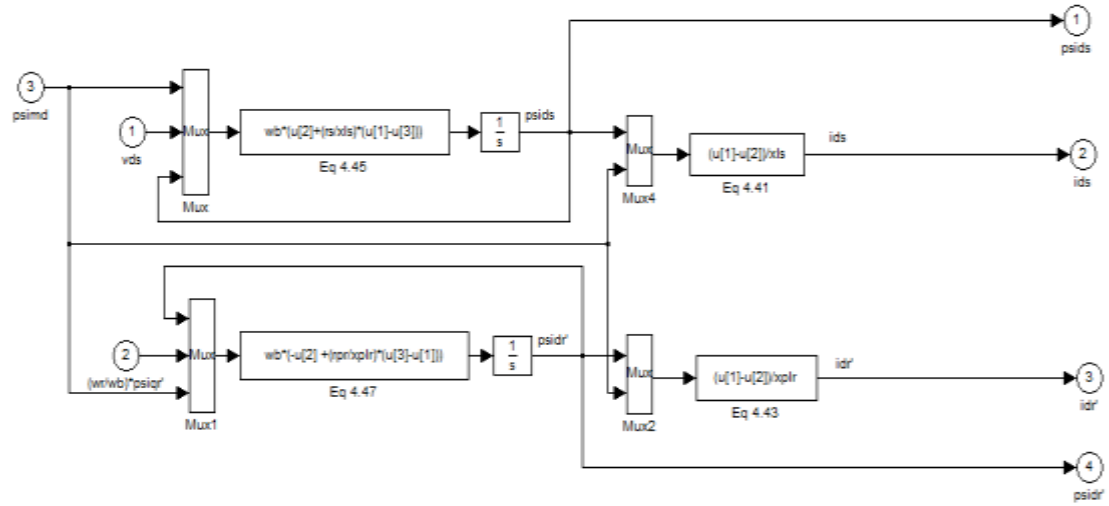


Figure 4.5 MATLAB/SIMULINK simulation model of induction motor



(a)



(b)

Figure 4.6 Simulation model of q and d- axis equivalent circuit

Figure 4.7 shows the simulation model of rotor of induction motor given in equation (4.53) - (4.55). When T_{mech} is negative the machine will be generating and in the motoring mode it will be positive. Finally, the saturation model of induction motor given in equations (4.57) – (4.63) is shown in Figure 4.8.

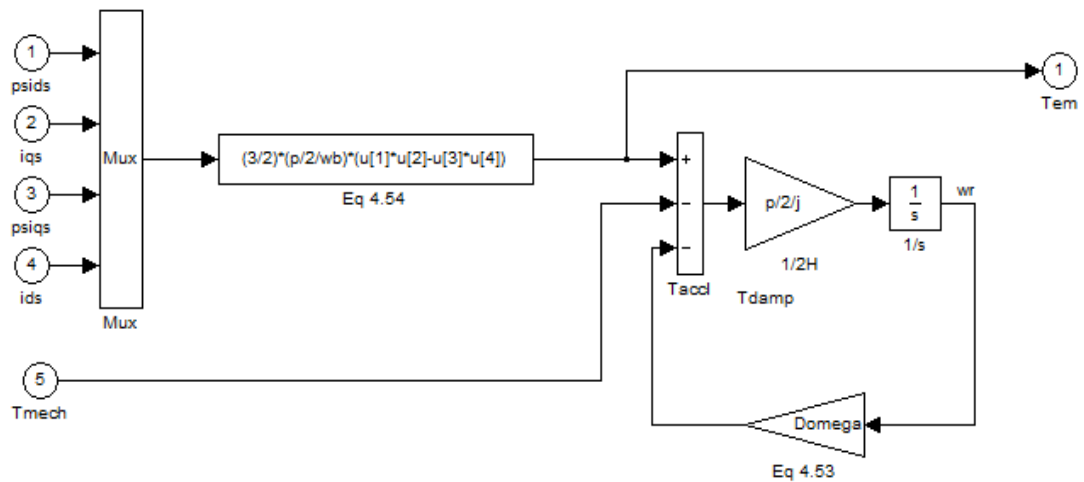


Figure 4.7 Simulation model of motor motion and electromagnetic torque

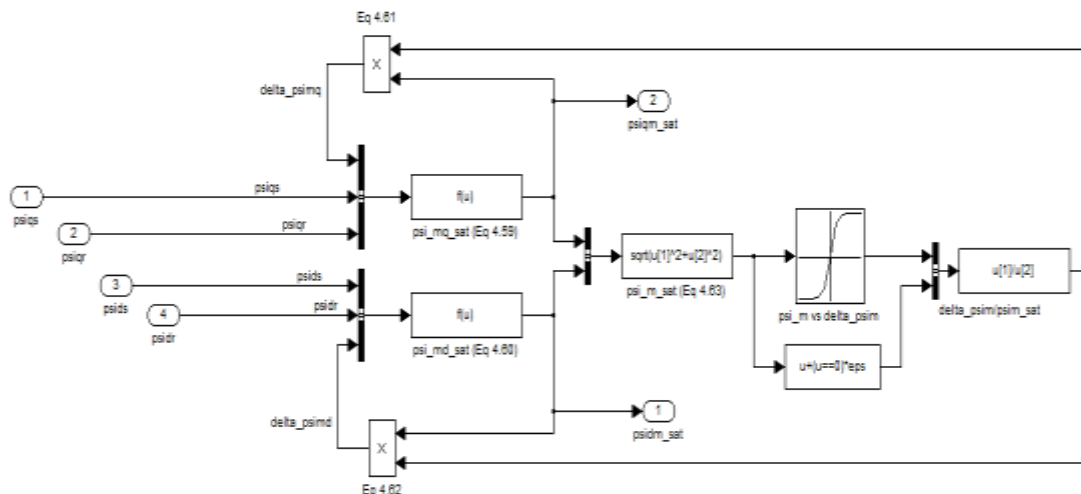


Figure 4.8 Simulation model of mutual flux saturation

4.2.1 Comparison of Simulation and Experimental Results of Induction Motor

In order to verify the machine model, simulation and experimental results of the induction machine during free acceleration are compared. Figure 4.9 shows the startup speed response of induction motor obtained from both simulation and experimental. It can be seen from Figure 4.9 that the results in both experiment and simulation are close. When the machine is starting in standstill, and when it is unloaded, the simulation and experimental speed reaches to synchronous speed (1500 rpm) approximately in 0.6 sec.

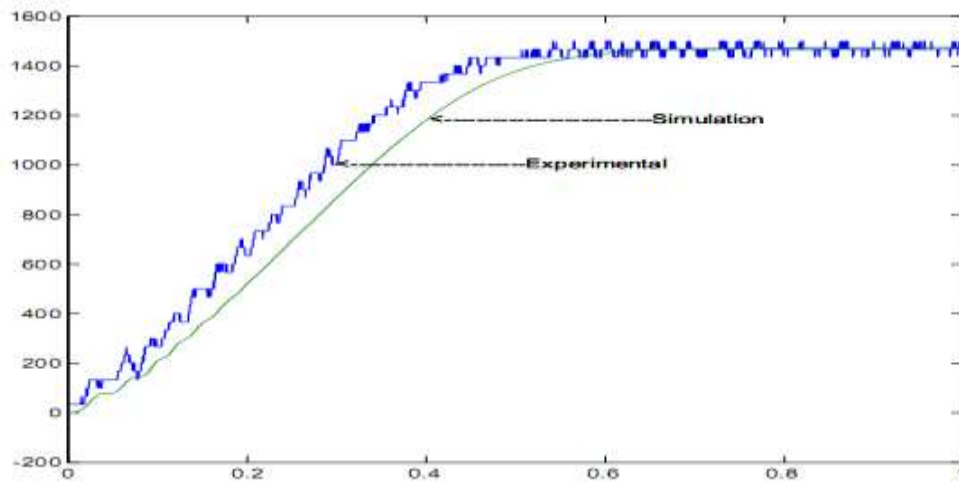


Figure 4.9 Rotor speed (RPM) response of induction motor during free acceleration test

Figure 4.10 shows the stator current of induction motor obtained from both simulation and experiment. It can be seen that, the value of stator current in experiment at the transient time is higher than that of the simulation results. In the simulations, it is assumed that the only magnetizing reactance is affected by the saturation. However, the stator and rotor leakage reactance are also affected by the saturation due to high currents at startup. As a result of the decrease in leakage reactance due to saturation, the stator currents increase. It can be seen that at $t=0.5$ sec the machine stator current decreases to the no-load value in both simulation and experiment.

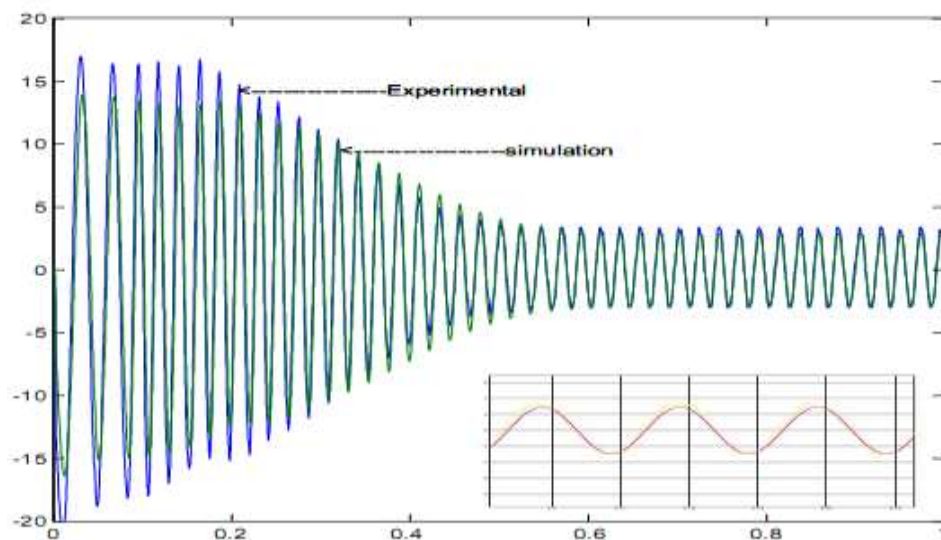


Figure 4.10 Stator current (A) of induction motor during free acceleration test

4.3 Dynamical Model of Fixed Capacitor Self Excited Induction Generator

In the previous section, the induction motor had been analyzed in q-d axes and the simulation of this machine explained. In this section, the dynamical model of self-excited induction generator will be studied. Figure 4.11 shows the self excited induction generator equivalent circuits in q and d axes with the capacitor and resistive load connected to the stator of machine.

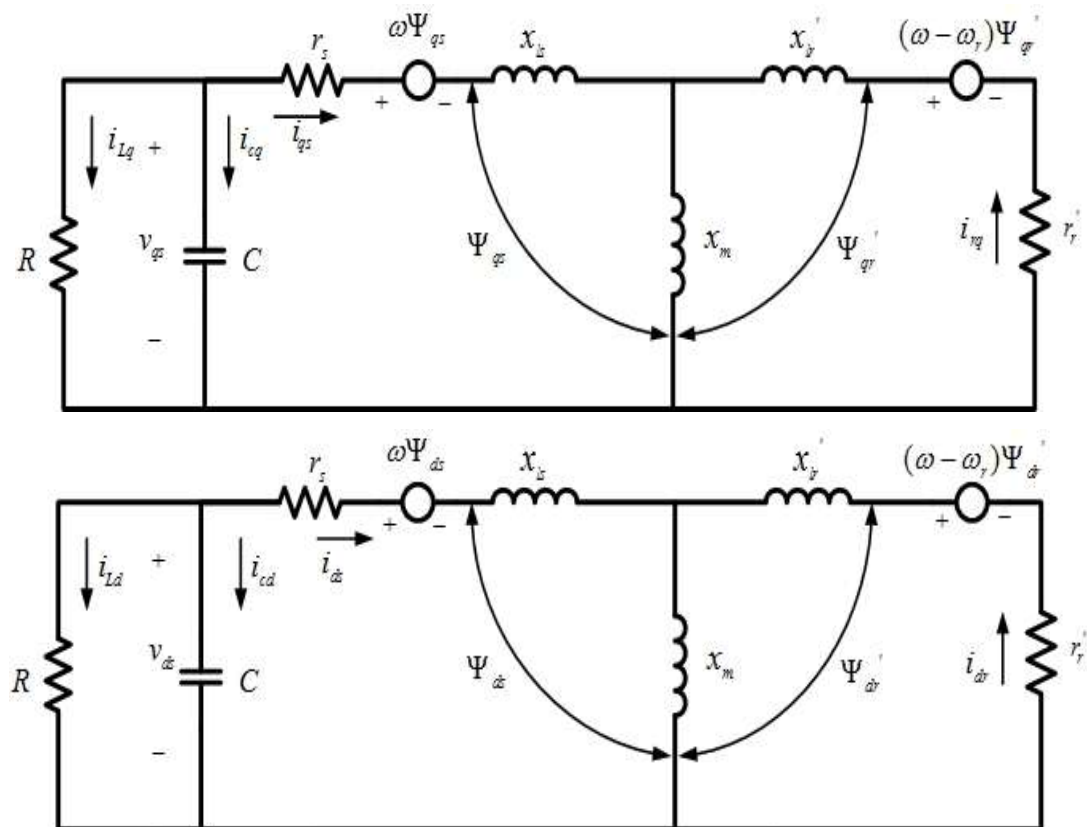


Figure 4.11 q and d axis equivalent circuits of fixed capacitor self excited induction generator

When compared to induction motor model, the differences in the SEIG model are the rotor speed, which is determined by the prime mover and the stator voltage equations, which are determined by the capacitor bank. In this case, the current of capacitor and the stator terminal voltage of SEIG can be expressed by using following equations, (Avinash & Kumar, 2006; Kishore & Kumar, 2006; Seyoum, Grantham & Rahman, 2001):

$$i_{cq} = -(i_{qs} + i_{Lq}) \quad (4.66)$$

$$i_{cd} = -(i_{ds} + i_{Ld}) \quad (4.67)$$

It can be seen from Figure 4.11, that the capacitor (and also load) voltages are equal to the stator phase voltages. Therefore, the capacitor voltages can be expressed as

$$v_{qs} = \int \frac{1}{C} (-i_{qs} - i_{Lq}) dt \quad (4.68)$$

$$v_{ds} = \int \frac{1}{C} (-i_{ds} - i_{Ld}) dt \quad (4.69)$$

Finally, the load currents are expressed as

$$i_{Lq} = \frac{V_{qs}}{R} \quad (4.70)$$

$$i_{Ld} = \frac{V_{ds}}{R} \quad (4.71)$$

Figure 4.12 shows the stator voltages of SEIG in q-d stationary reference frame, which are implemented by using equations (4.69) – (4.72).

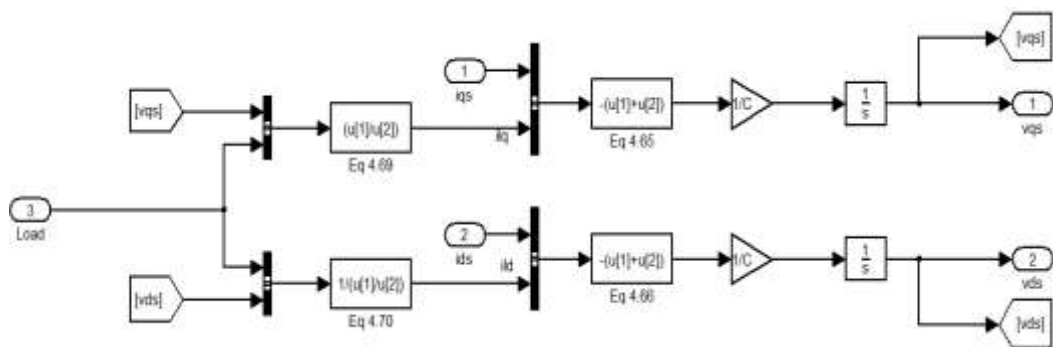


Figure 4.12 Simulation model of SEIG with fixed capacitor and load

Figure 4.13 shows the computer simulation model of constant-speed fixed capacitor self-excited induction generator. The saturation curve in both motoring and generating mode is the same.

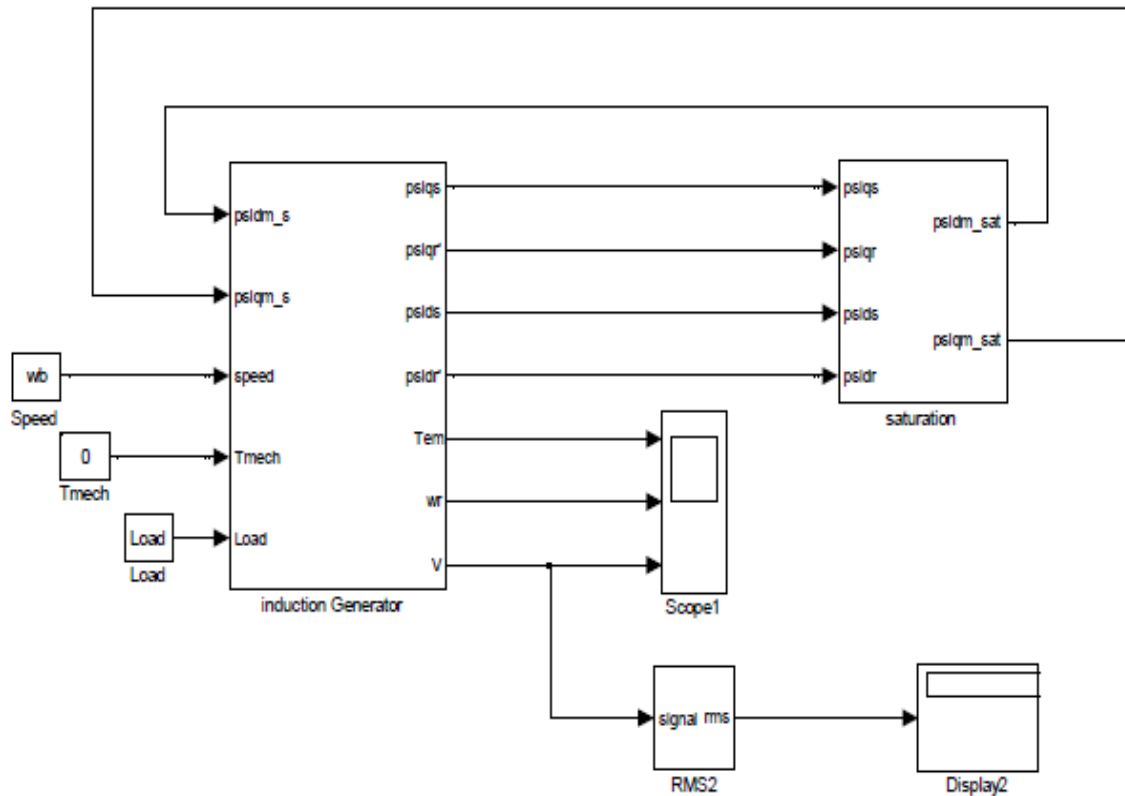


Figure 4.13 Simulation model of self excited induction generator

4.3.1 Comparison of Simulation Results with Experimental and Steady-State Analysis Results of SEIG

In laboratory setup, in order to drive the rotor of SEIG in constant speed, a DC motor driven by a four quadrant dc motor drive was used. The simulation results of SEIG voltage build-up are verified by experiment. Also, the results of dynamic simulations are verified by the results obtained from steady-state analysis.

Table 4.2 shows the results of experiment, steady state analysis and dynamical analysis in constant speed operating mode of SEIG. As it can be seen from this table, all results are in close agreement with each other.

Table 4.2 Comparison of experimental, steady state and simulation results at constant speed operation

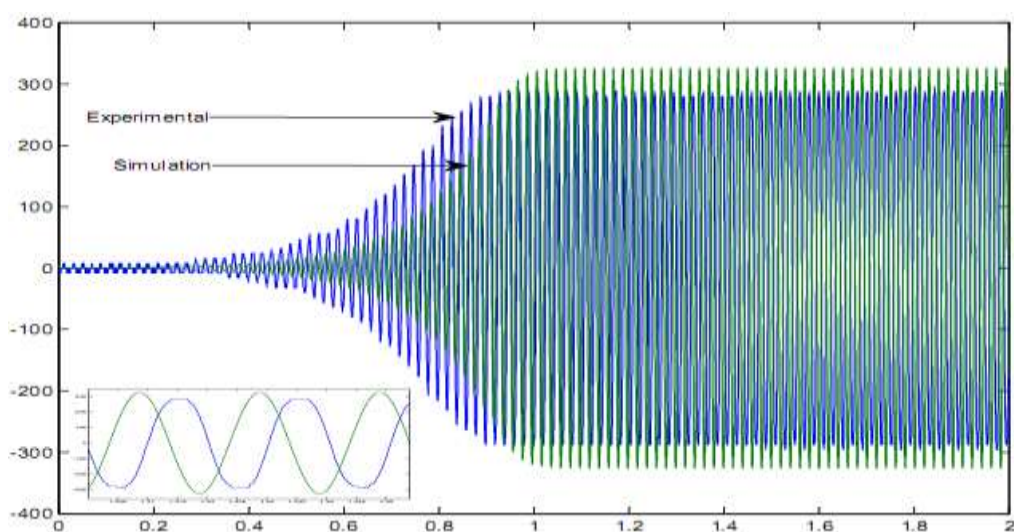
Operation	Load (Ω)	Stator Voltage (V)	Load Current (A)	Stator Frequency (Hz)
Experimental Results	∞	230	0	50
	384	200	0.52	48.9
	288	190	0.66	48.6
	192	157	0.82	48.1
	160	131	0.81	47.6
Steady-State Analysis Result	∞	230	0	50
	384	195	0.5	48.5
	288	185	0.64	48.1
	192	150	0.78	47.5
	160	133	0.83	47.2
Dynamic Results	∞	230	0	50
	384	202	0.52	48.5
	288	193	0.67	48.2
	192	160	0.83	47.6
	160	131	0.81	47.5

The stator voltage values are decreased by increasing the load. The dynamic model's results are closer to the experimental results.

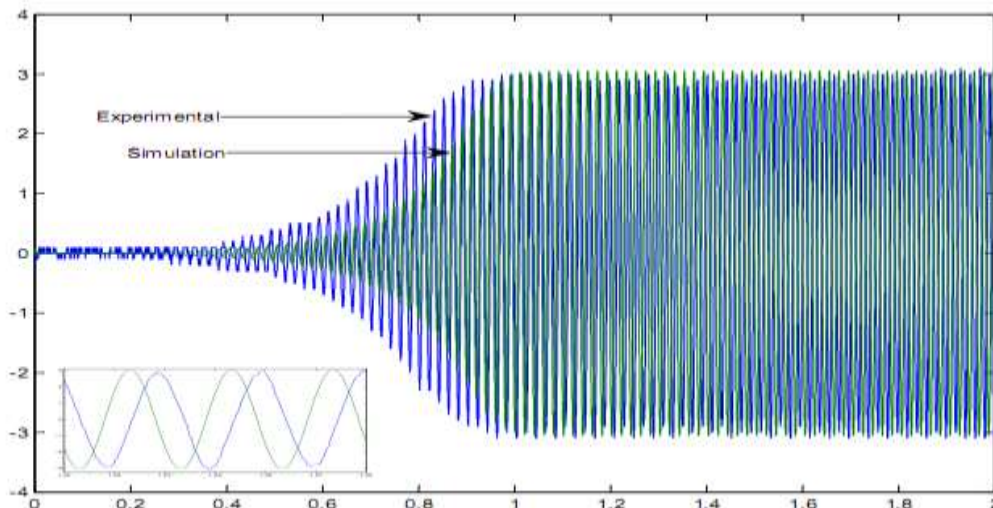
4.3.1.1 Voltage Buildup under No-Load

In order to verify the dynamic performance of the machine, results of experimental laboratory setup and simulation are compared. Excitation under no-load process is provided by employing a three phase balanced capacitor and driving the shaft of the machine at a constant speed by a dc motor fed from a four quadrant dc motor drive.

Figure 4.14(a) and 4.14(b) shows the experimental and simulation results of voltage and current build-up under no-load condition, respectively. In Figure 4.14(a), the magnitude of the generated voltage in simulation is higher than the experimental results. In experiments, the waveform of the generated voltage is flattened due to saturation and contain 3rd harmonic dominantly, therefore, there is a difference in magnitude between the experimental and simulation results. But, in both of them, the measured voltage in RMS is equal to 230 volts. Also, the magnitudes of stator current in both simulation and experiment are closer as shown in Figure 4.14 (b). When generator is driven at a constant speed (1500 rpm) and it is excited with a three phase capacitor bank ($C=30 \mu\text{F}$), the value of generated voltage attains its steady state value of 230 volts (RMS) at 1 sec. The magnitude and frequency of generated voltage in both simulation and experiment are close to each other.



(a)



(b)

Figure 4.14 Voltage and current build up of SEIG in simulation and experiment. (a) stator voltage (V) build-up and zoomed view (b) stator current (A) build-up and zoomed view

4.3.1.2 Load Variation after Full Excitation

When the machine's speed is constant, any variation in the connected load affects the terminal voltage of SEIG. In order to simulate this operation, in the first time the machine excited under no load, then at $t=1.3$ sec, a 400 ohms load is connected to the terminal of SEIG. At $t=1.7$ sec, by connecting a 144 ohms load to the stator terminal of SEIG, the terminal voltage is collapsed. This process is illustrated in figure 4.15.

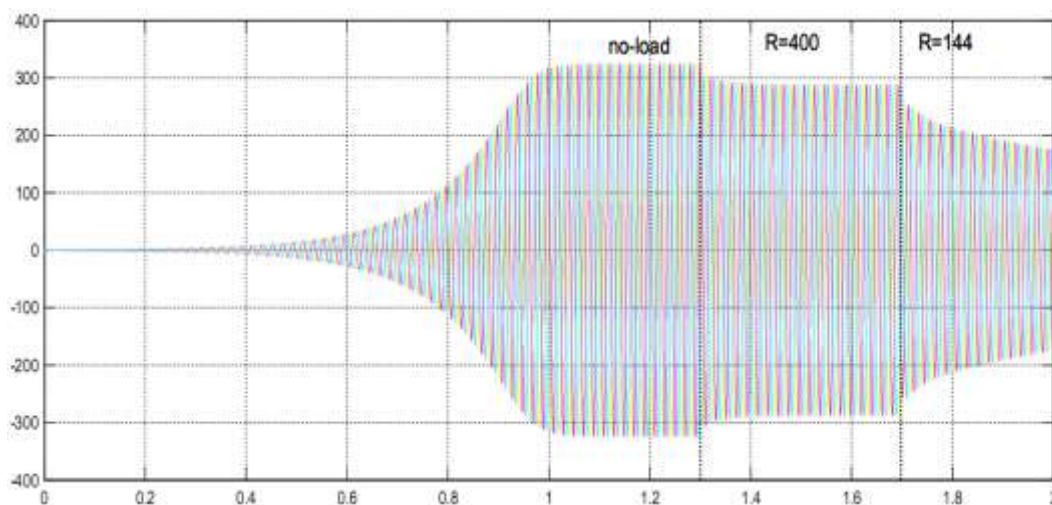


Figure 4.15 Stator voltage variation under different load values

CHAPTER FIVE

MODELING OF VOLTAGE REGULATION METHODS FOR STAND-ALONE SELF EXCITED INDUCTION GENERATOR

In this chapter, terminal voltage regulation methods of stand-alone SEIG are studied through simulations. In order to regulate the voltages on the stator terminals of SEIG, different kinds of circuits are examined. These are (a) variable capacitor bank, (b) voltage source inverter (VSI) and (C) STATCOM. The dynamic performances of the SEIG and controller are tested by applying load variations in computer simulations.

5.1 Voltage Regulation by using Variable Capacitor Bank

In order to control the generated voltage on the terminal of SEIG, there is variety of VAR generators. Some methods have been used such as connecting variable capacitors bank in series with the connected load and the stator. Unfortunately, this scheme limits the capability of the control (Saffar, Nho & Lipo, 1998). Also, regulation of terminal voltage is possible by adding more capacitor bank to the stator that is called shunt voltage regulation, as shown in Figure 5.1. This voltage regulation method is able to generate leading reactive power. The disadvantage of this method is step variation of the terminal voltage (Saffar, Nho & Lipo, 1998).

The control scheme is designed such that the magnitude of the generated voltage is sensed and compared with a reference voltage. If the magnitude of the generated voltage drops down to a specific value, the additional capacitor bank will be switched on.

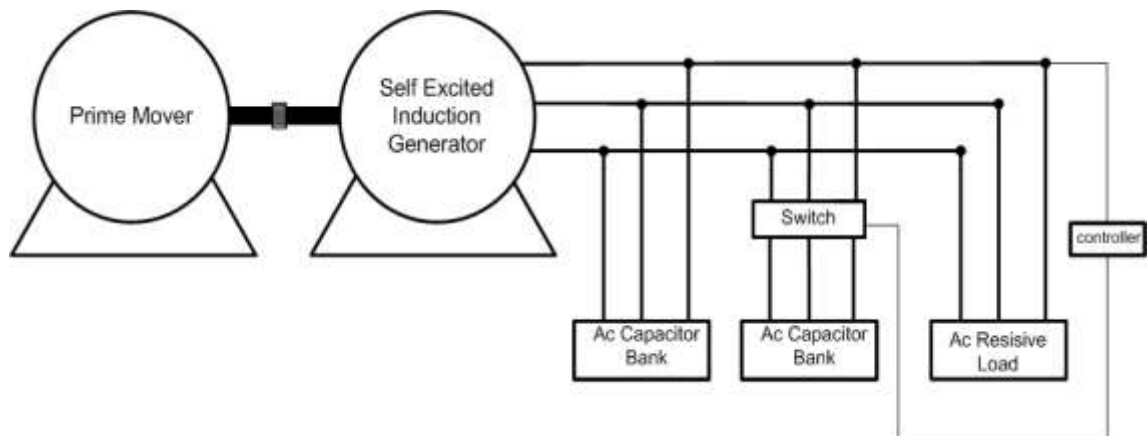


Figure 5.1 Excitation and regulation of the terminal voltage by using variable capacitor bank

5.1.1 Simulation Model of Voltage Regulation by Variable Capacitor Bank

By connecting 30 μF capacitor bank to the stator of SEIG, the generated voltage by the machine at no-load is nearly 230 volts in RMS. By changing the resistive load from infinite to 384 ohms, the generated voltage decreases from 230 to 202 volts. In order to restore the terminal voltage to its original value, capacitor value must be changed from 30 μF to 35 μF . In simulations, the load is modeled as R and RL. Figure 5.2 shows the simulation model of voltage regulation by variable capacitor bank implemented in MATLAB/SIMULINK.

The induction generator with saturation and capacitor excitation blocks were explained in Chapter 4. An additional control block was built by using an If Function and an If Action Subsystem to adjust the shunt capacitor value. For control purpose, the magnitude of the generated voltage can be obtained from q-d components as follows:

$$V_s = \sqrt{V_{qs}^2 + V_{ds}^2} \quad (5.1)$$

where V_s is the peak magnitude of the terminal voltage. The controller adds suitable capacitor bank when the magnitude of the generated voltage drops down below 290 Volts.

5.1.2 Simulation Results of using Variable Capacitor Bank

Variation of the stator frequency and terminal voltage by changing the load is shown in Figure 5.2 and Figure 5.3, respectively. It can be seen from Figure 5.2 that at no-load time the value of frequency is nearly 49.8 Hz. The stator frequency is decreased to 48.5 Hz when the load value is increased to 384 ohms at $t=1.3$ sec. From Figure 5.3, it can be seen that the generated voltage after connecting 384 ohms load at $t=1.3$ sec is reduced to 202 volts in RMS. The proper capacitor bank ($35\mu\text{F}$) is switched on if the magnitude of the terminal voltage drops down to the specific value (202 in RMS). After switching on the additional capacitor bank, the value of generated voltage attains its original value of 230 volts at 1.4 sec.

At $t=1.7$ sec, RL ($R=288$ and $L=800\text{mh}$) load is connected. In this case, the reactive power demand of the load is increased. Therefore, in order to keep the terminal voltage in a constant value the value of connected capacitor is increased to $39.5\mu\text{F}$, that cause the generated voltage attains its original value again.

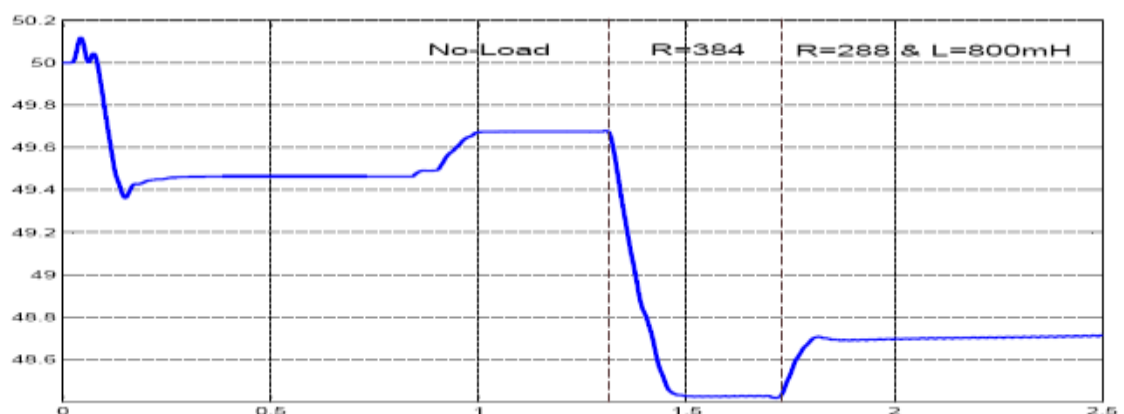


Figure 5.2 Variation of the stator frequency (Hz)

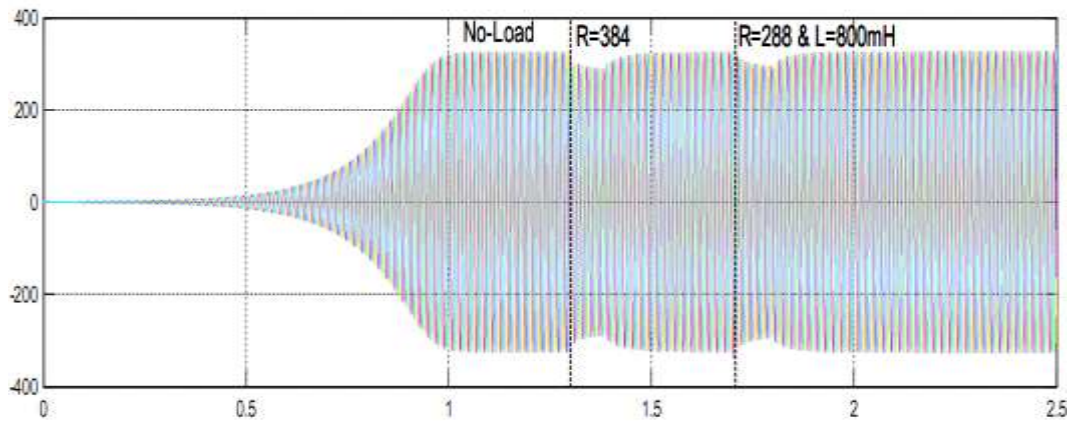


Figure 5.3 Stator voltage regulation of SEIG by using variable capacitor bank

Figure 5.4 shows the consumed reactive power by the SEIG and load. At no-load, the consumed reactive power by the machine is equal to

$$Q = 3 \frac{v^2}{x_c} = 3 \frac{230^2}{106} \approx 1500\text{VAR} \quad (5.2)$$

It is well known that the consumed reactive power is increased by connecting load to the stator terminals. By connecting 384 ohms load at $t=1.3$ sec, the value of capacitor is increased to $35\mu\text{F}$. In this case the consumed reactive power by the system is equal to

$$Q = 3 \frac{v^2}{x_c} = 3 \frac{230^2}{93.7} \approx 1700\text{VAR} \quad (5.3)$$

The demand of RL load to the reactive power is more than the R load. In this case by connecting a $39.5\mu\text{F}$ capacitor bank, the required reactive power by the machine and load is supplied. The amounts of reactive power consumed by the induction generator for the given R and RL load conditions are almost the same as shown in Figure 5.5. The reactive power consumed by the SEIG is calculated from

$$Q = \frac{3}{2} (v_{qs} i_{ds} - v_{ds} i_{qs}) \quad (5.4)$$

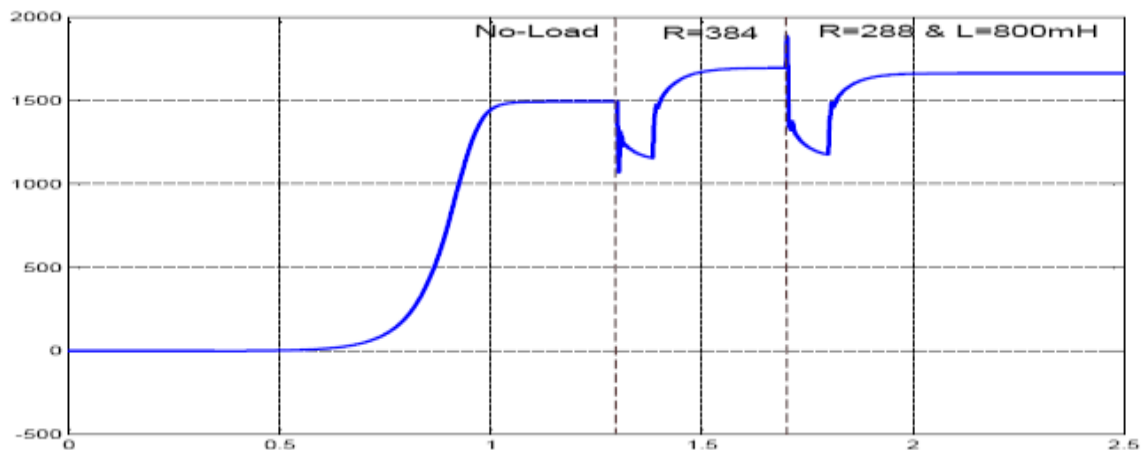


Figure 5.4 Consumed reactive power (VAR) by SEIG under R and RL loads

At the no-load the generated active power by the machine is zero. The application of 384 ohms load at $t=1.3$ sec, the generated active power by the SEIG is equal to 413 W. Also, by connecting the RL load to the stator terminals of machine, the generated active power by the machine is reduced to 323 W. As shown in Figure 5.5. The active power delivered by the induction generator is calculated from

$$p = \frac{3}{2} (v_{qs} i_{qs} + v_{ds} i_{ds} + 2v_{0s} i_{0s}) \quad (5.5)$$

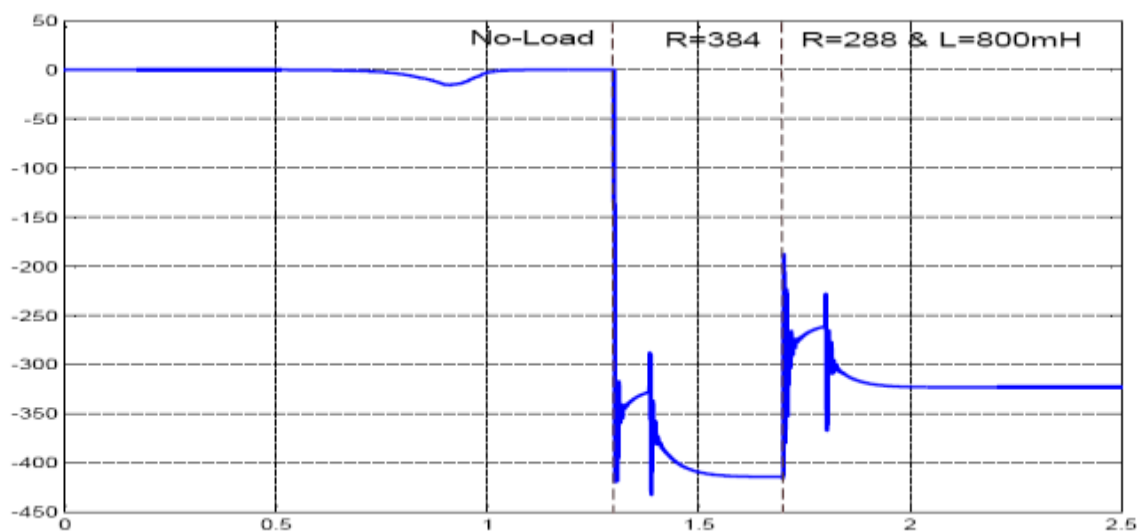


Figure 5.5 Generated active power (W) by SEIG under R and RL loads

5.2 Regulation of the Generated Voltage by using Voltage Source Inverter

In order to supply the reactive power to SEIG, a voltage source inverter (VSI) can be connected directly to the stator of machine. Also, the VSI deliver the generated active power by the SEIG to the connected dc load. The VSI is able to control the amplitude and frequency of stator voltage. The responsibility of VSI in this scheme is control the amplitude of the DC bus voltage. Figure 5.6 shows the system configuration (Hazra & Sensarma, 2008; Hazra & Sensarma, 2010; Murthy & Ahuja, 2010).

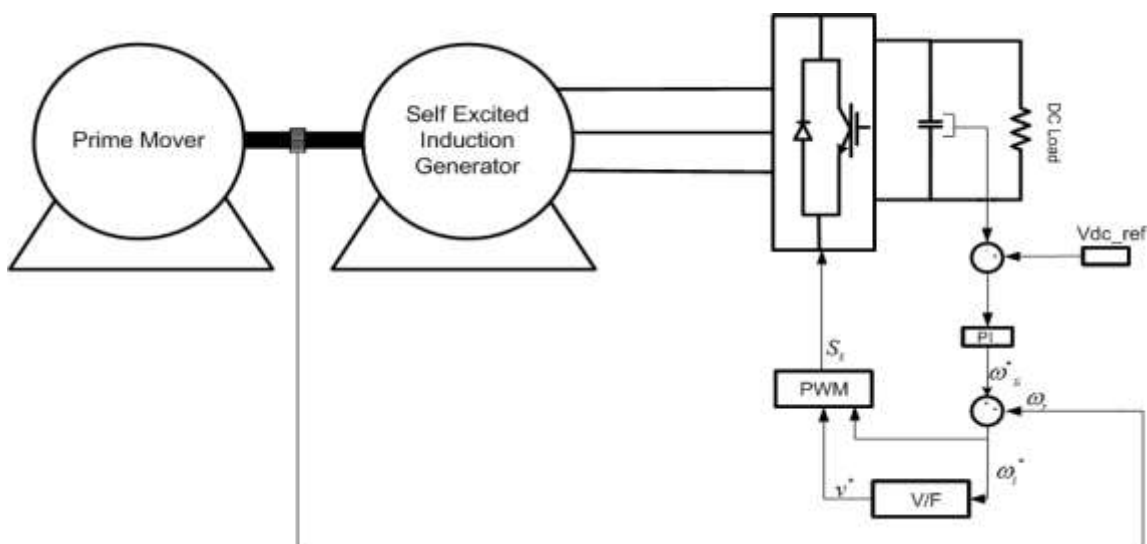


Figure 5.6 Stator voltage regulated by using VSI-PWM

In this control scheme, in order to regulate the generated voltage by the SEIG, a controller is designed based on control of slip speed (ω_{sl}). When the machine is driven at constant speed, any variation on the dc load affects the dc capacitor voltage. The capacitor voltage will be increased by any decrease in the connected load and vice versa. Therefore, by comparing the dc voltage with a reference dc voltage and using a PI controller, the dc bus voltage can be controlled by adjusting the slip of the induction machine. By adjusting the slip of induction machine to a negative value, the induction machine operates as a generator and supplies active power to the dc bus. As a result, dc capacitor will be charged and voltage build-up will occur.

The error between the measured dc voltage and the reference dc voltage is the input of PI controller. The PI controller output gives us a negative slip speed command. By adding this value to the rotor speed, the frequency of inverter excitation can be obtained. To maintain an optimum flux level in the induction machine, the voltage per frequency ratio is kept constant. By using the obtained frequency, we are able to calculate the voltage command to the VSI in order to implement V/F control method, which is suitable for controlling induction machine in motoring and generating mode (Hazra & Sensarma, 2010). Inverter command voltage is obtained from the constant V/F ratio and reference sine waveforms are generated from the frequency and voltage commands. Finally, inverter gate pulses are generated by means of PWM pulse generator. In order to achieve fast excitation, the load is connected to the dc bus after the dc bus voltage is fully build-up. The terminal voltage regulation and voltage build-up are examined through simulation models.

5.2.1 Modeling of the VSI and DC Load

The power circuit of the three-phase VSI is shown in Figure 5.7. The inverter consists of six switching devices and each leg has an anti-parallel diode. The upper side signals are shown by S_1, S_2, S_3 and the lower side signals are shown by $\bar{S}_1, \bar{S}_2, \bar{S}_3$. The valid switch state of each branch is shown in Table 5.1 (Lee & Ehsani, 2001; Singh, Murthy & Gupta, 2004; Shokrollah, 2006).

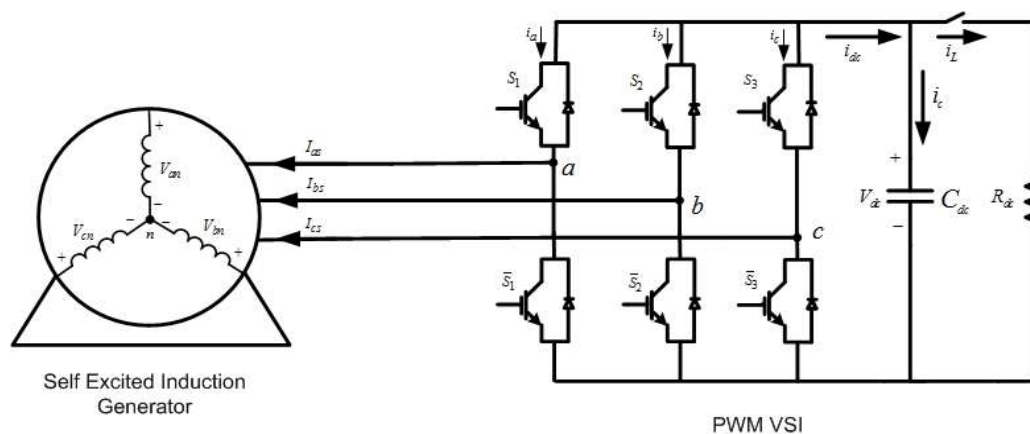


Figure 5.7 The scheme of SEIG voltage regulation by using VSI

Table 5.1 Valid switch states of three-phase PWM voltage source inverter

S_1	1	$\bar{S}_1=0$
	0	$\bar{S}_1=1$
S_2	1	$\bar{S}_2=0$
	0	$\bar{S}_2=1$
S_3	1	$\bar{S}_3=0$
	0	$\bar{S}_3=1$

The phase voltage of SEIG stator winding can be written as

$$V_{an} = V_{dc}S_1 - \frac{V_{dc}}{3}(S_1 + S_2 + S_3) \quad (5.6)$$

$$V_{bn} = V_{dc}S_2 - \frac{V_{dc}}{3}(S_1 + S_2 + S_3) \quad (5.7)$$

$$V_{cn} = V_{dc}S_3 - \frac{V_{dc}}{3}(S_1 + S_2 + S_3) \quad (5.8)$$

The transformation of variables to q-d coordinates in stationary reference frame is given by the following expressions:

$$f_q = \frac{1}{3}(2f_a - f_b - f_c) \quad (5.9)$$

$$f_d = \frac{1}{\sqrt{3}}(-f_b + f_c) \quad (5.10)$$

where the variable f represents quantities such as voltage, current or flux. By substituting the equation (5.9) - (5.10) into equations (5.5) and (5.6), the q-d stator voltage are expressed as

$$V_q = V_{dc} S_q \quad (5.11)$$

$$V_d = V_{dc} S_d \quad (5.12)$$

The DC side current is equal to

$$i_{dc} = -(i_{as} S_1 + i_{bs} S_2 + i_{cs} S_3) \quad (5.13)$$

The dc current in stationary q-d reference frame can be written as

$$i_{dc} = -\frac{3}{2}(i_q S_q + i_d S_d) \quad (5.14)$$

Finally, the value of capacitor voltage can be obtained from

$$V_{dc} = \frac{1}{C} \int i_c dt \quad (5.15)$$

where the i_c is the dc capacitor current and expressed as

$$i_c = i_{dc} - i_L = i_{dc} - \frac{V_{dc}}{R_{dc}} \quad (5.16)$$

5.2.2 Simulation Model of SEIG and VSI

This model was implemented in MATLAB simulink and shown in Figure 5.8. The VSI is connected directly to the stator terminals of SEIG and a dc load is connected to the dc side of VSI. The reactive power requirement by the induction machine is produced by the VSI. The computer simulation model of VSI subblock is shown in Figure 5.9. This model is the implementation of equations (5.11) – (5.16). The simulation model of PWM pulse generation block is shown in Figure 5.10. and Figure 5.11 shows the dc bus voltage control block diagram.

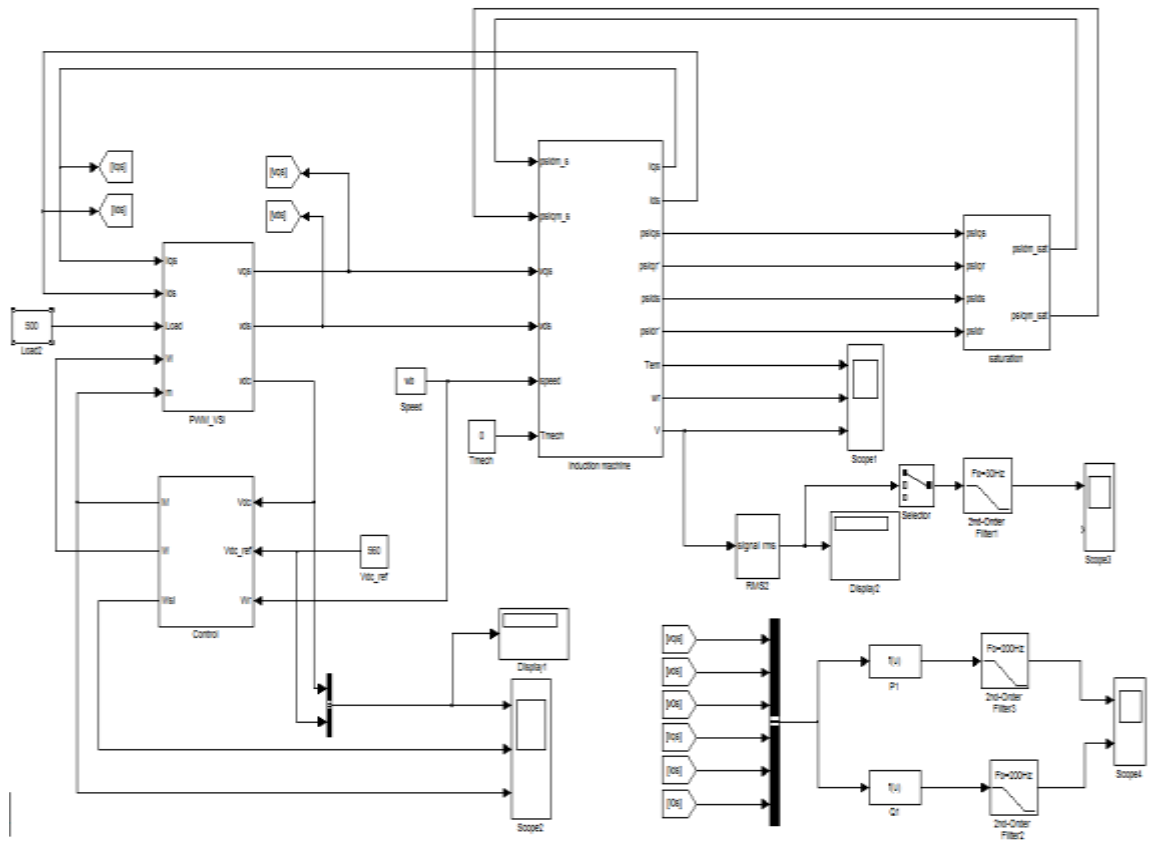


Figure 5.8 MATLAB Simulink model of SEIG and VSI

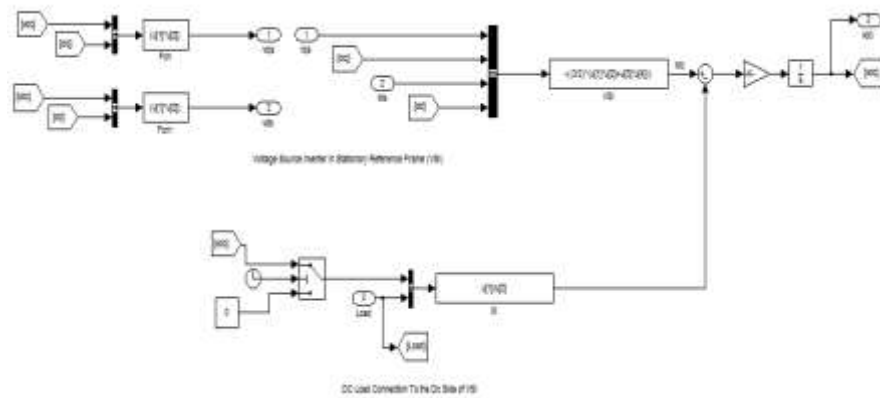


Figure 5.9 Simulation model of VSI in d-q stationary reference frame

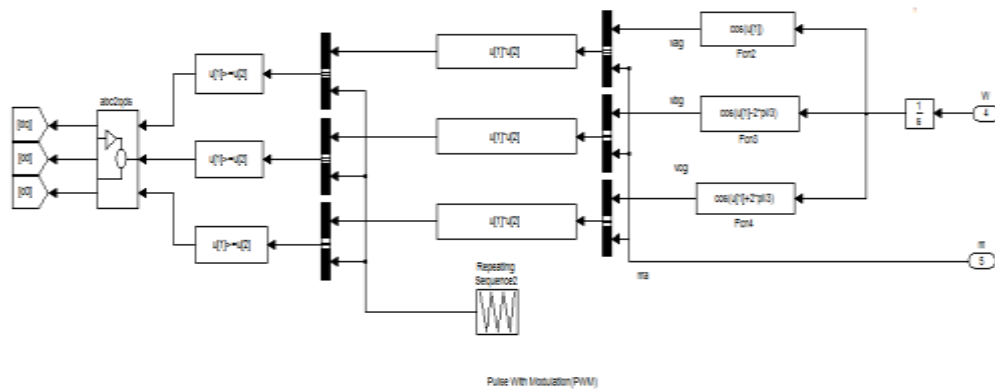


Figure 5.10 Simulation model of PWM pulse generation block

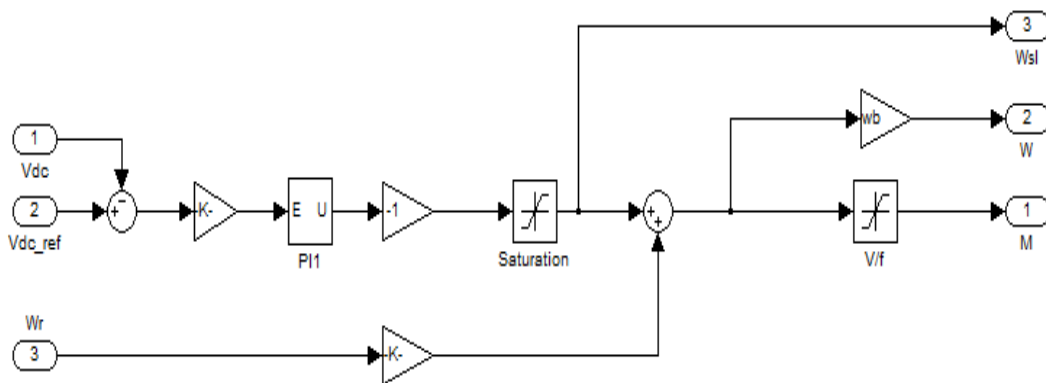


Figure 5.11 Simulation model dc bus voltage control

5.2.3 Results of Voltage Regulation by using VSI

Figure 5.12-Figure 5.20 show the dc bus voltage build-up, variation of the stator voltage in steady-state, stator voltage magnitude, dc bus voltage, slip speed command (ω_{sl}^*), modulation index, generated active and consumed reactive power by the machine in response to a change in resistive dc load, respectively. Value of the dc capacitor is set to 1000 μF which its initial value is assumed 15 Volts, $V_{dc}^* = 560$ volts and the gains in PI controller are $k_i = 0.01$ and $k_p = 3.5$, respectively.

At the no-load, the generated active power by the SEIG is delivered to the dc bus by VSI, which case the dc capacitor voltage takes its steady-state at $t=1.3$. Figure

5.13 shows the stator voltage variation. It can be seen that the terminal voltage build-up is totally completed at $t=1.3$ with the dc bus voltage. This time is dependent to the dc capacitor value, as shown in Figure 5.12. It can be seen that by connecting a 500 ohms load at $t=1.5$ sec, the value of the stator voltage drops nearly 4 volts, Figure 5.14 and Figure 5.15. On the other hand the value of dc bus voltage drops nearly 8 volts and slip is increased in negative side from 0 to -0.06 in order to produce more torque in the machine, as shows in Figure 5.16 and Figure 5.17, respectively. Figure 5.18 shows the value of modulation index that is kept constant in its maximum value (0.9). The generated active power and consumed reactive power by the SEIG is shown in Figure 5.19 and Figure 5.20, respectively. It can be seen that the consumed reactive power by the SEIG is increased by decreasing the load value also; the generated active power is variable dependent to the connected load value.

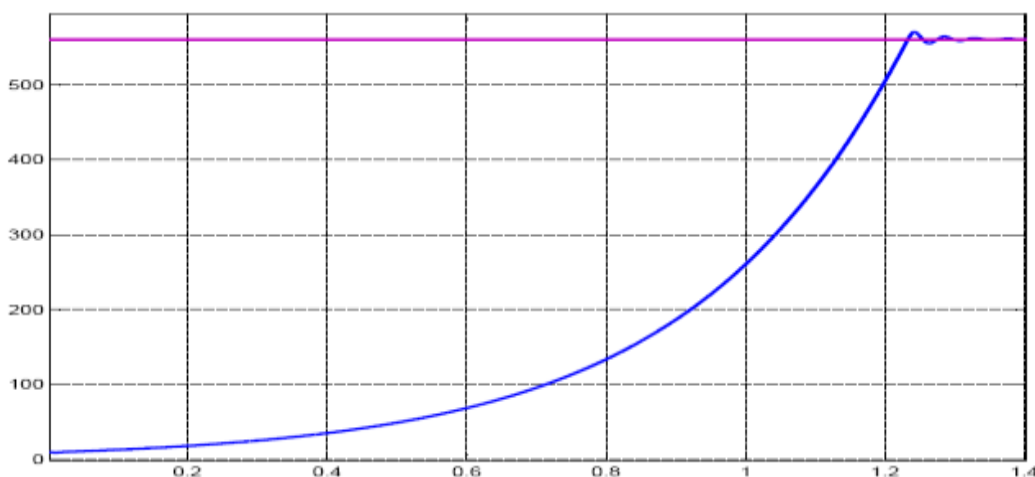


Figure 5.12 DC bus voltage (V) build-up at no-load

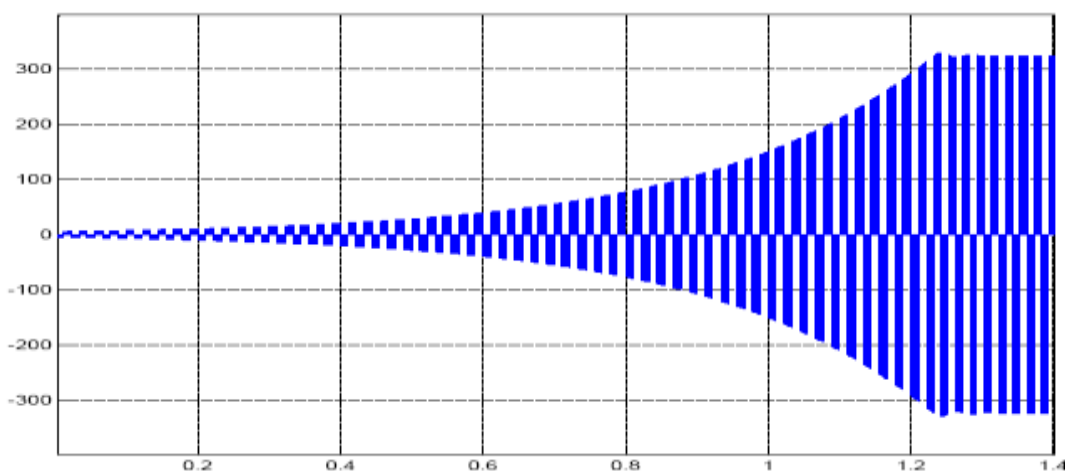


Figure 5.13 Stator voltage (V) build-up at no-load

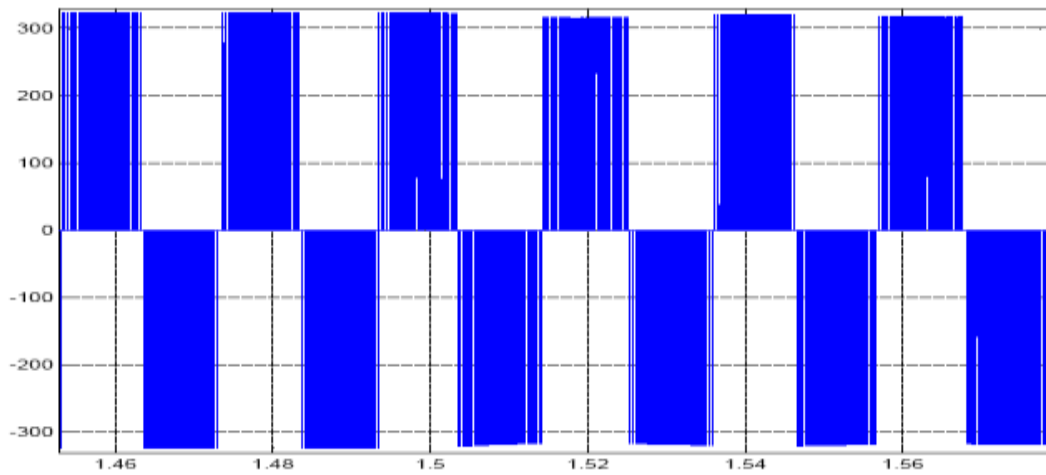


Figure 5.14 Steady-state waveform of the stator voltage (V) under 500Ω dc load

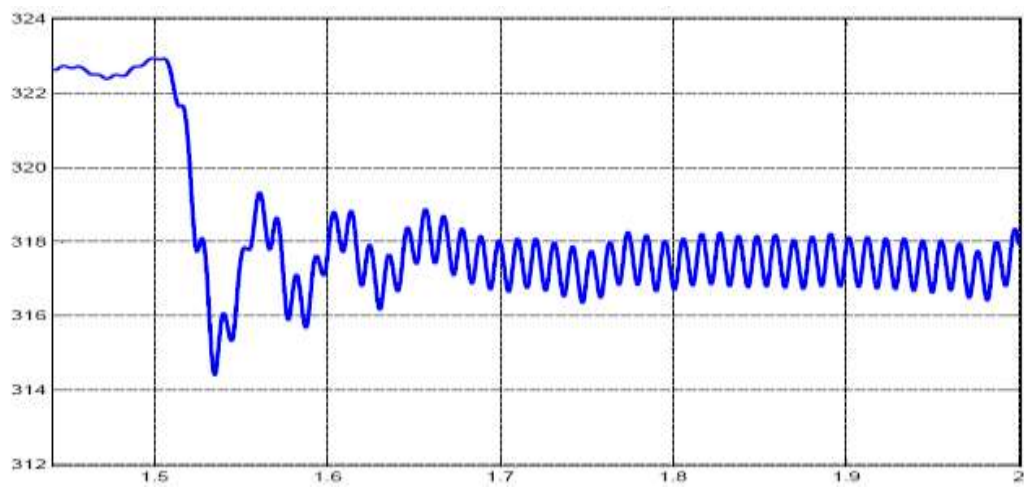


Figure 5.15 Variation of the stator voltage magnitude (V) with 500Ω dc load

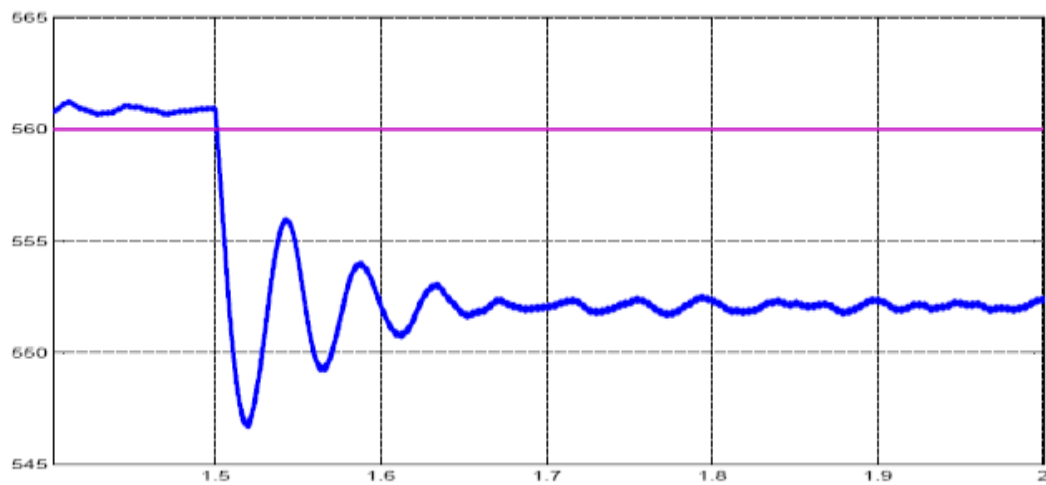


Figure 5.16 DC bus voltage (V) variation from no-load to 500 ohms dc load

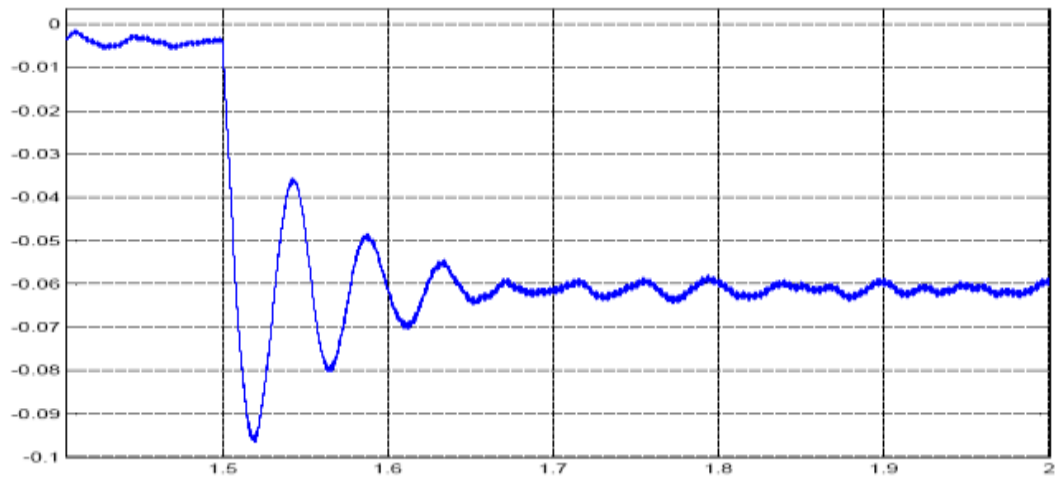


Figure 5.17 Variation of slip speed command with 500 ohms dc load

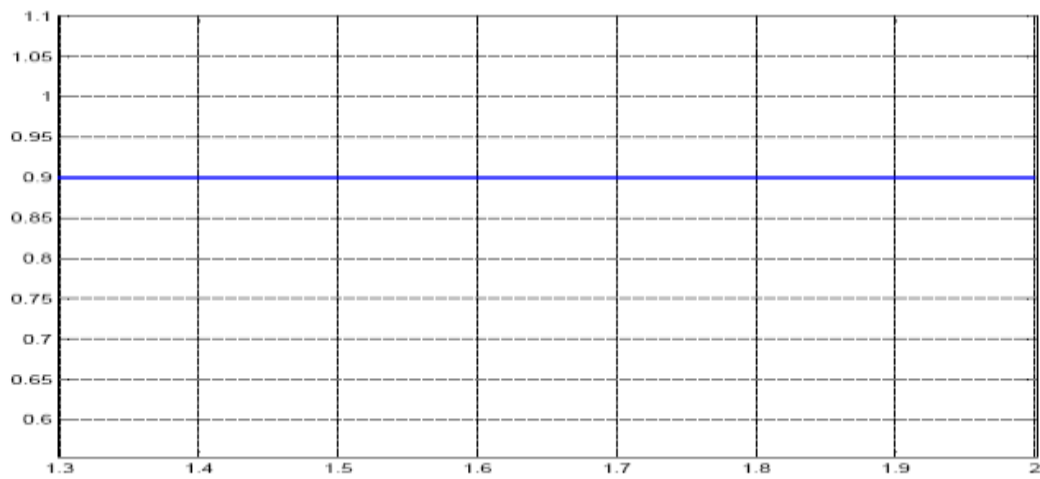


Figure 5.18 Behavior of modulation index with 500 ohms dc load

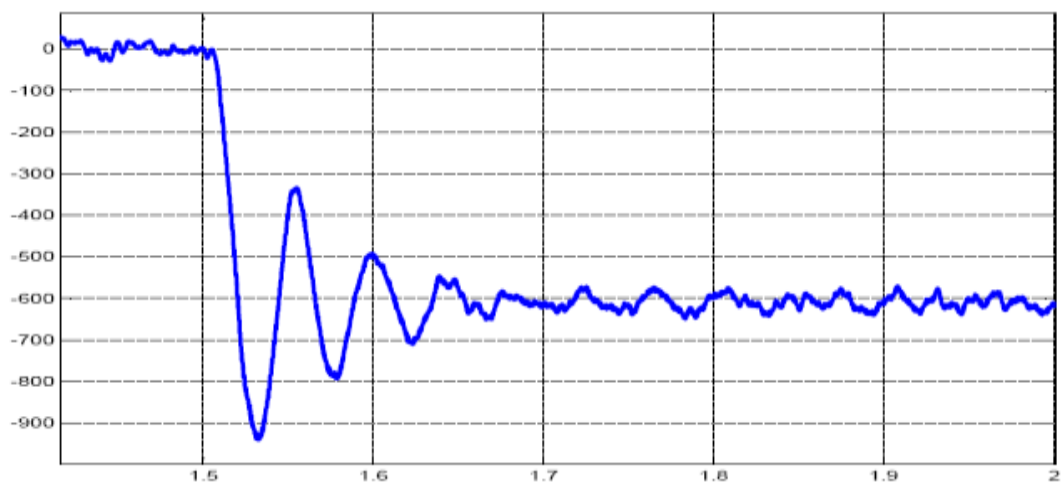


Figure 5.19 Generated active power (W) by SEIG with 500 ohms dc load

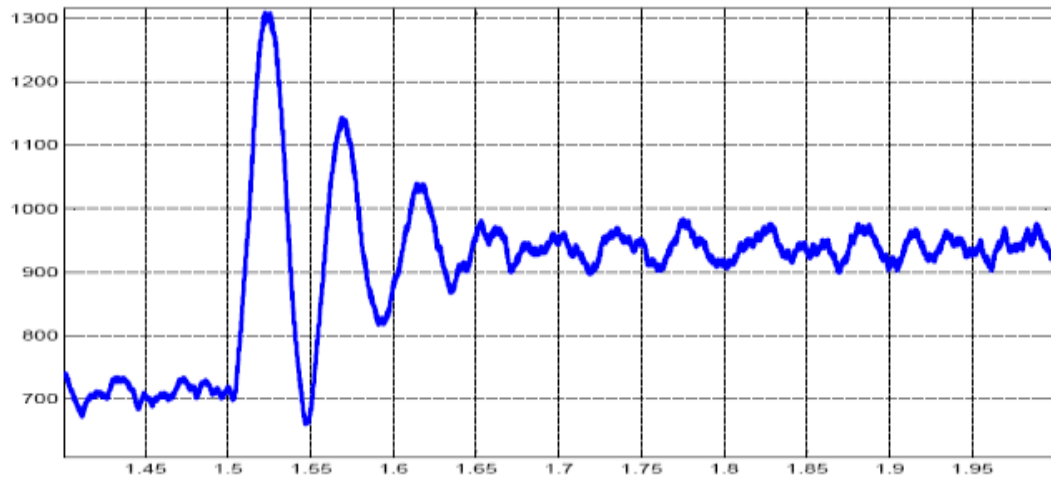


Figure 5.20 Consumed reactive power (VAR) by SEIG with 500 ohms dc load

5.3 Regulation of the Generated Voltage by using STATCOM

In this scheme, the ac capacitor bank across the stator is used to provide the major reactive power requirement of SEIG and the STATCOM is used to tune the reactive power needed by the machine and load when the machine is working in constant speed. Various control methods have been proposed in the literature such as instantaneous power control algorithm (Jayaramaiah & Femandes, 2008). Also, this scheme can be used with an energy storage unit (battery bank) at the dc bus to provide frequency and voltage regulation (Dastagir & Lopes, 2007; Lopez & Almeida; 2006; Geng, Xu, Wu & Huang, 2011). In this thesis, slip speed control method given in Section 5.2 is applied to STATCOM for controlling the magnitude of the generator terminal voltage and its viability is examined by simulations. The system configuration is shown in Figure 5.21.

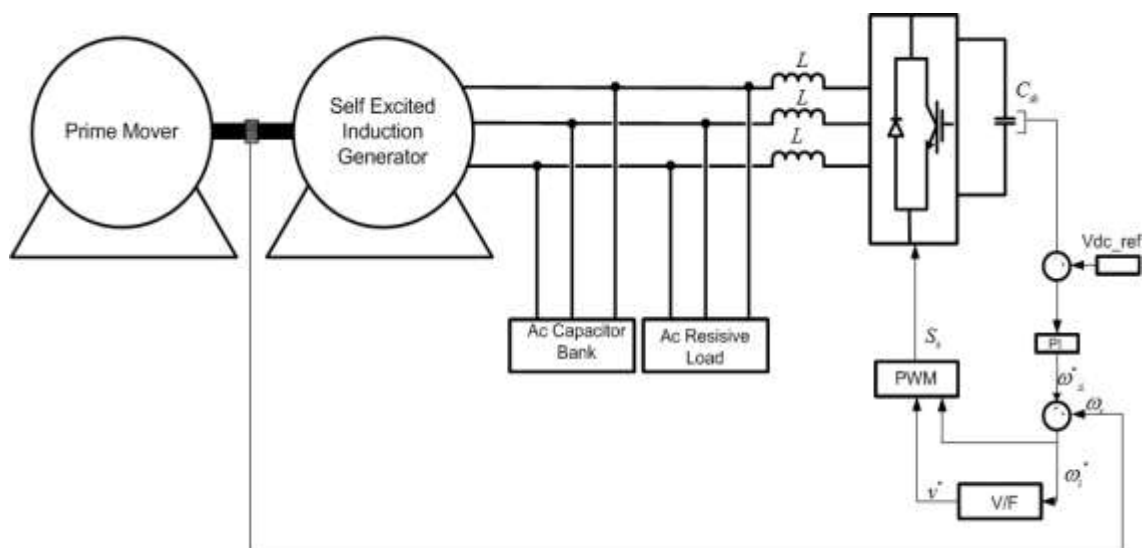


Figure 5.21 Shunt voltage regulation by using STATCOM and slip speed control method

5.3.1 Modeling of the Connected AC Load and STATCOM

Figure 5.22 shows the shunt connection type of STATCOM. By using the state space model, it is possible to define the STATCOM dynamics model (Jayaramaiah & Femandes, 2006).

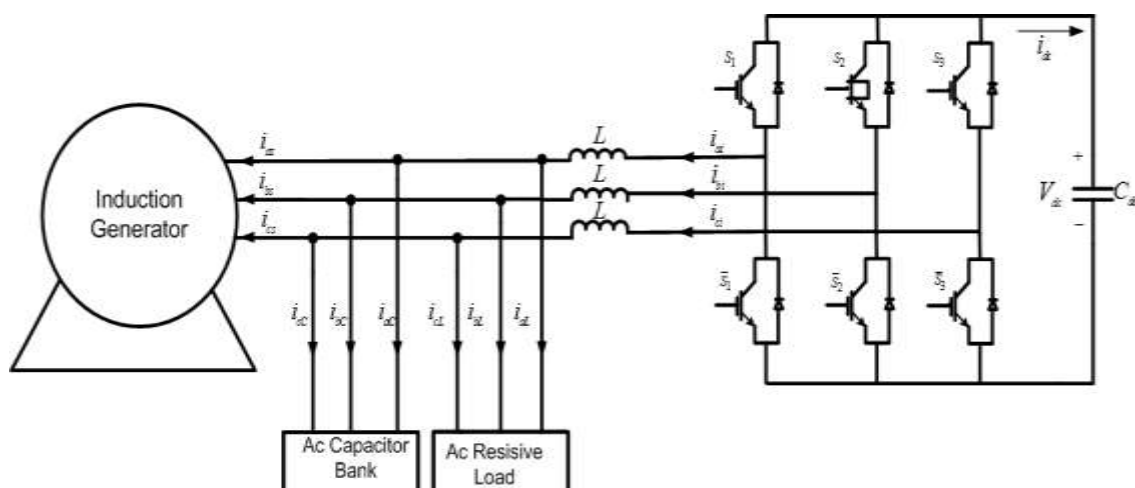


Figure 5.22 Shunt connection of STATCOM for terminal voltage regulation of SEIG

As mentioned in Section 5.2, the voltage and current expressions of three-phase induction circuit are determined by the switching states S_1, S_2, S_3 . Referring to Figure 5.23, the DC side current can be expressed as

$$i_{dc} = -(i_{ai}S_1 + i_{bi}S_2 + i_{ci}S_3) \quad (5.17)$$

The dc current in stationary qd reference frame can be written as

$$i_{dc} = -\frac{3}{2}(i_{qi}S_q + i_{di}S_d) \quad (5.18)$$

Finally, the value of capacitor voltage in the DC side can be obtained from

$$v_{dc} = \frac{1}{C_{dc}} \int i_{dc} dt \quad (5.19)$$

The STATCOM voltage behind the filter inductance (L) in stationary q-d reference frame can be written as

$$V_{qi} = V_{dc}S_q \quad (5.20)$$

$$V_{di} = V_{dc}S_d \quad (5.21)$$

The SEIG terminal voltages and STATCOM currents are then obtained as

$$V_{qs} = V_{qi} - L \frac{di_{qi}}{dt} \quad (5.22)$$

$$V_{ds} = V_{di} - L \frac{di_{di}}{dt} \quad (5.23)$$

$$i_{qi} = \int \frac{1}{L} (V_{qi} - V_{qs}) \quad (5.24)$$

$$i_{di} = \int \frac{1}{L} (V_{di} - V_{ds}) \quad (5.25)$$

In these equations, the subscript s represents the stator variables of SEIG and i represents the STATCOM variables. The voltage and current equations of RL load can be expressed as

$$V_{qs} = R_L i_{Lq} + L_L \frac{di_{Lq}}{dt} \Rightarrow i_{Lq} = \int \left(\frac{V_{qs}}{L_L} - \frac{R_L}{L_L} i_{Lq} \right) \quad (5.26)$$

$$V_{ds} = R_L i_{Ld} + L_L \frac{di_{Ld}}{dt} \Rightarrow i_{Ld} = \int \left(\frac{V_{ds}}{L_L} - \frac{R_L}{L_L} i_{Ld} \right) \quad (5.27)$$

where the subscript L represents the load variables. The current of the STATCOM can be written as

$$i_{qi} = i_{qs} + i_{qc} + i_{Lq} \quad (5.28)$$

$$i_{di} = i_{ds} + i_{dc} + i_{Ld} \quad (5.29)$$

where the subscript C represents the shunt capacitor variables. From above equations, the capacitor currents and capacitor voltages which are equal to the stator terminal voltages can be expressed as (Geng, Xu, Wu & Huang, 2011)

$$i_{qC} = i_{qi} - i_{qs} - i_{Lq} \quad (5.30)$$

$$i_{dC} = i_{di} - i_{ds} - i_{Ld} \quad (5.31)$$

$$V_{qs} = V_{qc} = \frac{1}{C} \int i_{qC} dt \quad (5.32)$$

$$V_{ds} = V_{dc} = \frac{1}{C} \int i_{dC} dt \quad (5.33)$$

5.3.2 Simulation Model of Shunt Voltage Regulation by using STATCOM

In this model, the STATCOM is connected parallel to the stator terminals, capacitor bank and load. The complete computer simulation model is shown in

Figure 5.23 and its subblocks are given in Figure 5.24 – Figure 5.28. The model is the implementation of equations (5.17) – (5.33).

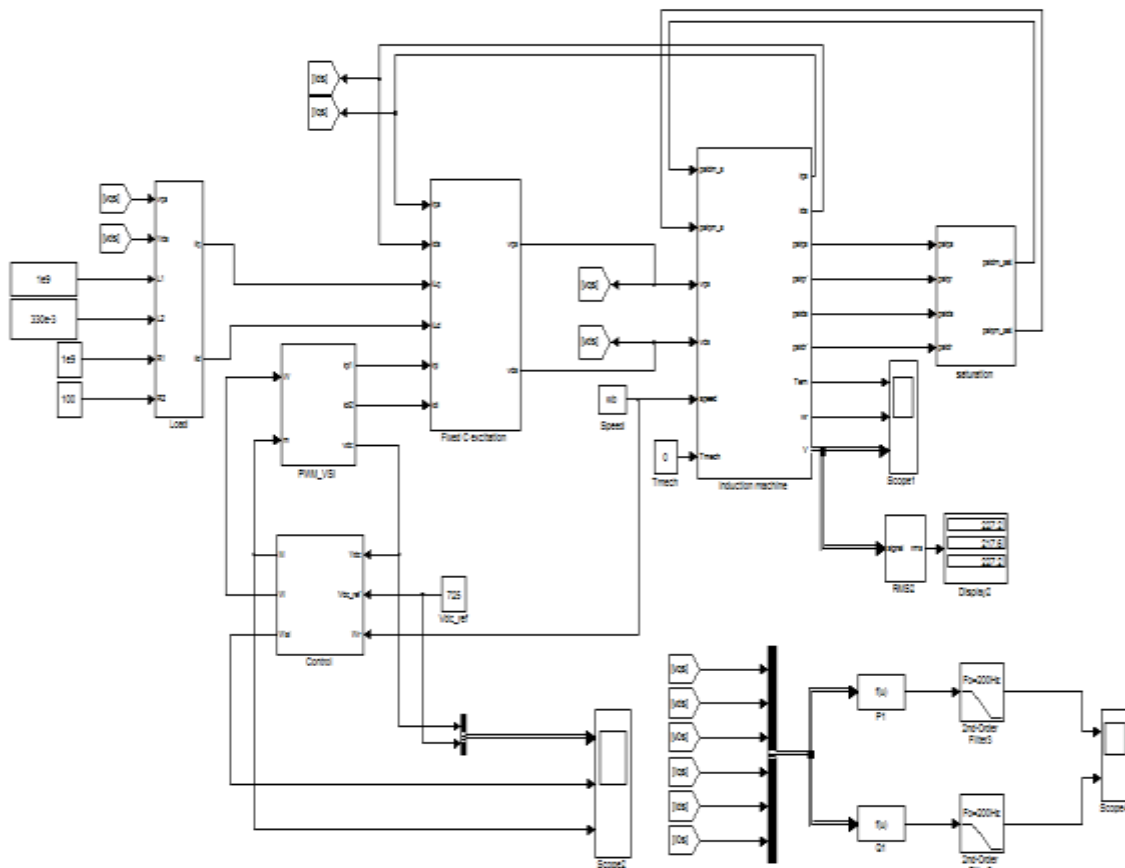


Figure 5.23 MATLAB Simulink model of SEIG and STATCOM



Figure 5.24 Simulation model of DC bus voltage in q-d stationary reference frame

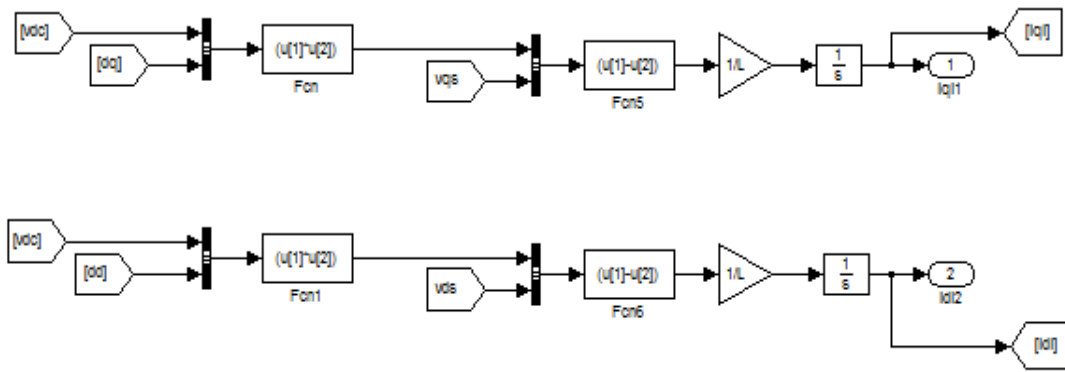


Figure 5.25 Simulation model of STATCOM currents in q-d stationary reference frame

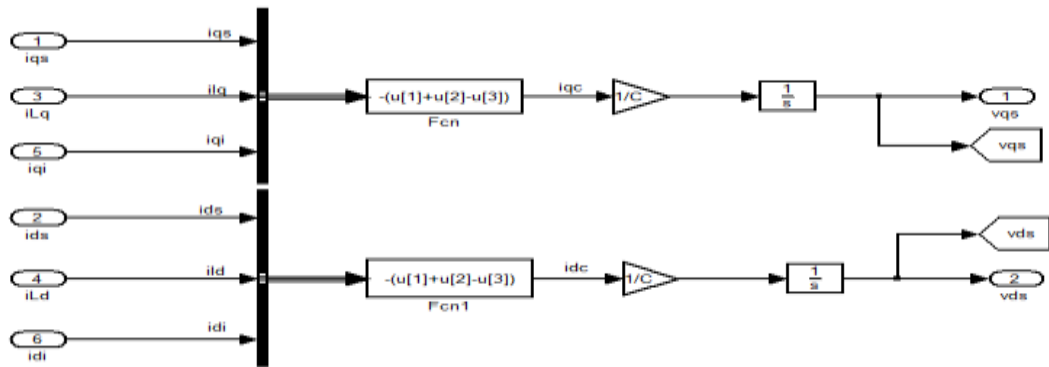


Figure 5.26 Simulation model of stator voltages of SEIG in q-d stationary reference frame

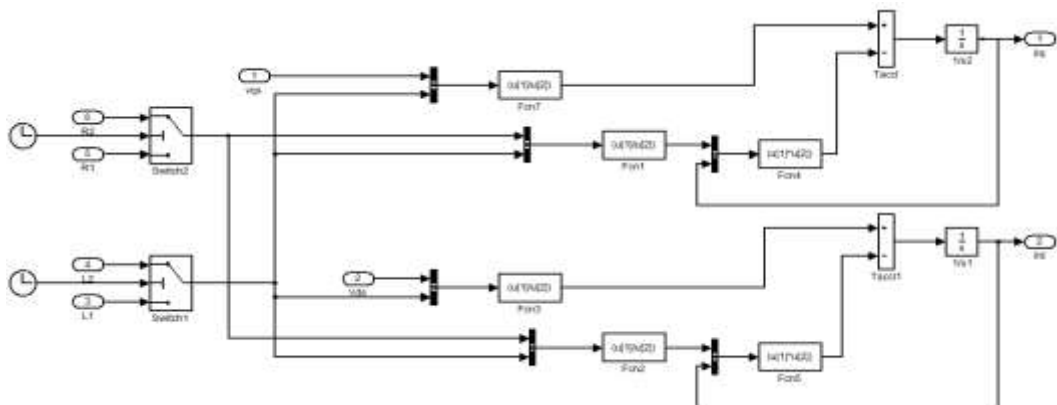


Figure 5.27 Simulation model of load in q-d stationary reference frame

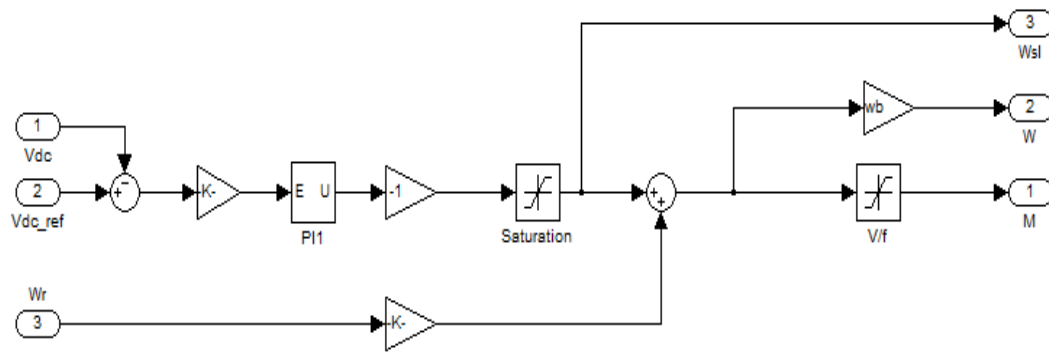


Figure 5.28 Simulation model of slip regulation method

5.3.3 Results of Shunt Voltage Regulation by using STATCOM

Simulations were performed to examine the voltage control capability of the STATCOM applied to the SEIG. In these simulations, variation of the DC link voltage, slip speed command, stator voltage in both RMS and reference value, consumed reactive power by the SEIG, generated reactive power by the STATCOM, generated active power by the SEIG and the active power consumed by the STATCOM with ac load connected to the stator of SEIG with R and RL load are shown, respectively. The value of the dc capacitor is set to 1000 μF and the gains of PI controller are $k_i = 0.01$ and $k_p = 3.5$, respectively. Also, the value of ac capacitor bank is set to 30 μF in the simulation. The simulations are in two cases: (i) applying resistive ac load of $R=144\Omega$, (ii) applying RL ac load of $R=100\Omega$ and $L=330\text{mH}$.

Case (i) $R=144\ \Omega$

In Figure 5.29, the dc bus voltage decrease nearly 10 volts by connecting 144 ohms load when the system operates at no-load initially. By applying this load in the absence of STATCOM the terminal voltages were collapsed as shown in Chapter 3 and Chapter 4. Figure 5.30 shows the variation of the slip speed command that is increased by increasing load value. It can be seen that the slip speed command is increased from -0.01 to -0.07 by increasing the load value from no-load to full-load (144 ohms). Figure 5.31 and Figure 5.32 show the instantaneous terminal voltages

and their peak value, respectively. Figure 5.33 shows the instantaneous stator voltage waveforms during the transition from no-load to full-load. Generated active power and consumed reactive power by the SEIG are shown in Figure 5.34 and Figure 5.35, respectively. At no-load, the generated active power is equal to zero. By applying 144 ohms load, the generated active power by the machine is increased to the rated value (1100 W). Also, the consumed reactive power by the machine is increased from 1500 VAR to 2100 VAR. This reactive power demanded by the machine under load is produced by the STATCOM. Figure 5.36 shows the generated reactive power by the STATCOM under loading conditions. The consumed active power by the STATCOM at steady-state is approximately zero and it draws real power from the induction machine to charge the dc capacitor as shown in Figure 5.37.

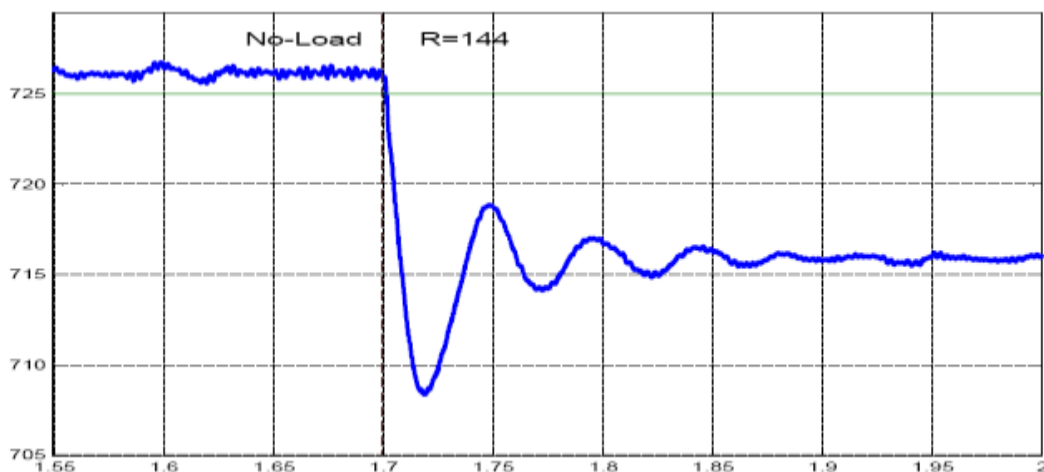


Figure 5.29 DC bus voltage (V) variation of STATCOM with 144Ω ac load

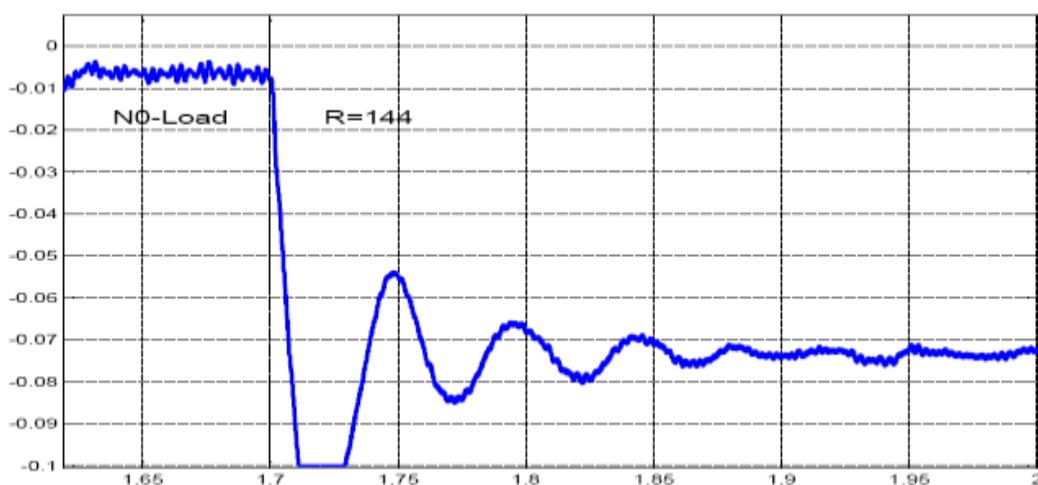


Figure 5.30 Slip speed command variation with 144Ω ac load

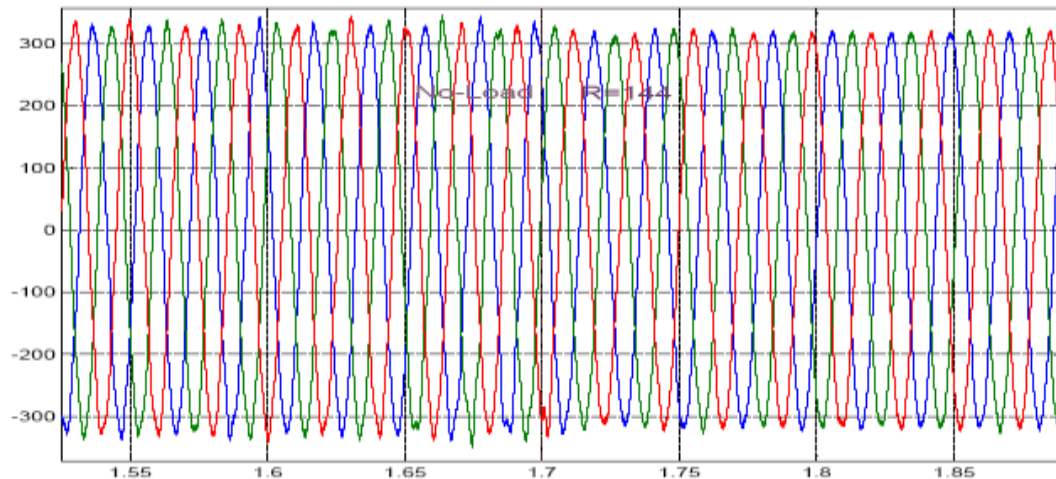


Figure 5.31 Terminal voltages (V) of SEIG with 144Ω ac load

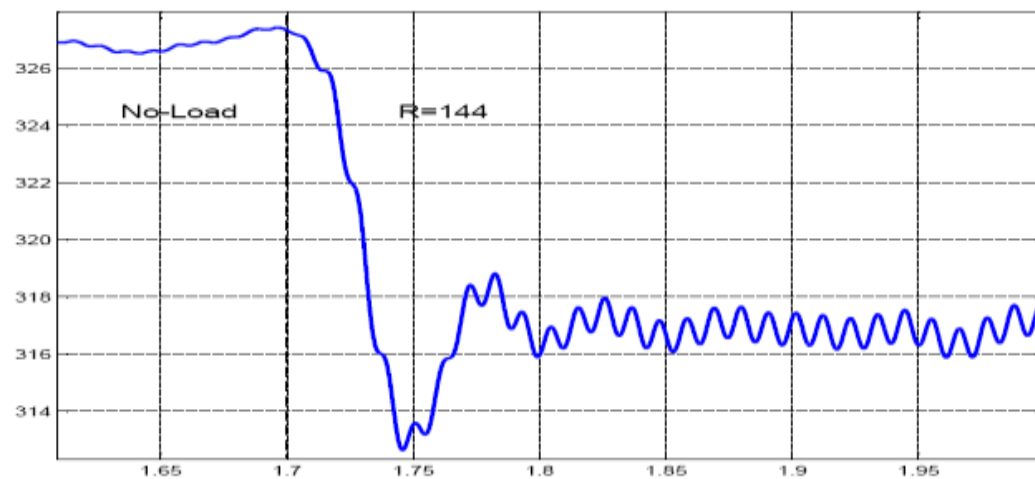


Figure 5.32 Peak terminal voltage magnitude (V) variation with 144Ω ac load

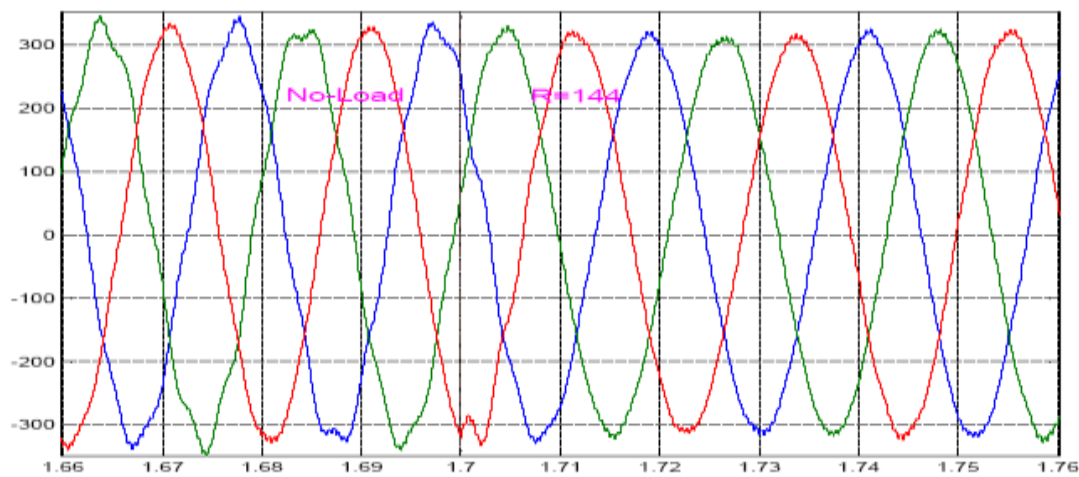


Figure 5.33 Variation of stator voltages of SEIG during the transition from no-load to full-load

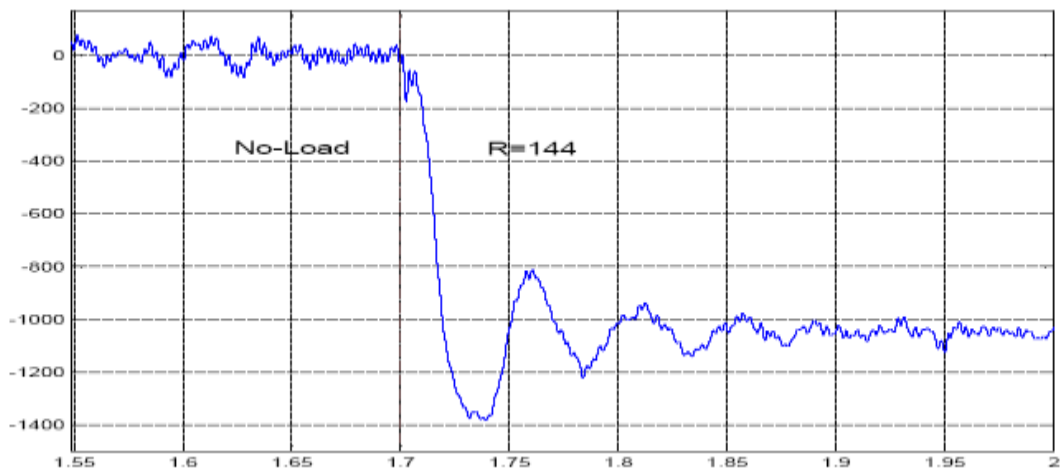


Figure 5.34 Generated active power (W) by the SEIG with 144Ω ac load

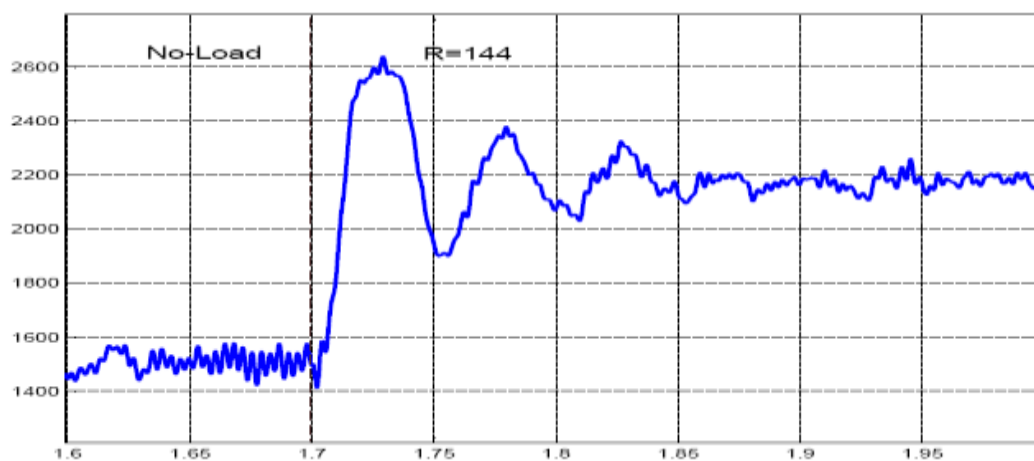


Figure 5.35 Consumed reactive power (VAR) by SEIG with 144Ω ac load

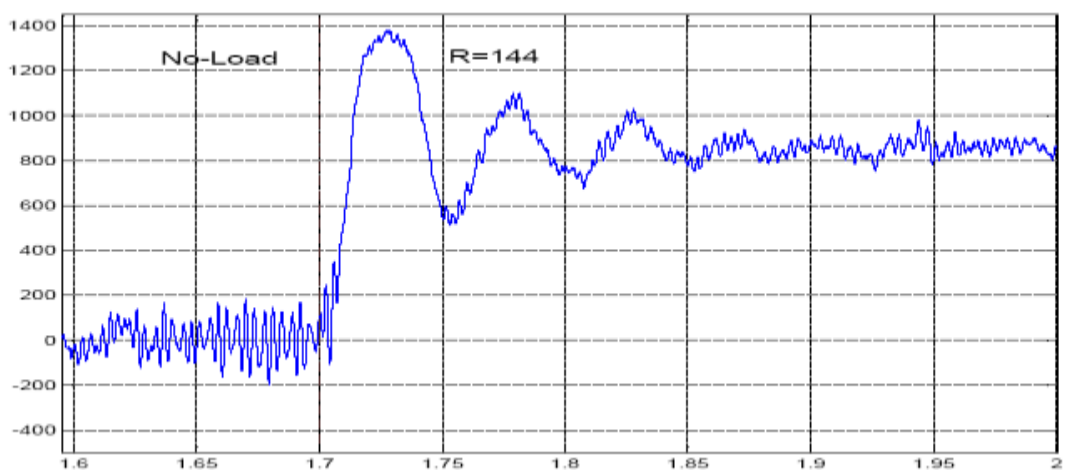


Figure 5.36 Generated reactive power (VAR) by the STATCOM with no-load and 144Ω load

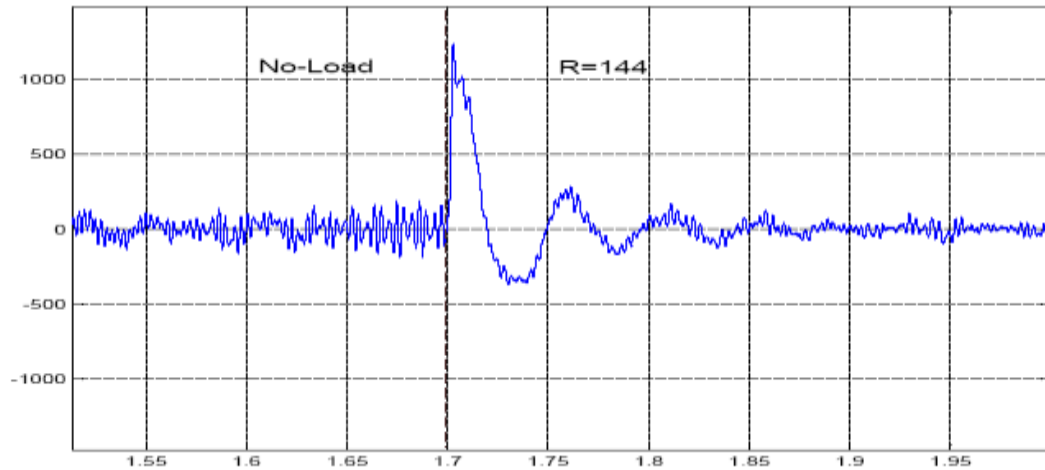


Figure 5.37 The instantaneous active power (W) of STATCOM

Case (ii) $R=100\ \Omega$ and $L=330\text{mH}$

The results of simulation for the quantities that are examined under the RL load case are shown in Figure 5.38 – Figure 5.46. The dc bus voltage, instantaneous stator voltages and their peak values during no-load and full-load are shown in Figure 5.38, 5.40, and 5.41, respectively. Similar to the case (i) the dc voltage drop is nearly 10 volts, because the impedance seen by the machine in case (i) and case (ii) is equal. Variation of slip speed command is illustrated in Figure 5.39, which is lower than case (i) because the load demand less active power while its reactive power demand increased. By applying rated RL load to the terminals of SEIG, the reactive power demand of the load is increased. The reactive power that is being supplied from STATCOM is the sum of the reactive powers of the load and machine. It is more in this case when compared to case (i) and shown in Figure 5.45.

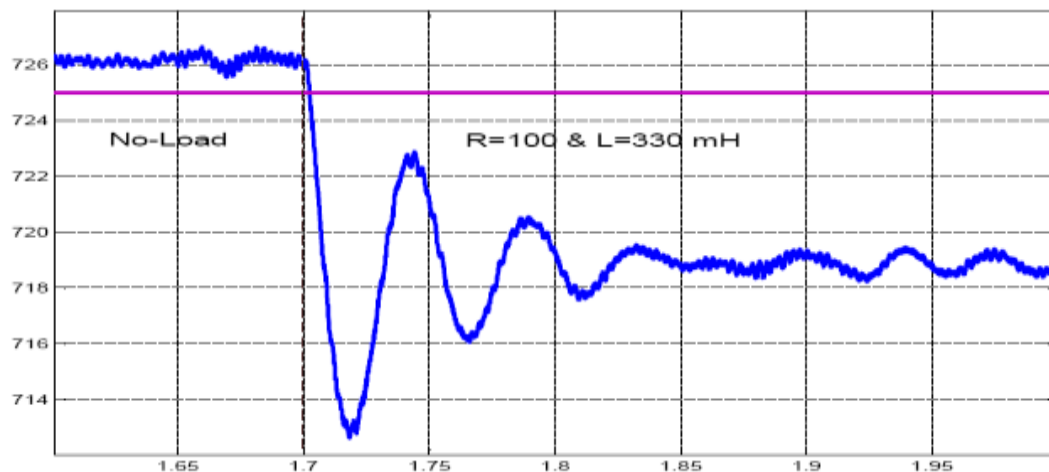


Figure 5.38 DC bus voltage (V) variation with $R=100\ \Omega$ and $L=330\text{mH}$ ac load

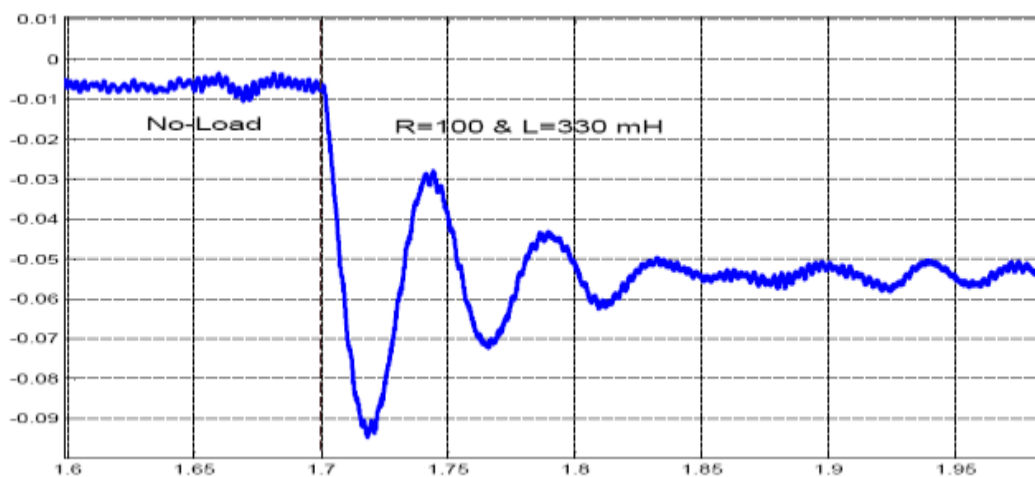


Figure 5.39 Slip speed command variation with $R=100\ \Omega$ and $L=330\text{mH}$ ac load

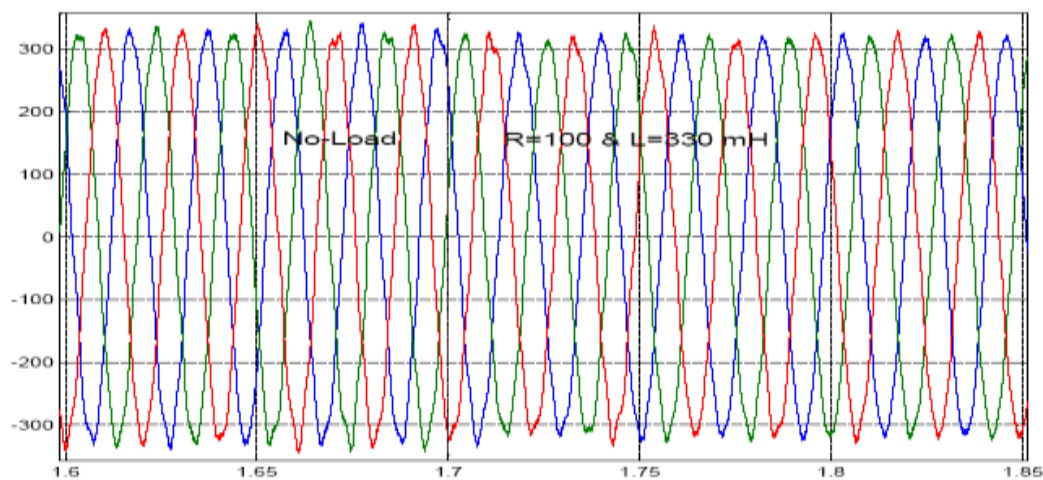


Figure 5.40 Instantaneous terminal voltages of SEIG with $R=100\ \Omega$ and $L=330\text{mH}$ ac load

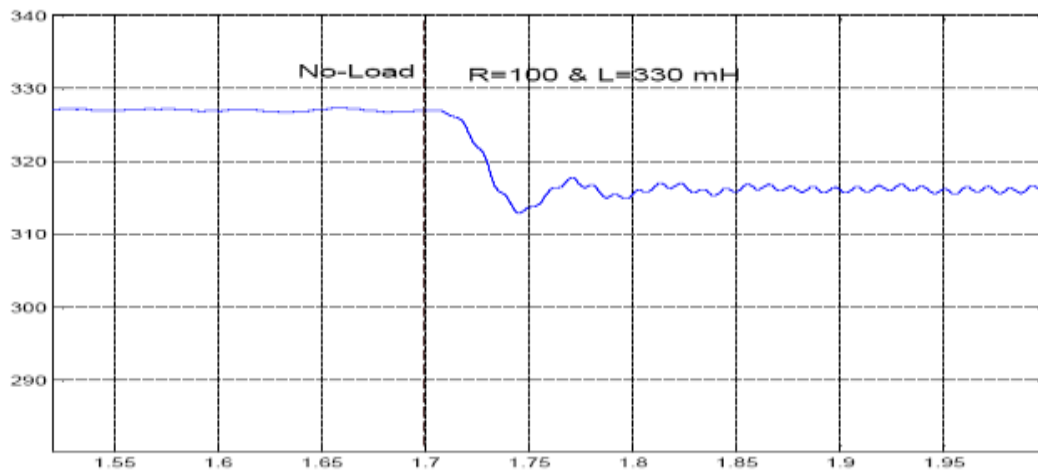


Figure 5.41 Peak terminal voltage magnitude (V) variation with $R=100\ \Omega$ and $L=330\text{mH}$ ac load

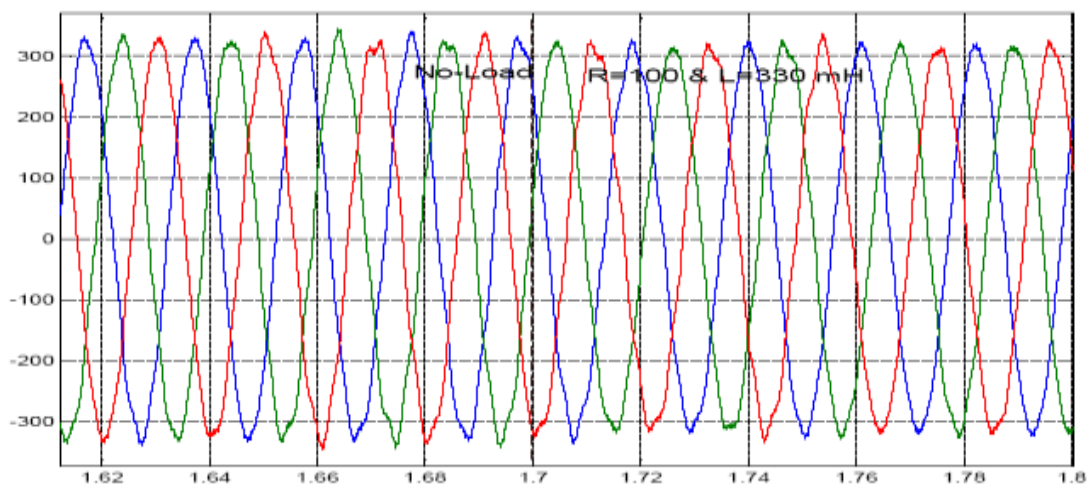


Figure 5.42 Variation of stator voltages of SEIG during the transition from no-load to full-load

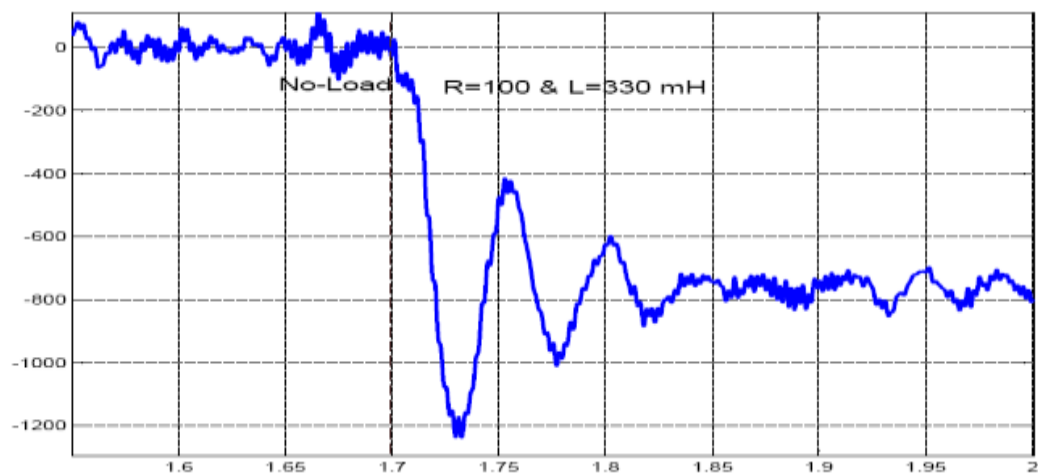


Figure 5.43 Generated active power (W) by the SEIG with $R=100\ \Omega$ and $L=330\text{mH}$ ac load

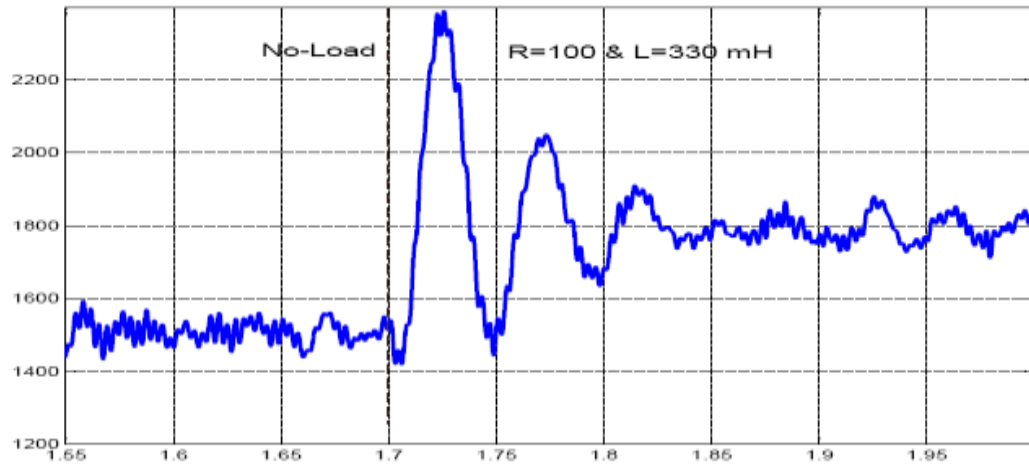


Figure 5.44 Consumed reactive power (VAR) by SEIG with $R=100\ \Omega$ and $L=330\text{mH}$ ac load

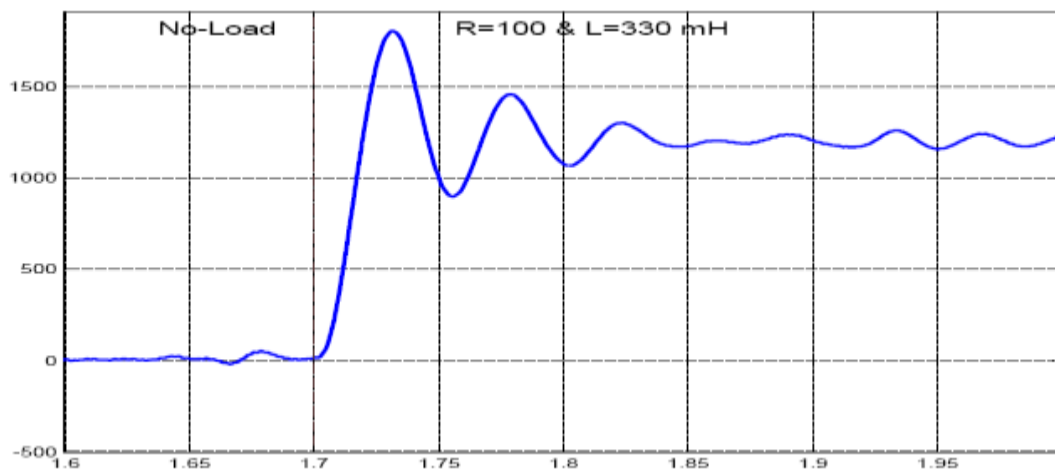


Figure 5.45 Generated reactive power (VAR) by the STATCOM

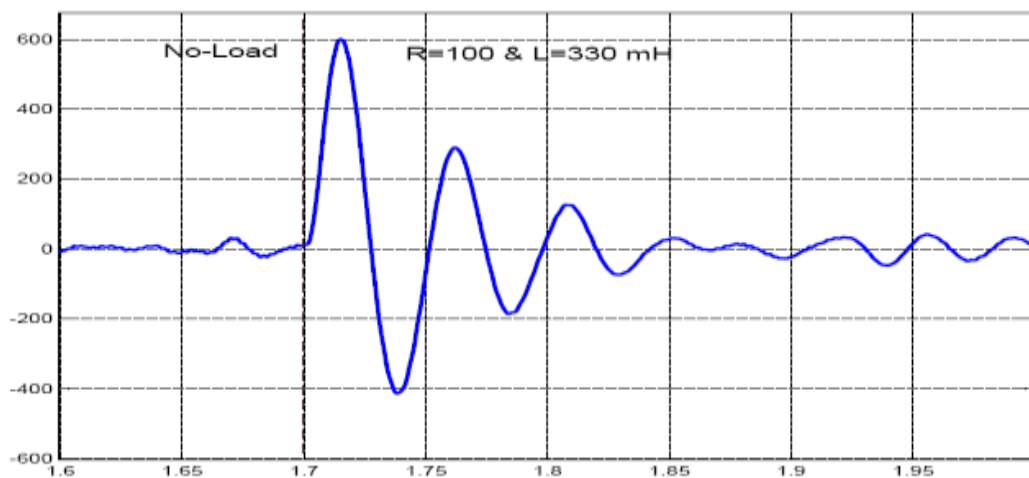


Figure 5.46 The instantaneous active power (W) of STATCOM

5.4 Shunt Voltage Regulation using Feedback from Stator Voltage

In the above voltage regulation mode, in order to control the stator voltage, the dc bus voltage was sensed. Also, it is possible to design a controller by sensing the stator voltage. The simulation results of voltage regulation by sensing the stator voltage is shown in Figure 5.47 and Figure 5.48. The value of the connected load is equal to 144 ohms. The variation on the terminal voltage with the dc voltage feedback is slightly less than with feedback from ac voltage. Both methods yield to approximately same results with the same PI parameters.

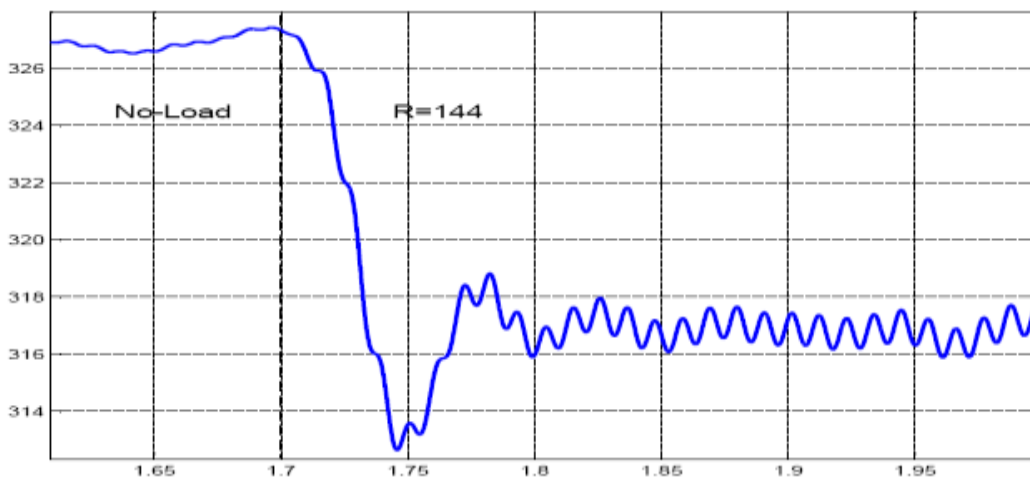


Figure 5.47 Peak terminal voltage magnitude (V) variation of SEIG using feedback from dc voltage

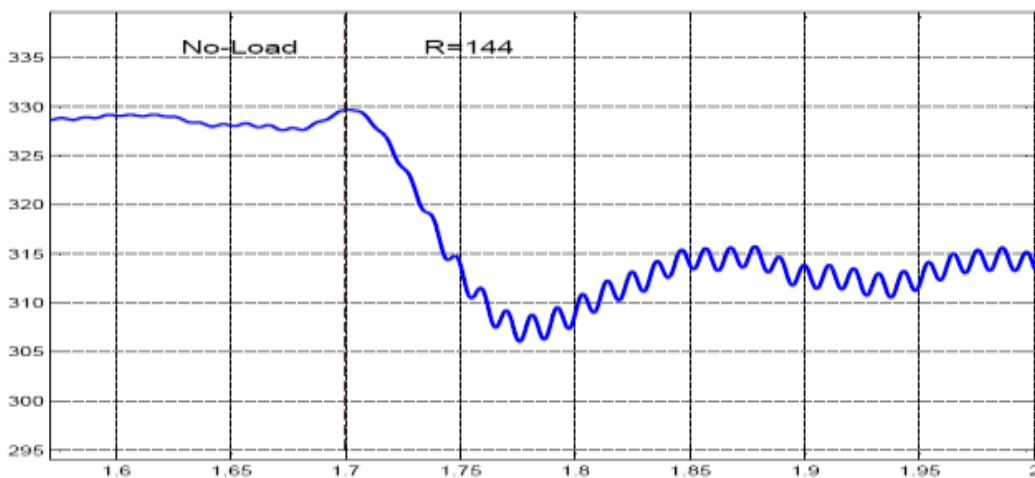


Figure 5.48 Peak terminal voltage magnitude (V) variation of SEIG using feedback from ac voltage

CHAPTER SIX

CONCLUSION

In this thesis, the capability and excitation issues of the stand-alone self-excited induction generator have been studied. In order to better understand the SEIG's behavior, the steady-state and dynamic analysis of the machine were accomplished and results are compared with the experimental study. The excitation methods to control the terminal voltage in stand-alone application were studied.

The steady-state analysis for constant frequency and constant speed was studied in MATLAB. Dynamical modeling of the induction machine based on stationary reference frame was explained in detail using $qd0$ reference frame theory. The simulated systems in both transient and steady-state were compared by the laboratory setup results. Comparing the experimental results with the dynamical and steady-state results verified that the dynamical model closely characterizes the behavior of the real machine. The terminal voltage control methods using variable capacitor bank, VSI and STATCOM were explained through simulations in MATLAB/Simulink. For VSI and STATCOM systems, a control scheme based on slip speed control methodology was studied. The control task was performed by a PI regulator, which generates the slip speed command for the induction generator. As shown in simulation results, the controller can maintain an approximately constant voltage at the induction generator terminal and across the dc capacitor by adjusting the STATCOM frequency under different loading conditions. Also, STATCOM can supply the reactive power required by the load. The applicability of this control scheme to STATCOM system is shown by means of computer simulations. The modeling studies that have been accomplished in this thesis can be extended to practical implementation of the systems examined as future work.

REFERENCES

- Ahmed, T., & Noro, O. (2003). Three-phase self excited induction generator driven by variable speed mover for clean renewable energy utilization and its terminal voltage regulation characteristics by static VAR compensator. *IEEE Transactions on Industry Applications*, 693-700.
- Ahmed, T., & Noro, O., Matso, K., Shindo, Y., & Nakaoka, M. (2003). Minimum excitation capacitor requirement for wind turbine coupled stand-alone self excited induction generator with voltage regulation based on SVC. *IEEE International Symposium on Power Electronics*, 396-403.
- Anagreh, Y.N., & Al-Refae'e, M.I. (2003). Teaching the self excited induction generator using Matlab. *International Journal of Electrical Engineering Education*, 40(1).
- Avinash, K.G., & Kumar, S. (2006). Dynamic modeling and analysis of three phase-self excited induction generator using generalized state-space approach. *IEEE International Symposium on Power Electronics*, 15-52.
- Barrado, J. A., Grino, R., & Valderrama, H. (2007). Stand-alone self-excited induction generator with a three-phase four wire active filter and energy storage system. *IEEE Conference Publications*, 600-605.
- Bansal, R. C. (2005). Three-Phase Self-Excited Induction generator: an overview. *IEEE Transactions on Energy Conversion*, 20(2), 292-299.
- Boldea, I. (2002). *Three-phase induction generators. The Induction Machine Handbook*. Boca Raton London New York Washington, D.C: CRC Press.
- Chan, T.F., & Lai, L.L. (June 2001). A novel single-phase self regulated self excited induction generator using a three phase machine. *IEEE Transactions on Energy Conversion*, 16(2), 204-208.
- Dastagir, G., & Lopes, A. C. (2007). Voltage and frequency regulation of stand-alone self-excited induction generator. *IEEE Canada Electrical Power Conference*, 502- 506.

- Geng, H., Xu, D., Wu, B., & Huang, W. (2011). Direct voltage control for a stand-alone self-excited induction generator with improved power quality. *IEEE Transactions on Power Electronics*, 26(8), 2358-2368.
- Haque, M. H. (2008). Self excited single-phase and three- phase induction generator in remote areas. *IEEE 5th International Conference on Electrical and Computer Engineering*, 38-42.
- Hashemnia, M.N., & Kashiha, A., & Ansari, K. (2010). A novel approach for the steady-state analysis of a three-phase self excited induction generator including series compensation. *IEEE Symposium on Industrial Electronics and Applications*, 371-375.
- Hazra, S., & Sensarma, P. S. (2008). Dc bus voltage build up and control in stand-alone wind energy conversion system using direct vector control of SCIM. *Conference of IEEE Industrial Electronics*, 2143- 2148.
- Hazra, S., & Sensarma, P.S. (2010). Self-excitation and control of an induction generator in a stand-alone wind energy conversion system. *IET renewable power generation*, 4(4), 383-393.
- Jayaramaiah, G. V., & Fernandes, B.G. (2006). Novel Voltage Controller for Stand-alone Induction Generator using PWM-VSI. *IAS Annual Meeting, Industry Applications*, 1, 204-208.
- Jayaramaiah, G.V., & Fernandes, B.G. (2008). Voltage controller for stand-alone induction generator using instantaneous power control. *IEEE Power Electronics Systems and Applications* , 102-106.
- Joshi, D., & Sandhu, K. S., & Soni, M.K. (2006). Constant voltage constant frequency operation for a self-excited induction generator. *IEEE Transactions on Energy Conversion*, 21(1), 228-234.
- Kishore, A., & Kumar G. S. (2006). Dynamic modeling and analysis of three phase self excited induction generator using generalized state-space approach. *IEEE International Symposium on Power Electronics*, 52-59.

- Krause, P.C. (2002). *Analysis of electric machinery and drive system* (2th ed). IEEE Press.
- Kumar, D. B., & Mohanty, K. B. (2011). Analysis, voltage control and experiments on a self-excited induction generator. *International Conference on Renewable Energy and Power Quality*.
- Kuperman, A., & Rabinovici, R. (2005). Shunt voltage regulators for autonomous induction generators, part II: Circuit and systems. *International Conference on Electric Power Systems*, 124-129.
- Lee, B. K., & Ehsani, M. (2001). A simplified functional simulation model for three-phase voltage source inverter using switching function concept. *IEEE Transaction on Industrial Electronics*, 48(2), 309-321.
- Meier, A.V. (2006). *Electric power system*. Canada: IEEE Press.
- Mosaad, M.I. (5th June 2011). Control of Self Excited Induction Generator using ANN based SVC. *International journal of computer application*, 23, 22-25.
- Murthy, S. S., & Ahuja, R. Kr. (2010). A novel solid state voltage controller of three phase self excited induction generator for decentralized power generation. *IEEE Power, Control and Embedded Systems (ICPCES)*, 1-6.
- Murthy, S.S., & Bhuvaneshwari, G., & Ahuja, K., & Gao, S. (2010). Analysis of self excited induction generator using MATLAB GUI methodology. *IEEE International Conference on Power Electronics, Drives and Energy Systems (PEDES)*.
- Ong, C. M. (1998). *Dynamic simulation of electric machinery*. USA: Prentice Hall PTR Press.
- Ouazene, L., & Mcpherson. G. (august 1983). Analysis of the isolated induction generator. *IEEE Transaction on Power Apparatus and Systems*, 102(8), 2793-2798.

- Phumiphak, P., & Uthai C.C. (2009). Optimal Capacitances Compensation for short-shunt self excited induction generator under inductive load. *IEEE International Conference on Electrical Machines and Systems*.
- Saffar, M. A. AL., Nho, E. Ch., & Lipo, Th. A. (1998). Controlled shunt capacitor self-excited induction generator. *IEEE Industry Applications Conference*, 1486-1490.
- Sandhu, K.S., & jain, S.P. (2008). Steady state operation of self excited induction generator with varying wind speeds. *International Journal of Circuits, Systems and Signal Processing*, 2(1), 26-33.
- Seyoum, D., Grantham, C., & Rahman, F. (2001). The dynamics of an isolated self excited induction generator driven by a wind turbine. *Annual Conference of the IEEE Industrial Electronics Society*, 1364-1369.
- Sharma, S., & Sandhu, K. S. (2008). Role of reactive power source on power quality of three-phase self excited induction generator. *International Conference on Power Electronics, Drives and Energy Systems*, 3 (4), 216-225.
- Shokrollah, H. (2006). Voltage source inverter for voltage and frequency control of a stand alone self excited induction generator. *IEEE Canadian Conference on Electrical and Computer Engineering*, 2241-2244
- Singh, B., Murthy S. S., & Gupta S. (2004). Analysis and design of STATCOM based voltage regulation for self-excited induction generator. *IEEE Transactions on Energy Conversion*, 19(4), 783-790.
- Singh, G. K. (2003). Self excited induction generator research-a survey. *IEEE Transactions on Energy Conversion*, 107-114.
- Wang, L., & Cheng, C. M. (2000). Excitation capacitance required for an isolated three-phase induction generator supplying a single-phase load. *IEEE Power Engineering Society Winter Meeting*, 1, 299-303.

- Wang, L., & Su, J.Y. (1997). Dynamical performances of an isolated self-excited induction generator under various loading conditions. *IEEE Transactions on Energy Conversion*, 14(1), 93-100.
- Wu, J. C. (2008). AC/DC power conversion interface for self excited induction generator. *IET Renewable Power Generation*, 3(2), 144–151.